

Some Results on Structure in Graphs and Numbers

by

Tomas Boothby

M.Sc., University of Washington, 2010

B.Sc., University of Washington, 2008

Dissertation Submitted in Partial Fulfillment
of the Requirements for the Degree of
Doctor of Philosophy

in the
Department of Mathematics
Faculty of Science

© Tomas Boothby 2015
SIMON FRASER UNIVERSITY
Fall 2015

All rights reserved.

However, in accordance with the *Copyright Act of Canada*, this work may be reproduced without authorization under the conditions for “Fair Dealing.” Therefore, limited reproduction of this work for the purposes of private study, research, criticism, review and news reporting is likely to be in accordance with the law, particularly if cited appropriately.

Approval

Name: Tomas Boothby
Degree: Doctor of Philosophy (Mathematics)
Title: *Some Results on Structure in Graphs and Numbers*
Examining Committee: **Dr. Luis Goddyn** (chair)
Professor

Dr. Matt DeVos
Senior Supervisor
Professor

Dr. Petr Lisonek
Supervisor
Professor

Dr. Bojan Mohar
Internal Examiner
Professor

Dr. Wendy Myrvold
External Examiner
Professor

Date Defended: November 30, 2015

Abstract

This thesis present three results.

The first is a result in structural graph theory. It demonstrates a large family of complete graphs embedded (clique embeddings) as minors of the grid-like Chimera graph, which is an abstract graph representing the D-Wave quantum adiabatic processor where vertices of the Chimera graph represent qubits in the processor. These particular embeddings are uniform in the sense that each vertex of the complete graph is represented by an equal number of vertices in the Chimera graph, which is thought to improve performance of the D-Wave processor. We present a polynomial-time algorithm to find a largest clique in this family in arbitrary induced subgraphs. Then we use the output of our algorithm as a measure of quality of a particular induced subgraph and show that the size of a largest clique embedding grows logarithmically in the grid size when a fixed percentage of qubits have been deleted.

The second is a result in design theory and combinatorial number theory; constructing a family of designs called Heffter arrays. A Heffter array is a $(m \times n)$ integer matrix whose entries' absolute values cover the interval $[1, mn]$, where every row and column sums to zero modulo $2mn + 1$. Archdeacon [2] uses Heffter arrays to construct embeddings of the complete graph K_{2mn+1} into orientable surfaces such that every edge appears in an m -cycle and an n -cycle, provided either m or n is odd. This chapter establishes that $m \times n$ Heffter arrays exist if and only $m > 2$ and $n > 2$.

The third is a result in combinatorial number theory and structural graph theory. For subsets A, B of a group G define the product set $AB = \{ab : a \in A, b \in B\}$. Presented in this chapter is a classification the sets A, B such that $|AB| \leq |A| + |B|$ when $H < G$ and B is the union of two H -cosets by reducing the problem to, and classifying, vertex- and edge-transitive d -regular graphs with edge cuts of size at most $2d$. That classification necessitates the classification d -regular vertex- and edge-transitive graphs with girth g such that $dg \leq 2(d + g)$: with a provided finite list of exceptions, each edge belongs to at most two g -cycles.

Keywords: graph theory, structural graph theory, combinatorial number theory, quantum computing, topological graph theory, design theory

Dedication

This is yet another variation on the Cuckoo.

Acknowledgements

I need to thank some individuals. Many more are due thanks, but I can't fit them all here.

Megan: this thesis is a testament to her dedication every bit as much as it is to mine.

Matt: for teaching me to uncross, for reading and refuting strange conjectures via SMS after midnight, and so much more.

Jeff: for taking over Dan's many projects, and generally helping clean up Chapter 2.

Dan: for giving me such an interesting, and surprisingly tractable problem.

Andrew: for encouraging me towards an internship at D-Wave, and pointing me in the direction of native clique embeddings.

Aidan: for his enduring patience during my intership at D-Wave.

Mom: for instilling me with the confidence that I will succeed.

Dad: for instilling me with the tenacity to accomplish the above.

Additional thanks go to Amber, Fred, John, Kevin, Megan, Paolo, Renin, Ronnie, Sam, Sophie, Stefan, Tara and Thryn. You know what you've done.

Also, the research in Chapter 1 was supported by the Mitacs Accelerate program and by D-Wave. Thanks to everybody who made that possible.

Table of Contents

| | |
|---|-------------|
| Approval | ii |
| Abstract | iii |
| Dedication | iv |
| Acknowledgements | v |
| Table of Contents | vi |
| List of Tables | viii |
| List of Figures | ix |
| 0 Introduction | 1 |
| 0.1 Native Clique Embeddings in Chimera Subgraphs | 1 |
| 0.2 Heffter Arrays Exist | 2 |
| 0.3 A Step Beyond DeVos When One Set is Two Cosets | 4 |
| 1 Native Clique Embeddings in Induced Chimera Subgraphs | 6 |
| 1.1 Introduction and Motivation | 6 |
| 1.1.1 The Chimera graph and triangle embeddings | 7 |
| 1.2 Native Clique Embeddings | 8 |
| 1.3 Finding Optimal Native Clique Embeddings in Induced Subgraphs | 13 |
| 1.3.1 Induced and General Subgraphs | 17 |
| 1.4 Comparison With Previous Work | 18 |
| 1.5 Expected Clique Yield | 19 |
| 2 Heffter Arrays Exist | 21 |
| 2.1 Introduction | 21 |
| 2.1.1 A Brief History of Skolem Sequences | 21 |
| 2.1.2 Heffter Systems and Heffter Arrays | 23 |
| 2.1.3 Main Theorem | 24 |
| 2.1.4 Motivation | 24 |

| | | |
|----------|---|------------|
| 2.1.5 | Outline | 26 |
| 2.2 | High-Level Description of the Constructions | 27 |
| 2.2.1 | The Only Good Idea Here: A Dramatic Interlude | 28 |
| 2.3 | Both Dimensions Even | 29 |
| 2.4 | Some Small Heffter Arrays | 31 |
| 2.5 | Short Heffter Arrays of Odd Height | 32 |
| 2.5.1 | Constructing Heffter Systems From Near Skolem Sequences | 32 |
| 2.5.2 | Constructions of Skolem Sequences | 34 |
| 2.5.3 | Long Lines of Short Tiles | 36 |
| 2.5.4 | The Final Short Tile | 36 |
| 2.6 | The Last Five Cases | 37 |
| 2.7 | Complete Description of Heffter Arrays and Proofs That They Are Heffter Arrays: The Section That My Computer Wrote | 41 |
| 2.7.1 | Constructions of $3 \times n$ Heffter Arrays | 42 |
| 2.7.2 | Constructions of $5 \times n$ Heffter Arrays | 50 |
| 2.7.3 | Constructions For m and n Large | 58 |
| 2.8 | Future Work | 64 |
| 3 | A Step Beyond DeVos When One Set is Two Cosets | 66 |
| 3.1 | History | 66 |
| 3.2 | Introduction | 68 |
| 3.2.1 | Notation for Graphs | 68 |
| 3.2.2 | Reduction to Classifying Graphs | 71 |
| 3.3 | Classification Theorem | 72 |
| 3.3.1 | Tindell's Theorem | 72 |
| 3.3.2 | The Main Theorem | 74 |
| 3.4 | Observations on Vertex- and Edge-Transitive Graphs | 76 |
| 3.5 | Some Stability Theorems | 78 |
| 3.5.1 | Degree 3 | 78 |
| 3.5.2 | Degree 4 | 79 |
| 3.5.3 | Degree 5 | 85 |
| 3.5.4 | Degree 6 | 86 |
| 3.6 | Proof of The Main Theorem | 89 |
| | Bibliography | 96 |
| | Appendix A Skolem-like Sequences | 99 |
| | Appendix B Two Row Tiles | 104 |
| | Appendix C Additional Info for Chapter 3 and Main Theorem Tearout | 105 |

List of Tables

| | | |
|-----------|---|----|
| Table 2.1 | Case outline for constructions of $(4m + k) \times (4n + \ell)$ Heffter arrays. Blank cells are covered by symmetry. | 26 |
| Table 2.2 | Small Heffter arrays | 31 |
| Table 2.3 | Five seeds to be used in creating Heffter arrays with at least one odd dimension, and both dimensions at least 7. | 39 |

List of Figures

| | | |
|------------|--|----|
| Figure 1 | “Triangle” clique embedding in $\mathcal{C}_{4,4,4}$, which motivated the design of the Chimera graph. Every chain in this embedding has 5 qubits. . . | 2 |
| Figure 1.1 | A maximum native clique embedding and its corresponding block clique embedding. | 8 |
| Figure 1.2 | An example of the iterative construction of a block clique embedding. | 12 |
| Figure 1.3 | The four rectangles $R_i = R_{to}(X_i, c_i)$ with $(X_i, c_i) \in X_{to}(R)$. Gray ell blocks represent precomputed <i>maxPartialEmbedding</i> (R_i) as in Lemma 1.3.1. | 14 |
| Figure 1.4 | Comparison of clique yields for ell-shaped (red) and plus-shaped (blue) chains for various square grids with $L = 4$. The solid lines denote the median, and the shaded regions encompass the middle two quartiles. | 19 |

Chapter 0

Introduction

This chapter gives a brief introduction to the problems in this thesis. Aside from this introductory chapter, this thesis consists of three chapters. Each chapter contains a standalone result, and the results are largely disconnected. The individual chapters have their own introductions, will discuss the notation used therein, and the history and motivation behind the results. The central themes to the results are graph theory, and structure. First we will give a rough description of how these results fit our title, the “structure of graphs and numbers.”

Chapter 1 can be considered a result of structural graph theory with a significant industrial application. The chapter concerns a large family of minors in a class of graphs. It contains a precise description of the family, which gives rise to an algorithm to optimize over that family in a particular graph as well as a probabilistic argument to analyze the behavior of this optimum. This chapter is joint work with Andrew King and Aidan Roy.

Chapter 2 is largely motivated by graph theory, but is best described as a result on the structure of numbers. There, we solve a problem in design theory which generalizes magic squares – we find rectangular matrices with integer entries, whose row sums are zero in a particular cyclic group. This chapter is joint work with Dan Archdeacon and Jeff Dinitz.

Chapter 3 is indisputably structural graph theory. The core of the result is a classification of edge cuts of size $2d$ in d -regular graphs which are vertex- and edge-transitive. The motivation for this classification is from combinatorial number theory, so again, has to do with the structure of numbers, if weakly. This chapter is joint work with Matt DeVos.

Next, we dig in to the definitions and give a high-level view of our main results. Below, we briefly give enough detail to describe our results, and how we obtained them.

0.1 Native Clique Embeddings in Chimera Subgraphs

A D-Wave quantum annealing processor is a purpose-built analog computer [14] made to solve Ising spin glass problems. These processors are represented by *Chimera* graphs

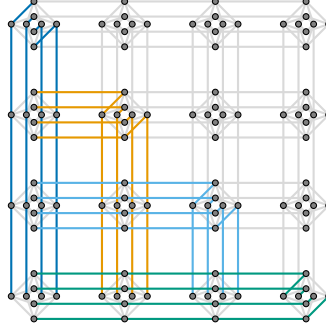


Figure 1: “Triangle” clique embedding in $\mathcal{C}_{4,4,4}$, which motivated the design of the Chimera graph. Every chain in this embedding has 5 qubits.

(defined in the next paragraph, see Figure 1 for an example Chimera graph). The first step to solving an Ising spin glass problem on a D-Wave computer is to look at the underlying graph of that problem and find that graph as a minor of the Chimera graph representing the processor that one has access to. Finding these minors is difficult in practice, so we restrict our attention to finding *clique embeddings*.

The Chimera graph $\mathcal{C}_{M,N,L}$ is an $M \times N$ grid of complete bipartite $K_{L,L}$ *unit cells*. Specifically, $\mathcal{C}_{M,N,L}$ has vertices $V = \{1, \dots, M\} \times \{1, \dots, N\} \times \{0, 1\} \times \{1, \dots, L\}$ which we refer to as *qubits* and edges:

$$\begin{aligned} (x, y, 0, k) &\sim (x + 1, y, 0, k), && \text{(horizontal inter-cell couplings)} \\ (x, y, 1, k) &\sim (x, y + 1, 1, k), \text{ and} && \text{(vertical inter-cell couplings)} \\ (x, y, 0, k_1) &\sim (x, y, 1, k_2) \text{ for } k_1, k_2 \in 1, \dots, L. && \text{(intra-cell couplings)} \end{aligned}$$

A particular D-Wave processor may have some defective vertices or edges, which we delete from our graph. Where the Chimera graph was designed in part to support a particular clique embedding called the *triangle* embedding, shown in Figure 1, a relatively small number of deleted qubits can conspire to invalidate large portions of an embedding.

We generalize the triangle embedding to a family of clique embeddings, called *native clique embeddings*, which grows exponentially with N in $\mathcal{C}_{N,N,L}$ for L fixed. We characterize this family of embeddings with a combinatorial description, which helps us find a dynamic programming approach to find a largest native clique embedding contained in an induced Chimera subgraph in polynomial time. Moreover, we are able to use this description to analyze a largest clique embedding that one can expect to find in a given induced Chimera subgraph.

0.2 Heffter Arrays Exist

An $m \times n$ matrix $H = (h_{ij})$ with integer entries is a *Heffter array* if

1. $\{|h_{ij}| : 1 \leq i \leq n, 1 \leq j \leq m\} = [1, mn]$,

2. $R_i = \sum_{j=1}^m h_{ij} \equiv 0 \pmod{2mn+1}$ for $1 \leq i \leq n$, and
3. $C_j = \sum_{i=1}^n h_{ij} \equiv 0 \pmod{2mn+1}$ for $1 \leq j \leq m$.

If the first two conditions replace $\equiv 0 \pmod{2mn+1}$ with $= 0$, then H is said to be an integer Heffter array. In Chapter 2, we show that $m \times n$ Heffter arrays exist for all plausible m and n , and likewise for integer Heffter arrays. Here, “plausible” means that m and n are large enough, and for the purpose of integer Heffter arrays, m and n satisfy a modular condition.

Chapter 2 has a peculiar structure. The result itself is a collection of a large number of constructions covering various residue classes of (m, n) modulo 4, with the cases $(3, n)$ and $(5, n)$ being exceptionally tricky, with n taken modulo 8. To convince ourselves that our constructions covered all $m, n > 3$, we implemented the constructions in Python. Later, we repurposed that code to produce proofs, easily verified by human, that our constructions are correct.

As nice as “easily verified by human” may sound, the full proof of Theorem 2.1.5 is rather tedious. Additionally, there is beauty behind our constructions that is utterly obscured by the computer-generated proofs. Thus, the majority of our effort is spent describing our constructions at a high level, without focusing too much on the pesky details.

In our constructions, we use two main ideas. The first is the signed sequence $x+1, -x-2, -x-3, x+4$, which sums to zero irrespective of the value of x . This idea proves useful in several contexts, which we outline in Section 2.2.1.

The second idea is the use of *Skolem sequences*, and some generalizations thereof. A Skolem sequence is (equivalent to) a labeling of an interval of integers of length $2n$ with the integers $[1, n]$ so that each label occurs precisely twice, and the integers a_d and b_d with label d have $|b_d - a_d| = d$. For example, such a labeling of $[6, 15]$

$$\begin{array}{cccccccccccc} 5 & 2 & 4 & 2 & 3 & 5 & 4 & 3 & 1 & 1 \\ \hline 6 & 7 & 8 & 9 & 10 & 11 & 12 & 13 & 14 & 15 \end{array}$$

gives rise to a partition $[1, 15]$ into triples $(d, a_d, -b_d)$,

$$\begin{array}{ccccc} 1 & 2 & 3 & 4 & 5 \\ 14 & 7 & 10 & 8 & 6 \\ -15 & -9 & -13 & -12 & -11 \end{array}$$

This gives a 3×5 matrix with column sums zero and entries covering the interval $[1, 15]$ in absolute value. By permuting the entries in various columns and negating some of those columns, one can change the row sums without affecting the column sums, hence obtain a

Heffter array

$$\begin{array}{ccccc} -1 & -9 & -3 & 8 & 5 \\ 15 & 2 & -10 & 4 & -11 \\ -14 & 7 & 13 & -12 & 6. \end{array}$$

The constructions depend on generalizing Skolem sequences by omitting a subset of the labels $\{1, 2\}$.

0.3 A Step Beyond DeVos When One Set is Two Cosets

Let G be a multiplicative group. Given two sets $A, B \subset G$, define the *product set* $AB = \{ab : a \in A, b \in B\}$. In 1813, Cauchy [13] proved that $|AB| \geq |A| + |B| - 1$, provided that $|G|$ is prime, $AB \neq G$ and $A, B \neq \emptyset$, a result rediscovered by Davenport [17] in 1935. A similar bound was established by Kneser [32] in 1953 for abelian groups, that $|AB| \geq |A| + |B| - |\text{Stab}_G(AB)|$, where $\text{Stab}_G(U) = \{g \in G : gU = U\}$ for any $U \subseteq G$.

In addition to these inequalities, a type of inverse problem has been studied. In 1956, Vosper [44] proved the following theorem.

Theorem 0.3.1 (Vosper). *For A, B nonempty subsets of a group G of prime order p , $|AB| < |A| + |B|$ if and only if*

1. $|A| + |B| > p$,
2. $|A| = 1$ or $|B| = 1$,
3. $B = c(G \setminus \{a^{-1} : a \in A\})$ for some $c \in G$, or
4. A and B are geometric progressions with the same ratio.

In 1960, Kemperman [29] found a similar *structural* theorem for the case of abelian groups, classifying those sets A, B for which $|AB| < |A| + |B|$. In 2013, DeVos [18] broke tradition by establishing a structural theorem for arbitrary groups first, and then unwinding that structure to find the appropriate bounding theorem. In 2009, Grynkiewicz [25] classifies those sets A, B for which $|AB| = |A| + |B|$, in a paper entitled ‘‘A Step Beyond Kemperman’s Structure Theorem.’’ Our goal is to make progress towards taking the analogous step beyond DeVos’s structural theorem.

One of the more difficult cases of DeVos’s study is when the set B is a union of two H -cosets, $B = Ha \cup Hb$ for some $H < G$ and $a, b \in G$. By constructing a bipartite graph Γ with vertex set $\{1, 2\} \times G$ with $(1, x) \sim (2, y)$ if $y \in xB$, DeVos shows that the vertices $\{2\} \times G$ have degree 2, so Γ is the incidence structure for the vertices and edges of a graph X . As it turns out, X is a vertex- and edge-transitive graph (due to the action of G upon itself), hence d -regular for some d . Furthermore, classifying those sets A for which $|AB| < |A| + |B|$ is equivalent to classifying edge cuts of size less than $2d$.

Now we are ready to discuss the results in this thesis. With an identical setup to DeVos, we are interested in d -regular graphs X which are vertex- and edge-transitive, and we want to classify the edge cuts of size at most $2d$. Our classification invokes two additional parameters, namely *girth*, the length of a smallest cycle in the graph, and *frequency*, the number of girth cycles that an edge belongs to. Since X is edge-transitive, frequency is well-defined. We describe DeVos's reduction to vertex- and edge-transitive graphs in Section 3.2.2.

In order to classify those graphs with small edge cuts, we classify the vertex- and edge-transitive graphs for which a minimum length cycle gives a small cut (in particular, where $dg \leq 2(d + g)$). We take advantage of an earlier classification of cubic graphs, and observe there are no such graphs for $d \geq 7$ since they would have $g \leq 2$. In particular, the 4-regular and 6-regular graphs admit a rather rich structure. In both we find large, essentially unclassifiable families where the frequency is 1 or 2, in addition to tilings of the torus where $k = 2$. The classification of 4-regular graphs of girth 4 was split off into a separate paper [10], in a slightly more general form (only assuming edge-transitivity and accepting infinite graphs).

In our classifications of graphs, the frequency is our primary tool. For the most part, we will use the fact that every edge in an edge-transitive graph is contained in the same number of girth-cycles, but the notion is much more general. For example Lemma 3.5.9 considers the number of times that a vertex v in a vertex-transitive graph occurs with degree 2 in induced copies of $K_{3,2}$. By looking at the frequency with which some substructure of a graph occurs inside another, we are able to explore the neighboring vertices of that substructure. If that graph has small diameter, we can rather quickly discover the whole graph. Otherwise, we learn that the graph is path-like, has a unique embedding on a surface, or in one case, belongs to a family too large to fully classify.

Chapter 1

Native Clique Embeddings in Induced Chimera Subgraphs

This chapter is joint work with Andrew King and Aidan Roy; it is very nearly identical to [11]. King provided the author with the rough idea of how native clique embeddings are structured, and both provided significant editorial input.

1.1 Introduction and Motivation

D-Wave quantum annealing processors are designed to sample low-energy spin configurations in the Ising model using open-system quantum annealing [1, 9, 19, 27]. Input to the processor consists of an *Ising Hamiltonian* (h, J) , where $h \in \mathbb{R}^n$ is a vector of *local fields* and $J \in \mathbb{R}^{n \times n}$ is a matrix of *couplings*, which we assume here to be symmetric. The *energy* of a spin configuration $s \in \{-1, 1\}^n$ is given as

$$E(s) = E(h, J, s) = s^T J s + s^T h. \quad (1.1)$$

The output of an *anneal* (i.e. a run) of the processor is a low-energy state s , which consists of an Ising spin (either -1 or 1) for each *qubit*.

Nonzero terms of J are physically realized using programmable *couplers*. These couplers only exist between certain pairs of physically proximate qubits. The input (h, J) is therefore restricted such that if $J_{i,j} \neq 0$, there must be a coupler between qubit i and qubit j . We rephrase this in graph-theoretic terms: The *connectivity graph* of (h, J) , which we denote by G_J , is the undirected graph on n vertices whose adjacency matrix has the same nonzero entries as J . Likewise, each processor has a *hardware graph* G representing the available qubits and couplers in the processor. For (h, J) to be input directly to the processor, G_J must be a subgraph of G . If this is not the case, we can indirectly input (h, J) to the hardware by embedding G_J as a graph minor of G . Implementing graph minors in the Ising

model involves putting a strong ferromagnetic coupling $J_{i,j} \ll 0$ between any two adjacent vertices i, j of G in the same vertex image. This coupling compels multiple qubits to take the same spin, thus acting like a single logical qubit. The method is studied in greater detail elsewhere [14, 43, 37, 30, 12].

In this paper we consider the problem of finding large clique minors in the hardware graph. This is sufficient for minor-embedding any problem of appropriate size in a given hardware graph, and allows the study of random, fully-connected spin glass problems, as in recent work [43]. Klymko et al. first provided a polynomial-time algorithm for generating large clique minors in subgraphs of hardware graphs [31]. In Section 1.4 we provide evidence that our algorithm uses fewer physical qubits and allows the embedding of larger minors.

1.1.1 The Chimera graph and triangle embeddings

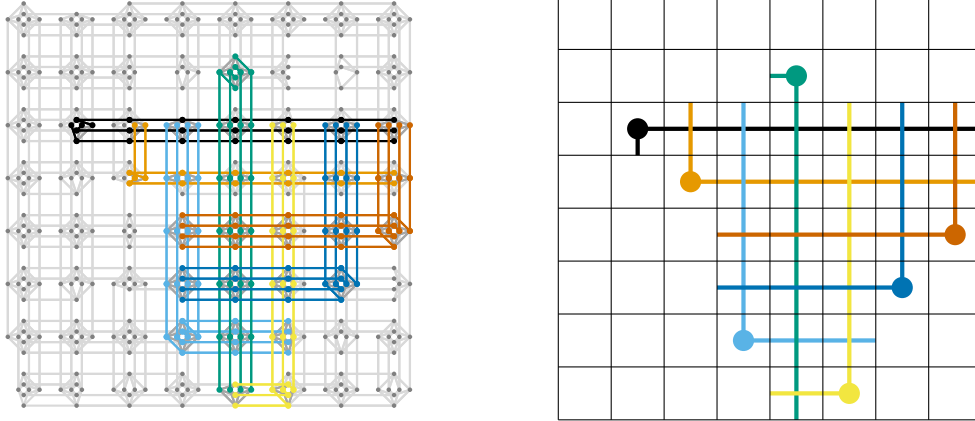
D-Wave processors currently operate using a *Chimera* hardware graph $\mathcal{C}_{M,N,L}$, which is an $M \times N$ grid of complete bipartite graphs $K_{L,L}$ called *unit cells*. D-Wave Two processors use a 512-qubit $\mathcal{C}_{8,8,4}$ hardware graph, and the most recent processors use a 1152-qubit $\mathcal{C}_{12,12,4}$ graph.

The Chimera graph was chosen, in part, because it contains a particularly nice clique minor [15] (see Figure 1). This *triangle embedding* is uniform in the sense that each vertex image (or *chain*) has the same number of vertices, and is near-optimal in the sense that it gives a K_{LM} minor in $\mathcal{C}_{M,M,L}$, whereas $\mathcal{C}_{M,M,L}$ has treewidth LM and therefore contains no K_{LM+2} minor¹. A degree argument also shows that any uniform K_{LM} minor requires chains of size at least M , while the triangle embedding has chains of size $M + 1$.

In practice, a given processor will have a number of inoperable qubits. If there are t inoperable qubits, up to t chains in a particular clique embedding can be rendered useless. These inoperable qubits force us to find a clique minor in an induced subgraph of $\mathcal{C}_{M,N,L}$. In the face of this, note that there are at least four triangle embeddings, which we can find by simply rotating the embedding shown in Figure 1. So a first attempt at minimizing the impact of inoperable qubits is to choose the triangle embedding for which the greatest number of chains survive.

Triangle embeddings can be generalized further. A triangle embedding consists of overlapping ell-shaped (L-shaped) “bundles” of chains, and each chain in a bundle joins a horizontal “wire” with a vertical “wire” via a matching at the corner of the bundle. First, the structure of overlapping ell-shaped bundles can be generalized from the triangle (we can avoid all four corner unit cells, for example). Second, the corner matchings can be chosen arbitrarily to minimize the impact of inoperable qubits (if there are three intact vertical wires and three intact horizontal wires, we can ensure that they are matched together to make three intact chains). These generalizations result in exponential expansion of the

¹Taking the triangle embedding and making an image of all the unused qubits gives a K_{LM+1} minor.



(a) A maximum native clique embedding of K_{24} in an induced subgraph of $\mathcal{C}_{8,8,4}$ with 26 randomly selected vertices deleted. (b) The corresponding block clique embedding, with dots indicating corners of the blocks.

Figure 1.1: A maximum native clique embedding and its corresponding block clique embedding.

number of clique embeddings available, but we can nevertheless optimize over them in polynomial time using a dynamic programming approach. Defining and efficiently optimizing over these clique embeddings are the main goals of this work.

In the next section we formalize the definition of *native clique embeddings* that generalize triangle embeddings, and give a combinatorial characterization of the same. In Section 1.3 we give a dynamic programming technique that, given an induced subgraph of $\mathcal{C}_{M,N,L}$, finds a maximum-sized native clique embedding in polynomial time. One desirable feature of native clique embeddings is uniform chain length, which results in uniform, predictable chain dynamics throughout the anneal [43]. Clique embeddings found through heuristic methods such as the algorithm described by Cai et al. [12] generally lack this property. In Section 1.4 we compare the results of our approach to those of the somewhat similar approach by Klymko et al. [31]. The shorter chains and larger cliques generated by our approach lead to improved tunneling dynamics and error insensitivity [23, 43, 47].

1.2 Native Clique Embeddings

We now formally define the structures required to construct and analyze native clique embeddings.

Recall that Chimera $\mathcal{C}_{M,N,L}$ is an $M \times N$ grid of $K_{L,L}$ unit cells. Specifically, $\mathcal{C}_{M,N,L}$ has vertices $V = \{1, \dots, M\} \times \{1, \dots, N\} \times \{0, 1\} \times \{1, \dots, L\}$ and edges:

$$\begin{aligned}
 (x, y, 0, k) &\sim (x + 1, y, 0, k) && \text{(horizontal inter-cell couplings),} \\
 (x, y, 1, k) &\sim (x, y + 1, 1, k) && \text{(vertical inter-cell couplings), and} \\
 (x, y, 0, k_1) &\sim (x, y, 1, k_2) && \text{(intra-cell couplings).}
 \end{aligned}$$

We construct native clique embeddings using *wires*. For $t \geq 1$, a *horizontal wire* of length t is a contiguous set of vertices $\{(x + i, y, 0, k) : i \in [0, t - 1]\}$, whose induced subgraph is a path on t vertices. Likewise, a *vertical wire* is a set $\{(x, y + i, 1, k) : i \in [0, t - 1]\}$. An *ell* is the union of a horizontal wire and a vertical wire where there is an edge between one end of the horizontal wire and one end of the vertical wire. Note that these ends are necessarily in the same unit cell, which we call the *corner* of the ell; for an ell ℓ we denote the corner by $c(\ell)$. In the embeddings we study, each chain is an ell. Our aim now is to specify an orderly way of arranging them into a clique minor.

Looking at Figure 1.1, one may notice that chains appear in sets that intersect the same unit cells. With this in mind, for an ell ℓ we define its *ell block* $(X(\ell), c(\ell))$: $X(\ell)$ is the set of unit cells intersecting ℓ , and again $c(\ell)$ is the corner of ℓ , which we must specify for the ell block in order to avoid ambiguity in the case of horizontal or vertical wires of length 1. We define an *ell bundle* B as a (possibly empty) set of vertex-disjoint ells ℓ_1, \dots, ℓ_p with the same ell blocks, i.e. such that $|\{(X(\ell), c(\ell)) \mid \ell \in B\}| \leq 1$.

A *block clique embedding* is a set \mathcal{X} of n ell blocks $\{(X_1, c_1), \dots, (X_n, c_n)\}$ such that

- each X_i contains n unit cells (so ells have length $n + 1$), and
- every distinct pair X_i, X_j in \mathcal{X} intersects at exactly one unit cell, which is in the horizontal component of one ell block and the vertical component of the other.

A *native clique embedding* respecting a block clique embedding \mathcal{X} is a collection \mathcal{B} of ell bundles $\{B_i, \dots, B_n\}$ such that for each i and for each $\ell \in B_i$, $(X_i, c_i) = (X(\ell), c(\ell))$, i.e. (X_i, c_i) is the ell block for each ell in B_i . From this definition and the above, we infer that

- any two ells ℓ and ℓ' in the same bundle have exactly two edges between them, both in the unit cell $c(\ell) = c(\ell')$, and
- any two ells ℓ and ℓ' in different bundles have exactly one edge between them, and it is in the unit cell $X(\ell) \cap X(\ell')$.

Hence a native clique embedding is a clique embedding.

We note a consequence of the requirement that every pair of ell blocks intersect at exactly one unit cell: in a block clique embedding $\mathcal{X} = \{(X_1, c_1), \dots, (X_n, c_n)\}$, the corners c_1, \dots, c_n form a permutation in the $n \times n$ matrix representing the unit cells of the graph $\mathcal{C}_{n,n,L}$. These permutations have a specific structure that is in direct correspondence with a class of permutations representable by circular point sets studied recently by Vatter and Waton [42].

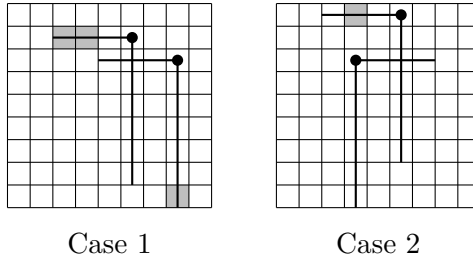
The following theorem provides a constructive classification of block clique embeddings and shows that, in contrast with triangle embeddings, native clique embeddings exist in abundance.

Theorem 1.2.1. *In a $\mathcal{C}_{n,n,L}$ Chimera graph for $n \geq 2$, there are 4^{n-1} block clique embeddings that contain n ell blocks. In particular, they are in natural bijection with the set $\{E, W\} \times \{NE, NW, SE, SW\}^{n-2} \times \{N, S\}$.*

To prove Theorem 1.2.1, we first show that each ell block in a block clique embedding has a distinct shape. Define the *width* of an ell as the number of vertices in its horizontal wire, and its *height* as the number of vertices in its vertical wire. All ells in an ell bundle have the same width and height, so define the width and height of an ell bundle or an ell block as the width and height of its constituent ells.

Lemma 1.2.2. *Let $\mathcal{X} = \{(X_1, c_1), \dots, (X_n, c_n)\}$ be a block clique embedding in $\mathcal{C}_{n,n,L}$. Then the ell blocks of \mathcal{X} have distinct heights.*

Proof. We will establish that \mathcal{X} has a unique ell block of height i for each $1 \leq i \leq n$. Clearly two ells of height 1 or two ells of height n cannot intersect properly (i.e. in exactly one unit which is horizontal for one ell block and vertical for the other). Assume for contradiction that \mathcal{X} contains two ells (X, c) and (X', c') of height $1 < i < n$. Their horizontal and vertical components must occupy different rows and columns respectively. Up to symmetry, there are two cases to consider where ells of the same height intersect properly, shown below. In both cases, we name the upper ell block (X, c) .



Since there are n ell blocks and n cells per block, every non-corner cell of every ell block must intersect another ell block. In Case 1, we have shaded cells for which the horizontal or vertical coordinate is unique among the two ells. Consider an ell block (Y, d) which properly intersects (X, c) in a shaded cell. To properly intersect (X', c') , (Y, c) cannot intersect (X, c) again, so must intersect (X', c') in a shaded cell also. Therefore, Y must have size greater than n , a contradiction. In Case 2, we have shaded the cell which lies directly north of a corner. In this case, it is clear that no ell block can properly intersect (X, c) at the gray cell and also intersect (X', c') properly. \square

By Lemma 1.2.2 we can assign unique labels to every ell block $(X_i, c_i) \in \mathcal{X}$ so that X_i has height i and width $n - i + 1$. Central to our proof is the notion of the *working rectangle*. We partition an ell block (X_i, c_i) of height i into three parts,

1. the corner $c_i = (x_i, y_i)$,

2. the horizontal component, $h_i = \{(x', y') \in X_i : y' = y_i, x' \neq x_i\}$, and
3. the vertical component, $v_i = \{(x', y') \in X_i : x' = x_i, y' \neq y_i\}$,

We define

$$R_i = \left(\bigcup_{j=1}^i h_j \right) \setminus \left(\bigcup_{j=1}^i v_j \right).$$

Unwinding these definitions, we find that

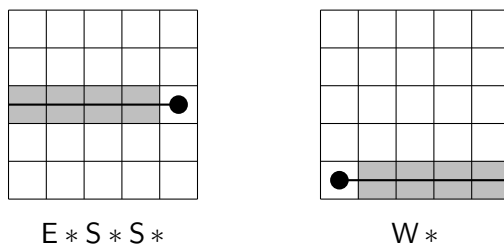
$$R_{i+1} = (R_i \setminus (R_i \cap X_i)) \cup (X_i \setminus (\{c_i\} \cup R_i)),$$

we'll prove that every R_i is a rectangle.

Proof of Theorem 1.2.1. We first give a mapping from the set of 4^{n-1} words to the set of block clique embeddings and then provide the inverse mapping.

Let $D = s_1 \cdots s_n$ be a word for which $s_1 \in \{E, W\}$, each of s_2, \dots, s_{n-1} is a word in $\{NE, NW, SE, SW\}$, and $s_n \in \{N, S\}$. We construct a block clique embedding from D in such a way that each ell block (X_i, c_i) corresponds to the subword s_i . We denote the location of a corner c_i by its Cartesian coordinates $(x_i, y_i) \in \{1, \dots, n\}^2$ and coordinates increase to the east (for x) and north (for y).

If $s_1 = W$ we place c_1 so that it is west of the remaining corners, i.e. $x_1 = 1$. If $s_1 = E$, we place c_1 so that it is east of the remaining corners, i.e. $x_1 = n$. We select y_1 so that there are $y_1 - 1$ Ss following the subword s_1 in the word D . Below, we show two initial ell block placements for words where $*$ denotes a (possibly empty) subword containing zero occurrences of the letter S.



The placement of the first ell block results in a working rectangle $R_1 = h_1$, which is in fact a rectangle. Now, suppose that the working rectangle after the selection of i ell blocks is $R_i = [x, x'] \times [y, y']$ in Cartesian coordinates, where $x \leq x'$ and $y \leq y'$. We choose corner c_i based on subword s_i as follows, noting that $x' = x + n - i - 1$ and $y' = y + i - 1$:

- If $s_i = NE$ or N , $c_i = (x', y' + 1)$.
- If $s_i = NW$, $c_i = (x, y' + 1)$.
- If $s_i = SE$ or S , $c_i = (x', y - 1)$.
- If $s_i = SW$, $c_i = (x, y - 1)$.

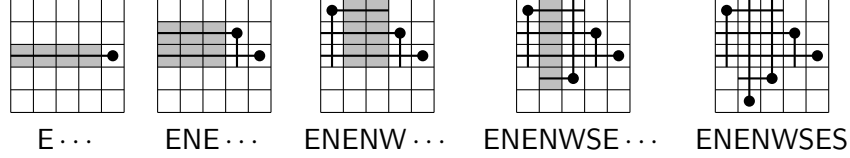


Figure 1.2: An example of the iterative construction of a block clique embedding.

Letting $c_i = (x_i, y_i)$, we then choose $X_i = (\{x_i\} \times [y, y']) \cup ([x, x'] \times \{y_i\})$ and update the working rectangle $R_{i+1} = ([x, x'] \setminus \{x_i\}) \times ([y, y'] \cup \{y_i\})$. Observe that every time that we find a W, x increases by 1 and every time we find an E, x' decreases by 1; every time we find an N, y increases by 1 and every time an S, y' decrease by 1. In particular, R_i is a rectangle one row taller and one column thinner than R_{i-1} , and the corner c_i is in the s_i -most corner of the rectangle $R_i \cup R_{i-1} \cup \{c_i\}$ (for example, if $s_i = \text{NW}$, c_i is in the cell in the north west corner of both its ell X_i and the aforementioned rectangle.)

Figure 1.2 shows an example of how the construction might proceed.

Note that R_i never shares a column with a corner in $\{c_j \mid j \leq i\}$, and the set of rows intersected by R_i is the same set of rows intersected by $\{c_j \mid j \leq i\}$. It therefore follows from the construction that $\{c_1, \dots, c_n\}$ is a permutation. Furthermore, by the construction, for $i < j$ there is always a unit cell $X_i \cap X_j$ in the working rectangle R_i – specifically, it is (x_j, y_i) . So $\mathcal{X} = \{(X_1, c_1), \dots, (X_n, c_n)\}$ is indeed a block clique embedding.

Now, we invert our construction. Let $\mathcal{X} = \{(X_1, c_1), \dots, (X_n, c_n)\}$ be a block clique embedding in which X_i has height i ; we will reconstruct our word D . We call $(x_n, y_1) = X_1 \cap X_n$ the center of \mathcal{X} , and say that a point (x, y) lies to the east or west of the center if $x > x_n$ or $x < x_n$ respectively, and likewise north and south.

- Let $s_1 = \text{E}$ if the corner c_1 lies to the east of the center, and W otherwise.
- For $1 < i < n$, let $s_i = a_i b_i$, where $a_i = \text{N}$ if c_i lies to the north of the center, and S otherwise; and $b_i = \text{E}$ if c_i lies to the east of the center, and W otherwise.
- Let $s_n = \text{N}$ if the corner c_n lies to the north of the center, and S otherwise.

Therefore, $D = s_1 s_2 \dots s_n$ is in $\{\text{E}, \text{W}\} \times \{\text{NE}, \text{NW}, \text{SE}, \text{SW}\}^{n-2} \times \{\text{N}, \text{S}\}$. To see that this construction is in fact the inverse, we observe that each ell block (X_i, c_i) is associated to the direction s_i in which the corner c_i lies from the center. If we start with a word D , then we see that the reverse construction reproduces that word D . Next, we'll show that the reverse construction is inverted by the forward construction, and hence that our sets are in bijection.

Furthermore, the ell block X_i , having height i , must intersect each previous ell block in precisely one cell. By construction, the vertical components v_j for $j < i$ are already “occupied” by the horizontal components h_j for $j < i$; $\bigcup_{i=1}^{j-1} v_j \subseteq \bigcup_{i=1}^{j-1} h_j$, and R_{i-1} is a rectangle of height $i - 1$ consisting of horizontal components less vertical components. Since

\mathcal{X} is a block clique embedding, the vertical component of X_i must overlap the horizontals of X_j for $j < i$, so $X_i \cap R_{i-1} = v_i$. As we argued in Lemma 1.2.2, v_i must overlap either the east-most or west-most cell of every $X_j \cap R_{i-1}$, or some pair of ell blocks will fail to overlap or overlap inappropriately. Similarly, the horizontal component of X_i must occupy the row one step north or south of R_{i-1} . Therefore, R_i is also a rectangle, one unit taller and thinner than R_{i-1} , and the corner c_i lies in the s_i -most corner of the rectangle $\{c_i\} \cup R_i \cup R_{i-1}$. Since X_i is the unique ell $\{c_i\} \cup (R_{i-1} \setminus R_i) \cup (R_i \setminus R_{i-1})$, the forward construction inverts our reverse construction. \square

1.3 Finding Optimal Native Clique Embeddings in Induced Subgraphs

In this section we describe an algorithm to find a largest native clique embedding $\mathcal{B} = \{B_1, \dots, B_n\}$ in an induced subgraph G of $\mathcal{C}_{M,N,L}$ with $n \leq M, N$. Our algorithm necessarily takes as input a parameter n , which determines the size of the chains, i.e. $n + 1$.

Our algorithm is inspired by the proof of Theorem 1.2.1. We use dynamic programming to maximize the block clique embeddings with each working rectangle R , and do so in an orderly way which results in a polynomial-time algorithm.

As a pre-processing step, for each ell block (X, c) we compute a maximum bundle and store it as $maxBundle(X, c)$ (it is straightforward to do this in $O(nL)$ time per ell block). We then use this information to construct block clique embeddings as in the proof of Theorem 1.2.1: adding one ell block at a time, with working rectangles of increasing height. Let (X, c) be an ell block of height i . If $1 \leq i \leq n - 1$, there is a unique working rectangle $R_{from}(X, c)$ that can be in effect immediately after (X, c) is placed. If $2 \leq i \leq n$, there is a unique working rectangle $R_{to}(X, c)$ that can be in effect immediately before (X, c) is placed. Note that for each working rectangle R , the sets

$$X_{from}(R) := \{(X, c) \mid R = R_{to}(X, c)\}$$

and

$$X_{to}(R) := \{(X, c) \mid R = R_{from}(X, c)\}$$

each have size at most four (see Figure 1.3).

For any set of ell bundles $\mathcal{B} = \{B_1, \dots, B_n\}$ where each B_i is contained in the ell block (X_i, c_i) and $\mathcal{X} = \{(X_1, c_1), \dots, (X_n, c_n)\}$, we define

$$\|\mathcal{X}\| := \left| \bigcup_{i=1}^n maxBundle(X_i, c_i) \right| \geq \left| \bigcup_{i=1}^n B_i \right|$$

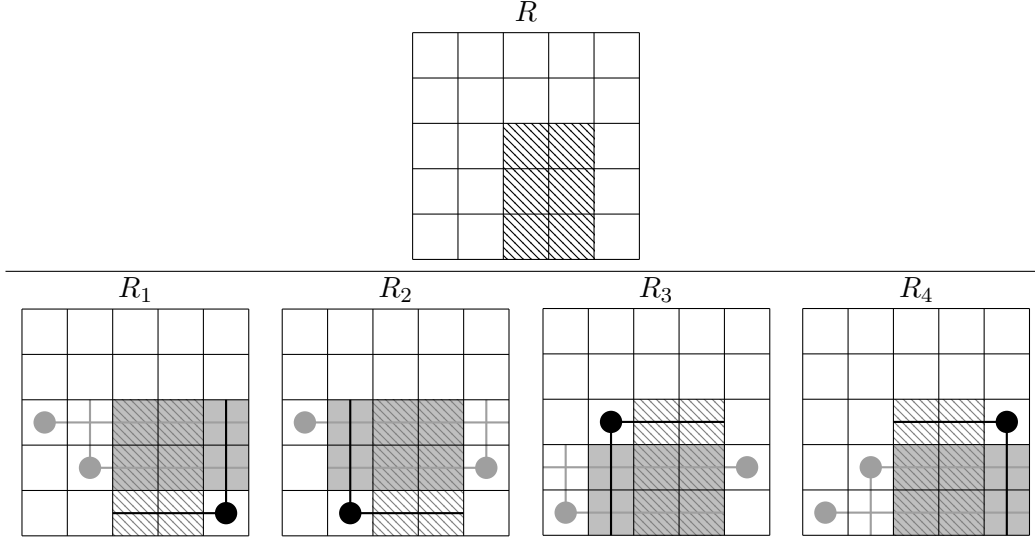


Figure 1.3: The four rectangles $R_i = R_{to}(X_i, c_i)$ with $(X_i, c_i) \in X_{to}(R)$. Gray ell blocks represent precomputed $maxPartialEmbedding(R_i)$ as in Lemma 1.3.1.

provided that the ell blocks are all distinct. This enables us to construct maximum native clique embeddings while only considering the ell blocks involved.

For each working rectangle R of height i (and width $n - i$), our algorithm computes and stores a *partial block clique embedding* with that working rectangle: a set of ell blocks $\mathcal{X}_i = \{(X_1, c_1), \dots, (X_i, c_i)\}$ such that

- $R = R_{from}(X_i, c_i)$,
- X_j has height j for all $1 \leq j \leq i$
- $R_{to}(X_j, c_j) = R_{from}(X_{j-1}, c_{j-1})$ for all $2 \leq j \leq i$.

In particular, we compute *maximum* partial block clique embeddings with working rectangle R ; those which maximize $\|\mathcal{X}_i\|$ over all partial block clique embeddings with a given working rectangle. We denote a particular maximum partial block clique embedding for a given working rectangle R by $maxPartialEmbedding(R)$, though many may exist. Our algorithm will operate by extending maximum partial block clique embeddings by ells, so we define $maxExtension(X, c) = maxPartialEmbedding(R_{to}(X, c)) \cup \{(X, c)\}$ when X has height $h > 1$, and $maxExtension(X, c) = \{(X, c)\}$ otherwise.

The following lemma encodes the key step of the algorithm: to find a maximum partial block clique embedding with working rectangle R , we need only consider partial block clique embeddings that include an ell block (X, c) such that $R = R_{from}(X, c)$.

Lemma 1.3.1. *Given a rectangle R of height $i \geq 1$ and width $n - i$,*

$$\| \mathit{maxPartialEmbedding}(R) \| = \max_{(X,c) \in X_{to}(R)} | \mathit{maxExtension}(X,c) |.$$

Proof. We proceed by induction on i . When $i = 1$, our claim follows immediately from definitions. Assume that $i > 1$ and that our claim holds for all working rectangles of height $i - 1$.

We consider the complete set of partial block clique embeddings with working rectangle R , $S = \{ \mathcal{X}_i \mid R_{from}(X_i, c_i) = R \} = \{ \mathcal{X}_i \mid (X_i, c_i) \in X_{to}(R) \}$ where (X_i, c_i) is the ell block with height i in \mathcal{X}_i . By definition, $\| \mathit{maxPartialEmbedding}(R) \| = \max_{\mathcal{X}_i \in S} \| \mathcal{X}_i \|$. For contradiction, pick some maximum $\mathcal{X}_i \in S$ and suppose that

$$\| \mathcal{X}_i \| > \| \mathit{maxPartialEmbedding}(R_{to}(X, c)) \cup \{(X, c)\} \|$$

for all $(X, c) \in X_{to}(R)$. In particular, letting $\mathcal{X}_{i-1} = \mathcal{X}_i \setminus \{(X_i, c_i)\}$,

$$\begin{aligned} \| \mathcal{X}_i \| &= \| \mathcal{X}_{i-1} \| + \| \{(X_i, c_i)\} \| \\ &> \| \mathit{maxPartialEmbedding}(R_{to}(X_i, c_i)) \| + | \mathit{maxBundle}(X_i, c_i) |, \end{aligned}$$

a contradiction since \mathcal{X}_{i-1} has working rectangle $R_{to}(X_i, c_i)$. □

We now present the algorithm, wherein we compute $\mathit{maxPartialEmbedding}(R)$ for rectangles of increasing height, as indicated by Lemma 1.3.1. To do so we treat the set of possible working rectangles as a digraph, where $R \rightarrow R'$ if and only if there is an ell block (X, c) for which $R \in R_{from}(X, c)$ and $R' \in R_{to}(X, c)$. This means that if $R \rightarrow R'$, the height of R' is one more than the height of R . The number of edges in this digraph is equal to the number of ell blocks. To compute $\mathit{maxPartialEmbedding}(R')$, assuming that we have computed $\mathit{maxPartialEmbedding}(R)$ for all rectangles of lesser height, we simply set $\mathit{maxPartialEmbedding}(R')$ to be a maximum partial block clique embedding in the set

$$\{ \mathit{maxExtension}(X, c) \mid (X, c) \in X_{to}(R') \}.$$

Once we have computed $\mathit{maxPartialEmbedding}(R)$ for all rectangles R of height $n - 1$ and width 1, we pick a maximum-sized clique embedding from the set

$$\{ \mathit{maxExtension}(X, c) \mid (X, c) \text{ has height } n - 1 \text{ and width } 1 \}.$$

Pseudocode is given in Algorithm 1.

Theorem 1.3.2. *The NativeCliqueEmbed algorithm finds a maximum-sized native clique embedding with chain length $n + 1$ in polynomial time.*

Algorithm 1 The algorithm to find a maximum-sized native clique embedding in an induced subgraph of a Chimera graph.

```

1: function NATIVECLIQUEEMBED( $G, n$ )
2:   for  $i = 1, \dots, n - 1$  do
3:     for each rectangle  $R$  of height  $i$  and width  $n - i$  do
4:        $maxPartialEmbedding(R) \leftarrow \emptyset$ 
5:     for each ell block  $(X, c)$  of height  $i$  and width  $n - i + 1$  do
6:        $\mathcal{B} \leftarrow maxPartialEmbedding(R_{to}(X, c)) \cup \{(X, c)\}$ 
7:       if  $\|maxPartialEmbedding(R_{from}(X, c))\| < \|\mathcal{B}\|$  then
8:          $maxPartialEmbedding(R_{from}(X, c)) \leftarrow \mathcal{B}$ 
9:      $\mathcal{B}_{max} \leftarrow \emptyset$ 
10:    for each ell block  $(X, c)$  of height  $n$  and width 1 do
11:       $\mathcal{B} \leftarrow maxPartialEmbedding(R_{to}(X, c)) \cup \{(X, c)\}$ 
12:      if  $\|\mathcal{B}_{max}\| < \|\mathcal{B}\|$  then
13:         $\mathcal{B}_{max} \leftarrow \mathcal{B}$ 
14:    return  $\{maxBundle(X, c, G) \mid (X, c) \in \mathcal{B}_{max}\}$ 

```

Proof. We first prove correctness, then the bound on running time.

Note that the loop beginning on line 5 of Algorithm 1 iterates over all ell blocks of height i and width $n - i$. Given a rectangle R , there are up to four ell blocks (X, c) for which $R = X_{to}(X, c)$. If we ignore all ell blocks except those incident to a particular rectangle R , this loop implements Lemma 1.3.1 directly. Therefore, when we reach line 9, we have computed $maxPartialEmbedding(R)$ for all R with height $n - 1$ and width 1.

Let $\mathcal{B} = \{B_1, \dots, B_n\}$ be a maximum native clique embedding where B_i is an ell bundle in the ell block (X_i, c_i) with height i . By Theorem 1.2.1, deleting the final ell block to obtain $\mathcal{X}_{n-1} = \{(X_1, c_1), \dots, (X_{n-1}, c_{n-1})\}$ gives a partial block clique embedding with working rectangle $R_{to}(X_n, c_n)$. By Lemma 1.3.1,

$$\|maxPartialEmbedding(R_{to}(X_n, c_n))\| \geq \|\mathcal{X}_{n-1}\|,$$

so we see a clique embedding of size at least $\|\mathcal{X}_{n-1}\| + |maxBundle(X_n, c_n)|$ when line 11 is reached with $(X, c) = (X_n, c_n)$. Therefore, when line 14 is reached, $\|\mathcal{B}_{max}\| \geq \|\mathcal{B}\|$ and a native clique embedding of maximum size has been found.

We can compute $maxBundle(X, c, G)$ in $O(nL)$ time, and there are polynomially many ell blocks and rectangles: There are at most MN possible locations of a rectangle's lower-left corner, and n possible shapes, thus at most nMN rectangles. Likewise there are at most MN possible locations for an ell block's corner, and at most $4(n - 1)$ ell blocks containing n unit cells with a given corner, thus at most $4nMN$ ell blocks.

It follows that each line in Algorithm 1 is evaluated $O(nMN)$ times, and the pre-processing step of computing $maxBundle(X, c, G)$ for each ell block (X, c) naively takes $O(n^2MNL)$ time. Consequently, with the rough bound that each line in Algorithm 1 takes

$O(nL)$ time for a single evaluation, we can bound the total running time of our algorithm by $O(n^2MNL)$. \square

Remark. The $O(n^2MNL)$ -time bound on Algorithm 1 is quadratic in the number of vertices in $\mathcal{C}_{N,M,L}$, i.e. $O(n^2MNL) \subseteq O((MNL)^2)$. Assume $M \leq N$ and L is constant. With a little more care, we can modify Algorithm 1 to achieve a bound of $O(N^3)$ instead of $O(N^4)$. Doing this involves (a) pre-computing all maximum horizontal and vertical line bundles in time $O(LNM^2 + LMN^2)$ with a dynamic programming approach, which allows us to compute $|maxBundle(X, c, G)|$ in $O(1)$ time, and (b) exploiting the fact that throughout the algorithm, we need only keep track of the size of maximum partial embeddings and the route used to reach it (replacing $maxPartialEmbedding(R)$ with a mapping $R \mapsto (X, c) \in X_{to}(R)$), rather than the embeddings themselves.

NativeCliqueEmbed gives a maximum native clique embedding for a fixed chain length. To find a maximum native clique embedding over all chain lengths for a given graph, we simply repeat the process for each choice of $n \in \{2, \dots, \min\{M, N\}\}$. For $M \leq N$ and constant L , this gives an overall running time on a subgraph of $\mathcal{C}_{M,N,L}$ of $O(N^5)$ with the naive implementation and $O(N^4)$ with the refinement discussed above.

1.3.1 Induced and General Subgraphs

We now discuss the motivation of using induced subgraphs and how to approach more general subgraphs.

Recall that we have restricted our attention to induced subgraphs rather than more general subgraphs because failed couplers adjoining working qubits are relatively rare. In an induced subgraph, we will still focus on horizontal and vertical wires, and it is easy to find a maximum set of such wires in a line of unit cells.

A *maximum ell bundle* is a maximum-sized set of vertex-disjoint ells that occupy an ell block, and the *size* of an ell bundle is the number of ells contained therein. It is simple to find a maximum ell bundle in a given ell block: finding maximum sets S_H and S_V of horizontal and vertical wires spanning a line of cells is trivial, and these lines may be paired off arbitrarily since the corner is a complete bipartite graph. Here there may be difficulty in generalizing even this relatively simple optimization problem in the face of arbitrary edge deletion. Finding a maximum ell bundle in an arbitrary Chimera subgraph is polynomially equivalent to finding a maximum clique in $D_2(\mathcal{L}(B))$ where B is a bipartite graph, $\mathcal{L}(B)$ is the line graph of B , and $D_2(G)$ is the distance-2 graph with vertex set $V(G)$ and edge set $\{uv : d_G(u, v) = 2\}$. We are unsure of the complexity of this problem, but expect that it is NP-complete.

Note that we can easily relax the requirement of an induced subgraph when couplers between unit cells are defective – in any case, one just computes the number of wires in a

line of cells where all qubits and couplers are contained in the subgraph. In short, failed inter-cell couplers don't increase the difficulty of the problem.

If we restrict our attention to Chimera graphs $\mathcal{C}_{N,N,L}$ where $L = O(\log N)$, or assume L to be a constant, then this difficulty at the corners can be swept under the rug. At present, this appears to be a reasonable consideration, as it is much easier from a manufacturing and design standpoint to increase N than it is to increase L .

However, there is a further challenge introduced by intra-cell couplers. Our algorithm intrinsically relies upon the assumption that couplers exist between any two cells whose unit cells intersect. Missing intra-cell couplers void that assumption. The easiest remedy for this obstruction is to consider vertex covers of the failed intra-cell couplers: Given a graph G that is the subgraph of $\mathcal{C}_{M,N,L}$ induced by vertex set W , i.e. $G = \mathcal{C}_{M,N,L}[W]$, let U_1, \dots, U_s be the list of minimal vertex covers of the failed intra-cell couplers. Then, for each $1 \leq i \leq s$, compute a largest clique minor considering $G[W]$ for the purpose of constructing cells, and $G[W \setminus U_i]$ for the purpose of growing cliques. This approach gives a fixed-parameter tractable algorithm for finding the maximum native clique embedding in an arbitrary subgraph of Chimera in terms of the number of missing edges with both endpoints intact – for the D-Wave Two processors installed at NASA Ames [43] and ISI [1], this parameter was zero.

1.4 Comparison With Previous Work

Klymko, Sullivan and Humble gave a greedy embedding algorithm that quickly produces similar embeddings to those in this paper [31]. Their algorithm produces plus-shaped chains (having nearly twice as many qubits), and restricts its search to embeddings where the vertical and horizontal components of pluses are only allowed to meet at the diagonal of a fixed square. While our algorithm is slower, taking $O(N^4)$ time compared to their $O(N^3)$ for $\mathcal{C}_{N,N,4}$, it is exhaustive, empirically embeds larger cliques, and produces chains of roughly half the size.

Given a family of clique minors, the *clique yield* of a graph G over that family is the size of the largest clique minor in the family which are subgraphs of G . In Figure 1.4, we compare ell- and plus-shaped chains as the grid size grows for several fixed percentages of operational qubits. In both families, a similar asymptotic behavior becomes clear: for a fixed qubit failure rate, increasing the grid size gives diminishing returns in terms of clique yield. However, the difference between these curves is significant, with ell-shaped chains producing much larger clique minors.

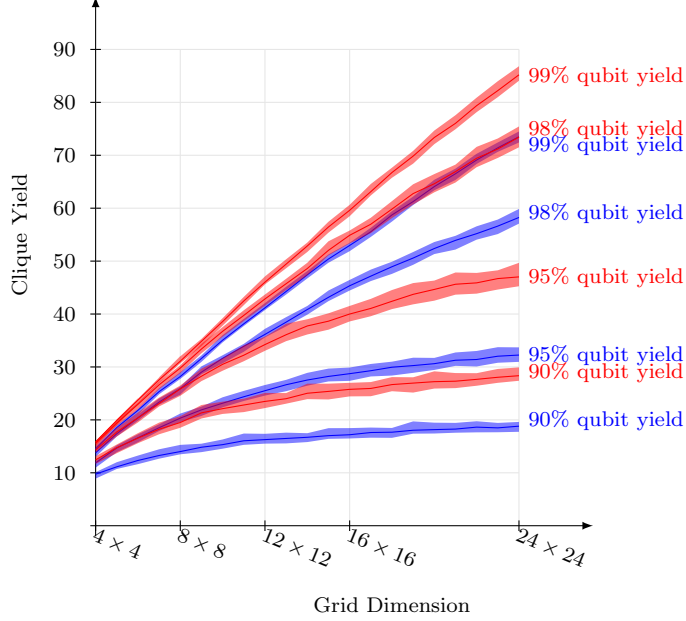


Figure 1.4: Comparison of clique yields for ell-shaped (red) and plus-shaped (blue) chains for various square grids with $L = 4$. The solid lines denote the median, and the shaded regions encompass the middle two quartiles.

1.5 Expected Clique Yield

In this section we consider the likelihood of a native clique embedding of a given size existing in an induced subgraph G' of $G = \mathcal{C}_{N,N,L}$. We assume a random model for G' in which each vertex of $\mathcal{C}_{N,N,L}$ is independently deleted with probability $1 - q$.

Theorem 1.5.1. *Define the clique yield $t_0 = t_0(N, L, q)$ as the largest value t for which we expect to see at least one native clique minor of size t in G' . For fixed $q < 1$ and fixed L , $t_0(N, L, q)$ is $O(\sqrt{\log N})$.*

Proof. Let X_t be the number of native clique minors of size at least t in G' . We bound t_0 by showing the expected value of X_t is less than 1 for sufficiently large t .

Let \mathbf{K}_w denote the set of native clique minors in G with ells of length $w + 1$. For a given clique minor $K \in \mathbf{K}_w$ and induced subgraph G' , let K' denote the largest subclique of K whose ells have no vertices deleted from G' . Let $|K'|$ be the number of vertices in K' . (In other words, $|K'|$ is the number of ells of K that survived in G' .) Then the expected number of induced native minors in which t or more ells survive deletion is

$$\begin{aligned}
 \mathbb{E}[X_t] &= \sum_{G' \subseteq G} q^{|G'|} (1 - q)^{|G \setminus G'|} \sum_{w=1}^N \sum_{K \in \mathbf{K}_w} \mathbf{1}_{|K'| \geq t} \\
 &= \sum_{w=1}^N \sum_{K \in \mathbf{K}_w} \mathbb{P}[|K'| \geq t],
 \end{aligned}$$

where $\mathbf{1}$ denotes the indicator function and $\mathbb{P}[|K'| \geq t] = \sum_{G' \subseteq G} q^{|G'|} (1-q)^{|G \setminus G'|} \mathbf{1}_{|K'| \geq t}$ is the probability that $|K'| \geq t$ by definition. As every qubit survives independently with probability q , every ell survives with probability q^{w+1} . Therefore every K' has the same binomial size distribution:

$$\mathbb{P}[|K'| = s] = \binom{Lw}{s} (q^{w+1})^s (1 - q^{w+1})^{Lw-s},$$

and $\mathbb{P}[|K'| \geq t] = \sum_{s=t}^{Lw} \mathbb{P}[|K'| = s]$. We have also shown that there are 4^{N-1} block clique embeddings in the $N \times N$ grid. Additionally, for each ell block, there are $L!$ different ell bundles of size L in that ell block. Therefore, the Chimera graph $\mathcal{C}_{N,N,L}$ has $|\mathbf{K}_w| = (N - w + 1)^2 (L!)^w 4^{w-1}$ clique minors with ells of length $w + 1$. Combining the above,

$$\begin{aligned} \mathbb{E}[X_t] &= \sum_{w=1}^N (N - w + 1)^2 (L!)^w 4^{w-1} \sum_{s=t}^{Lw} \binom{Lw}{s} (q^{w+1})^s (1 - q^{w+1})^{Lw-s} \\ &\leq N^2 \sum_{w=\lceil t/L \rceil}^N (L!)^w 4^{w-1} 2^{Lw} (q^{w+1})^t \\ &= \frac{1}{4} q^t N^2 \sum_{w=\lceil t/L \rceil}^N (cq^t)^w, \end{aligned}$$

where $c = 4L!2^L$. To upper bound t_0 , it is sufficient to find some t where $\mathbb{E}[X_t] < 1$. For large t we have $cq^t < 1/2$, and so the geometric sum is bounded:

$$\begin{aligned} \mathbb{E}[X_t] &\leq \frac{1}{4} q^t N^2 \sum_{w=\lceil t/L \rceil}^N (cq^t)^w \\ &\leq \frac{1}{2} q^t N^2 (cq^t)^{(t/L)}. \end{aligned}$$

The last expression is less than 1 if and only if

$$\log(1/2) + 2 \log(N) + t[\log(q) + \log(c)/L] + t^2 \log(q)/L < 0;$$

which implies that t is $O(\sqrt{\log N})$ for fixed q and L . \square

Chapter 2

Heffter Arrays Exist

This chapter is joint work with Dan Archdeacon and Jeff Dinitz, culminating a paper [4] which is a brief summary of this chapter, and a technical report [5] which is essentially [4] together with Section 2.7. Archdeacon gave the problem to the author, having resolved the question of $4n \times 4m$ Heffter Arrays with Dinitz (as well as a finite field construction which we did not need in the end), and met frequently with the author to discuss the constructions as the author found them. Unfortunately, Archdeacon died in early 2015, and Dinitz has been working diligently to tie up loose ends, including finalizing our paper for publication and providing editorial support for the author.

2.1 Introduction

2.1.1 A Brief History of Skolem Sequences

A Steiner triple system $STS(m)$ is a set of 3-element subsets, called *blocks*, of a set S such that every 2-element subset of S appears in exactly one of the blocks. In 1897, Lothar Heffter [26] reduced the problem of producing a Steiner triple system $STS(6n + 1)$ to the following problem, known as Heffter's first difference problem.

Problem 2.1.1. *Can a set $[1, 3n]$ be partitioned¹ into n ordered triples (a_i, b_i, c_i) , such that for each $1 \leq i \leq n$, either $a_i + b_i - c_i \equiv 0 \pmod{6n + 1}$ or $a_i + b_i + c_i \equiv 0 \pmod{6n + 1}$?*

Heffter's reduction was to take each triple $(a_i, b_i, a_i + b_i)$ and make a *base block* $(0, a_i, a_i + b_i)$. Then, for each $j \in [0, 6n]$, replicate a shift of the base block $(j, a_i + j, a_i + b_i + j)$, so that the Steiner triple system is

$$\{(j, a_i + j, a_i + b_i + j) : i \in [0, n], j \in [0, 6n]\},$$

¹We abuse notation a little here, as partitions are usually taken to be sets of sets. Our ordered triples, when unordered, form a partition. This shan't be mentioned again.

where each entry is reduced modulo $6n + 1$. For example, a solution to Heffter's problem for $n = 2$ is the pair of triples $\{(2, 5, 6), (1, 3, 4)\}$ corresponding to the base blocks $\{(0, 2, 7), (0, 1, 4)\}$ and Steiner triple system (half-columns are triples, separated by a line)

| | | | | | | | | | | | | |
|---|---|---|----|----|----|----|----|----|----|----|----|----|
| 0 | 1 | 2 | 3 | 4 | 5 | 6 | 7 | 8 | 9 | 10 | 11 | 12 |
| 2 | 3 | 4 | 5 | 6 | 7 | 8 | 9 | 10 | 11 | 12 | 0 | 1 |
| 7 | 8 | 9 | 10 | 11 | 12 | 0 | 1 | 2 | 3 | 4 | 5 | 6 |
| 0 | 1 | 2 | 3 | 4 | 5 | 6 | 7 | 8 | 9 | 10 | 11 | 12 |
| 1 | 2 | 3 | 4 | 5 | 6 | 7 | 8 | 9 | 10 | 11 | 12 | 0 |
| 4 | 5 | 6 | 7 | 8 | 9 | 10 | 11 | 12 | 0 | 1 | 2 | 3 |

Heffter posed a second difference problem yielding a construction of $STS(6n + 3)$, which is less relevant to us.

Rose Peltesohn [36] first solved Heffter's difference problems in 1939, with six explicit solutions for the various cases modulo 18. Independently, Thøger Bang [7] posed a problem to Thoralf Skolem, similar to Heffter's first difference problem,

Problem 2.1.2. *Can a set $[1, 2n]$ be partitioned into n ordered pairs (a_i, b_i) , such that $b_i - a_i = i$ for every $1 \leq i \leq n$?*

Bang's motivation was to find sufficient and necessary conditions on irrational α and β for which the sets $\mathbb{N}\alpha$ and $\mathbb{N}\beta$ form a partition of the natural numbers. Thoralf Skolem [41] found the sufficient and necessary conditions for Bang's difference problem in 1957; that $n \equiv 0, 3 \pmod{4}$. Skolem demonstrated sufficiency with two families of what are now known as *Skolem sequences*, and necessity with the simple observation (due to Bang) that

$$\frac{n(n+1)}{2} = \sum_{i=1}^n i = \sum_{i=1}^n (b_i - a_i) \equiv \sum_{i=1}^n (b_i + a_i) = \sum_{j=1}^{2n} j = \frac{(2n)(2n+1)}{2} \pmod{2}.$$

Since then, Skolem sequences have been well-studied, with many generalizations. One common generalization is that of a d -near Skolem sequence: partitions of the set $[1, 2n - 2]$ into $n - 1$ ordered pairs (a_i, b_i) , such that $b_i - a_i = i$ for every $1 \leq i \leq n$ except $i = d$? We further generalize near Skolem sequences in Section 2.5.

Skolem and Peltesohn both constructed what are now known as *starters*: partitions of the nonzero elements of a group G of odd order into pairs $\{s_i, t_i\}$ for $1 \leq i \leq \frac{|G|-1}{2}$ such that $\{\pm(t_i - s_i) : 1 \leq i \leq (|G| - 1)/2\} = G \setminus \{0\}$ (to obtain a starter in \mathbb{Z}_{2n+1} from a Skolem sequence, for example, create the set of pairs $\{\{b_i, -a_i\} : 1 \leq i \leq n\} \cup \{\{a_i, -b_i\} : 1 \leq i \leq n\}$). Dinitz [22] has a good summary of the literature on starters. We use a slight generalization of starters, allowing the collection of differences to be an arbitrary multiset D , and the pairs to partition an arbitrary set S . We call such an object a *partition of S into differences D* .

2.1.2 Heffter Systems and Heffter Arrays

We generalize Heffter's problem to the following.

Problem 2.1.3. *Partition the interval $[1, nm]$ into n m -tuples $\{x_1^{(i)}, \dots, x_m^{(i)}\}$ and find an assignment of signs $\sigma : [1, mn] \rightarrow \{-1, 1\}$ satisfying*

$$\sum_{j=1}^m \sigma(x_j^{(i)})x_j^{(i)} \equiv 0 \pmod{2nm+1}$$

for all $1 \leq i \leq n$.

We will call a solution to this problem, $\{\{\sigma(x_1^{(i)})x_1^{(i)}, \dots, \sigma(x_m^{(i)})x_m^{(i)}\} : i \in [1, n]\}$, a *Heffter system* S , and an element $s \in S$ a *m -set*. We will refer to Heffter systems consisting of 3-sets as *Heffter triple systems* and those of 5-sets as *Heffter quintuple systems*, or in general, *Heffter m -tuple systems*. We often refer to both ends of the interval $[1, mn]$, and we use m and n to denote quantities other than the array dimensions. To that end, we will use the variable \mathfrak{D} to denote the product of the matrix dimensions.

We say that two Heffter systems S and T are *orthogonal* when

- $\bigcup_{s \in S} s = \bigcup_{t \in T} t$ (that is, the elements of $[1, \mathfrak{D}]$ have the same sign in both systems), and
- $|s \cap t| = 1$ for all $s \in S$ and all $t \in T$.

Definition 2.1.4. An $m \times n$ matrix $H = (h_{ij})$ with integer entries is a *Heffter array* if

1. $\{|h_{ij}| : 1 \leq i \leq n, 1 \leq j \leq m\} = [1, \mathfrak{D}]$,
2. $R_i = \sum_{j=1}^m h_{ij} \equiv 0 \pmod{2\mathfrak{D}+1}$ for $1 \leq i \leq n$, and
3. $C_j = \sum_{i=1}^n h_{ij} \equiv 0 \pmod{2\mathfrak{D}+1}$ for $1 \leq j \leq m$.

An orthogonal pair of Heffter systems is equivalent to a Heffter array: given an orthogonal pair, label the sets $S = \{s_1, \dots, s_n\}$ and $T = \{t_1, \dots, t_m\}$ and set h_{ij} to be the unique element in $s_i \cap t_j$; conversely, the rows and columns of a Heffter array form an orthogonal pair.

We note that m and n must be greater than 2, since $|h_{11}| \neq |h_{12}|$ and $|h_{11}| + |h_{12}| < 2\mathfrak{D}$, and we will show that this is the only obstruction to the existence of Heffter arrays. If the rows and columns all sum to precisely the integer 0, then we say H is an *integer Heffter array*. Naturally, every integer Heffter array is a Heffter array. Note that for an integer Heffter array,

$$0 = \sum_{j=1}^n R_j = \sum_{i=1}^n \sum_{j=1}^m h_{ij} \equiv \binom{mn+1}{2} \pmod{2}$$

so either mn or $mn+1$ is divisible by 4 – thus $mn \equiv 0, 3 \pmod{4}$.

2.1.3 Main Theorem

In the sections to come, we present a complete solution to the existence problem for Heffter arrays and integer Heffter arrays. Before the author was introduced to the problem, Archdeacon and Dinitz had described the construction for $4m \times 4n$ Heffter arrays presented in Section 2.3 as well as a finite field construction for $m \times n$ Heffter arrays when $2mn + 1$ is prime.

Theorem 2.1.5. *For $m, n \in \mathbb{N}$, there exists a $m \times n$ Heffter array if and only if $m > 2$ and $n > 2$; and there exists a $m \times n$ integer Heffter array if and only if $m > 2$, $n > 2$, and $mn \equiv 0, 3 \pmod{4}$.*

But first, we will discuss an application of Heffter arrays to topological graph theory.

2.1.4 Motivation

If $m > 2$ and $n > 2$ are not both even, Archdeacon [2] describes a way to use a Heffter array to embed the complete graph K_{2mn+1} into an orientable (possibly pinched) surface so that

- all faces are either m -cycles or n -cycles,
- all m -faces are surrounded by n -faces, and
- all n -faces are surrounded by m -faces.

Such an embedding is called a *biembedding*. The reason that one would require an odd dimension is that the construction calls on a 1-face embedding of the complete bipartite graph $K_{m,n}$, which exists [45] if and only if at least one of m, n is odd. The other necessary ingredients used to produce Archdeacon's embeddings are cyclic orderings of each row and each column. We will briefly look at two properties of these orderings.

Given a cyclic ordering (t_1, t_2, \dots, t_m) of an m -set in an additive group, we define the *partial sum* $s_j = \sum_{i=1}^j t_i$, and say that the ordering is *simple* if every partial sum is distinct, $s_i \neq s_j$ for all $1 \leq i < j \leq m$. A Heffter system is *simple* if every part has a simple ordering. Further, a Heffter array is *simple* if both the row and column Heffter systems are simple. In the case that the row and column orderings are both simple, then every face of the biembedding is a cycle of K_{2mn+1} (that is, every vertex incident to a face is incident to precisely two edges bounding that face). We suspect that it is always possible to find simple orderings of our Heffter arrays; this is the subject of a conjecture of Alspach which we will discuss shortly.

Viewing the cyclic orderings ω_r and ω_c as permutations of the entries of a Heffter array, we say that ω_r and ω_c are *compatible* if $\omega_r \circ \omega_c$ is a cyclic permutation. If the orderings are both simple, then the biembedding is simple. If the orderings are compatible, there are no

pinch points, and the surface is a torus of genus

$$1 + \frac{1}{2} \binom{mn}{2} \left(\frac{1}{mn} - \frac{1}{m} - \frac{1}{n} + 1 \right)$$

Theorem 2.3 of [21] says that if at least one of m and n is odd, there exists a pair of compatible orderings, ω_r and ω_c .

Dinitz and Mattern [21] found simple, compatible orderings of $3 \times n$ Heffter arrays for all $n > 2$, using Heffter arrays constructed by the author which differ slightly from those in this thesis. Their methods do not work for our constructions for $5 \times n$ arrays for arbitrary n , though they did succeed for all $3 \leq n \leq 100$. Our collective experience suggests that it is relatively easy to find simple orderings for specific Heffter arrays, but generic constructions are more elusive. In Section 2.8, we describe a different approach to constructing $5 \times n$ Heffter arrays for which the reordering problem may be easier.

Rather than find explicit reorderings, it may be more worthwhile to attack the problem from the combinatorial number theoretical side. Archdeacon, Dinitz, Mattern and Stinson [3] conjecture:

Conjecture 2.1.6. *Every $A \subseteq \mathbb{Z}_n \setminus \{0\}$ has a simple ordering, i.e., A can be ordered so that all partial sums are distinct.*

Some progress has been made on this problem: Archdeacon *et al.* have computationally verified the conjecture for $n \leq 25$, have proved that it holds when $|A| \leq 6$, along with other useful-looking results. The author has computationally verified this conjecture for $n \leq 31$ with a simple recursive strategy, adding one element to the ordering at a time, provided it doesn't duplicate a previously-seen partial sum. Bode and Harborth [8] have shown it is true for $|A| = n - 1$, using the ordering

$$1, n - 2, 3, n - 4, \dots, 4, n - 3, 2, n - 1$$

of $\mathbb{Z}_n \setminus \{0\}$ for all n . Also, they find simple orderings for $|A| = n - 2$ if $n \equiv 1 \pmod{2}$ by taking a cyclic rotation of the above and removing the chosen element, and for $n \equiv 0 \pmod{2}$ with a significantly more complex construction.

To produce simple orderings of Heffter arrays, the following weaker conjecture is sufficient.

Conjecture 2.1.7. *Let n be an odd integer. Every $A \subseteq \mathbb{Z}_n$ with $\{-a : a \in A\} \cap A = \emptyset$ has a simple ordering.*

Among the computational experiments we have performed, we have computed the number of simple orderings for every subset $A \subset \mathbb{Z}_n \setminus \{0\}$ for $1 \leq n \leq 14$, and we make the following bold conjecture.

| $k \setminus \ell$ | 0 | 1 | | 2 | 3 | |
|--------------------|-------|--|--|-------|--|--|
| 0 | § 2.3 | 5×4 5×(8n+8) 5×(8n+12) (4m+9)×(4n+4) | § 2.4 § 2.7.2.2 § 2.7.2.6 § 2.7.3.6 | § 2.3 | 3×4 3×(8n+8) 3×(8n+12) (4m+7)×(4n+4) | § 2.4 § 2.7.1.2 § 2.7.1.6 § 2.7.3.7 |
| 1 | | 5×5 5×(8n+9) 5×(8n+13) (4m+9)×(4n+9) | § 2.4 § 2.7.2.3 § 2.7.2.7 § 2.7.3.4 | | | |
| 2 | | 5×6 5×(8n+10) 5×(8n+14) (4m+9)×(4n+6) | § 2.4 § 2.7.2.4 § 2.7.2.8 § 2.7.3.1 | § 2.3 | 3×6 3×(8n+10) 3×(8n+14) (4m+7)×(4n+6) | § 2.4 § 2.7.1.4 § 2.7.1.8 § 2.7.3.2 |
| 3 | | 5×3 5×(8n+7) 5×(8n+11) (8n+9)×3 (8n+13)×3 (4m+9)×(4n+7) | § 2.4 § 2.7.2.1 § 2.7.2.5 § 2.7.1.3 § 2.7.1.7 § 2.7.3.5 | | 3×3 3×(8n+7) 3×(8n+11) (4m+7)×(4n+7) | § 2.4 § 2.7.1.1 § 2.7.1.5 § 2.7.3.3 |

Table 2.1: Case outline for constructions of $(4m + k) \times (4n + \ell)$ Heffter arrays. Blank cells are covered by symmetry.

Conjecture 2.1.8. *If $A \subset \mathbb{Z}_n \setminus \{0\}$, then are at least $2^{|A|-1}$ simple orderings of A .*

The problem of producing a pair of simple orderings which are compatible still seems difficult, even armed with Dinitz and Mattern’s compatibility theorem and assuming Conjecture 2.1.6.

The next section gives a rough outline of the rest of this chapter.

2.1.5 Outline

Our presentation of our results is somewhat nonstandard. Our proof of Theorem 2.1.5 consists of 24 constructions, together with seven small Heffter arrays which are not covered by the constructions. Three of the constructions are very simple, and we will prove their viability in little more space than it takes to define them. The remaining cases are vastly more complicated. To check examples, we implemented the constructions in easy-to-read Python. Daunted by proving correctness of so many constructions, we automated the process. Initially, the thought was to produce a small “certificate” that could be verified, and included alongside the construction. The process of discovery and proof is outlined below.

- Code generates individual Skolem-like sequences.

- Code attempts to generalize an individual Skolem-like sequence, to produce a family of Skolem-like sequences. On success, output code that, given m , produces a Skolem-like sequence of order $2m + k$.
- Use code output by the previous step to automatically generate 16 families of Heffter arrays. Output code that, given m , produces a $3 \times (8m + k)$ or $5 \times (8m + k)$ Heffter array.
- Using the output by the previous step, use m as a symbolic variable to produce a single “sporadic tile” and a single “variable tile”.
- Repurpose the code of the other 5 constructions to produce a single sporadic tile and one or two variable tiles, along with the parameters passed into them.
- Code analyzes the tiles produced above, which computes row and column sums of the tiles, and the support of the tiles, and then prints out L^AT_EX code for a proof that the construction in question produces a Heffter array.

At this point, the reader is encouraged to skip ahead a few pages, to Section 2.7 and read the computer-written proof of one of the constructions found there. The proofs themselves are very easy to read and verify, if a bit tedious. Due to the readability of the proofs, we have a very high level of confidence in our results. However, discovering the constructions involved significant insight and effort, which are obscured rather than exposed by the proofs.

In the sections between here and Section 2.7, we will describe how we found our constructions. By walking the reader through the discovery process, we are able to showcase the more interesting features of the constructions. We do so at a rather high level, and do our best to avoid an indecent amount of detail. After all, the reader with an appetite for detail is cordially invited to gorge themselves on Section 2.7.

2.2 High-Level Description of the Constructions

The proof of our theorem is broken into several cases. At the coarsest scale, we consider the residue classes of m and n modulo 4. When both m and n are even, our job is fairly simple. The cases of $m = 3$ and $m = 5$ require particular attention, where we refine to residue classes of n modulo 8. After clearing those hurdles, we produce constructions of Heffter arrays for $m, n \geq 7$ for congruence classes containing at least one odd dimension. These constructions leave a few small holes, which are shown in Table 2.2. A summary of the cases involved can be found in Table 2.1.

But first, we’ll emphasize the key ingredient behind all of our constructions with a moment of levity².

²The following section has been preserved under objection of a minority of the examination committee.

2.2.1 The Only Good Idea Here: A Dramatic Interlude

Let's say some deranged entity points a loaded weapon at your head, and demands you to find an assignment of signs to the sequence

$$[x \ x + \alpha \ y \ y + \alpha]$$

so that it sums to zero, regardless of the values in the variables. Panic! How did you even get to this point in life? You blank. All that you can think of is the PIN number that you punch into ATM machines,

$$[1 \ 2 \ 3 \ 4]$$

and lucky you, that sequence has just the right form, and you quickly realize that there's only one way to do it,

$$[1 \ -2 \ -3 \ 4]$$

(and you're wrong about that, because the opposite sequence works just fine), and fortunately for you, your single example (really, you should change your PIN, and stop calling it a PIN number) generalizes perfectly! But you were too slow! The deranged entity screams "CLICK!" Apparently, its finger-pistol is out of ammo. You survive to read another thesis. Barely.

Using overlines to denote negation,

$$[x \ \overline{x + \alpha} \ \bar{y} \ y + \alpha]$$

sums to zero. This peculiar style of exposition was chosen to highlight [38] the crucial importance of this sign sequence. It will appear so many times in our constructions, some might call it "unreasonably effective," except that we understand the reasons quite well.

We'll abuse notation a little here, and refer to Heffter systems with polynomial entries, to show how we can "grow" Heffter systems. Given a Heffter m -system $T = \{T_0, \dots, T_{n-1}\}$ whose entries' absolute values partition $[1, \alpha] \cup [z - \beta, z] \subset \mathbb{Z}[z]$ and whose parts sum to zero in $\mathbb{Z}[z]/(2z + 1)$, we can construct a Heffter $(m + 4)$ -system $T' = \{T'_0, \dots, T'_{n-1}\}$ with

$$T'_i = T_i \cup \{\alpha + 4i + 1, \overline{\alpha + 4i + 2}, \overline{\alpha + 4i + 3}, \alpha + 4i + 4\}$$

for each $0 \leq i < n$. For example, the Heffter triple system (3-sets written as rows)

$$\begin{array}{ccc} 6 & 9 & 4 \\ 8 & \bar{7} & \bar{1} \\ 5 & \bar{2} & \bar{3} \end{array}$$

generalizes to a polynomial Heffter triple system with parameters $\alpha = 5$ and $\beta = 3$.

$$\begin{array}{ccc} z-3 & z & 4 \\ z-1 & \overline{z-2} & \overline{1} \\ 5 & \overline{2} & \overline{3} \end{array}$$

from which we can easily construct a polynomial Heffter septuple system,

$$\begin{array}{ccccccc} z-3 & z & 4 & 6 & \overline{7} & \overline{8} & 9 \\ z-1 & \overline{z-2} & \overline{1} & 10 & \overline{11} & \overline{12} & 13 \\ 5 & \overline{2} & \overline{3} & 14 & \overline{15} & \overline{16} & 17 \end{array}$$

and then specialize to a proper Heffter septuple system by assigning $z = 3 \cdot 7$,

$$\begin{array}{ccccccc} 18 & 21 & 4 & 6 & \overline{7} & \overline{8} & 9 \\ 20 & \overline{19} & \overline{1} & 10 & \overline{11} & \overline{12} & 13 \\ 5 & \overline{2} & \overline{3} & 14 & \overline{15} & \overline{16} & 17. \end{array}$$

In the following section, we show that the outer product of this sign sequence with itself leads us to a 4×4 Heffter array, which we will use to fill out almost all of the area of almost every Heffter array. In fact, that idea can be used to produce a multidimensional $4m_1 \times 4m_2 \times \cdots \times 4m_k$ integer Heffter array, but the investigation of such things is well outside of the scope of this thesis.

The sign sequence $+- -+$ also plays a role in constructing 3×8 and 5×8 tiles, though in those cases, not everything cancels out quite so easily and we concatenate its negative to obtain $+- -+ -+ +- -$. Later, we will construct 7×4 and 9×4 tiles whose topmost row is a signed increasing sequence $(x+1, \overline{x+2}, \overline{x+3}, x+4)$, which lend to an “ell” construction (filling the top- and left-most columns with these tiles).

2.3 Both Dimensions Even

First, we’ll show how certain even-dimensional arrays can be used to cover a different interval than they were discovered with. A matrix A can be *shifted by* x to obtain a matrix $A+x = (a_{ij} + x \operatorname{sgn}(a_{ij}))$. A Heffter array is *shiftable* if shifting by x preserves row and column sums. It is clear that a Heffter array is shiftable if and only if the number of negative entries is equal to the number of positive entries in each row and column, and therefore, the only shiftable arrays have both dimensions even. In this section, we will show that shiftable Heffter arrays exist for all even $m, n > 2$.

As we mentioned in the previous section, the sign sequence $+ - - +$ can be used to produce a 4×4 array directly,

$$H_{4 \times 4} = \begin{bmatrix} 1 & \bar{2} & \bar{3} & 4 \\ \bar{5} & 6 & 7 & \bar{8} \\ \bar{9} & 10 & 11 & \bar{12} \\ 13 & \bar{14} & \bar{15} & 16 \end{bmatrix}.$$

Note that this is in fact an integer Heffter array and each row and column has an equal number of pluses as minuses, hence we can shift the matrix by z

$$H_{4 \times 4} + z = \begin{bmatrix} z+1 & \overline{z+2} & \overline{z+3} & z+4 \\ \overline{z+5} & z+6 & z+7 & \overline{z+8} \\ \overline{z+9} & z+10 & z+11 & \overline{z+12} \\ z+13 & \overline{z+14} & \overline{z+15} & z+16 \end{bmatrix}$$

without changing its row and column sums – we call this a 4×4 tile. Thus, we can make $4n \times 4$ Heffter arrays by repeating these tiles in a line,

$$\left[H_{4 \times 4} \mid \cdots \mid H_{4 \times 4} + 16i \mid \cdots \mid H_{4 \times 4} + 16(n-1) \right]$$

and repeat such lines shifted to make $4n \times 4m$ integer Heffter arrays.

Next up,

$$H_{4 \times 6} = \begin{bmatrix} 1 & \bar{2} & 3 & \bar{4} & 11 & \bar{9} \\ \bar{7} & 8 & \bar{12} & 10 & \bar{5} & 6 \\ \bar{13} & 14 & \bar{18} & 16 & \bar{23} & 24 \\ 19 & \bar{20} & 21 & \bar{22} & 17 & \bar{15} \end{bmatrix}$$

is a shiftable 4×6 integer Heffter array, which can be used to construct shiftable $4n \times 6$ Heffter arrays, similar to the above. By stacking a $6 \times 4n$ array atop a shifted $4(m-1) \times 4n$ array, we can construct $4n \times (4m+2)$ integer Heffter arrays for all n and m feasible.

Finally, the 6×6 Heffter array

$$H_{6 \times 6} = \begin{bmatrix} 10 & 35 & 24 & \bar{13} & \bar{27} & \bar{29} \\ 7 & 26 & 9 & \bar{32} & \bar{8} & \bar{2} \\ 11 & 34 & \bar{17} & 16 & \bar{14} & \bar{30} \\ \bar{19} & \bar{36} & 21 & \bar{1} & 15 & 20 \\ \bar{6} & \bar{31} & \bar{33} & 25 & 22 & 23 \\ \bar{3} & \bar{28} & \bar{4} & 5 & 12 & 18 \end{bmatrix}$$

is shiftable, and we can construct $(4n + 2) \times (4m + 2)$ arrays with the construction

$$\left[\begin{array}{c|c} H_{6 \times 6} & H_{6 \times 4} + 36 \mid \cdots \mid H_{6 \times 4} + 36 + 24(m - 1) \\ \hline H_{4 \times 6} + 36 + 24m & \\ \hline \vdots & \\ \hline H_{4 \times 6} + 36 + 24(m + n - 1) & E + 36 + 24(m + n) \end{array} \right]$$

where E is a shiftable $4(n - 1) \times 4(m - 1)$ Heffter array.

This concludes the story for matrices with both dimensions even. The remaining cases are handled similarly: we will find constructions of ‘ribbons’ of odd height, some of which may be bent into ell shapes. These ribbons and ells will be placed along the border of an array, leaving an even-dimensioned hole which we fill with a certain shift of a shiftable Heffter array.

2.4 Some Small Heffter Arrays

We succeeded in finding constructions of large arrays which have small base cases. In this section, we have a very small number of Heffter arrays for those dimensions that are not covered by our constructions. These arrays were found with computer assistance, and shown in Table 2.2.

| | |
|---|---|
| $(3 \times 3) \quad \begin{bmatrix} 6 & 8 & 5 \\ 9 & \bar{7} & \bar{2} \\ 4 & \bar{1} & \bar{3} \end{bmatrix}$ | $(4 \times 5) \quad \begin{bmatrix} 7 & \bar{12} & \bar{2} & 6 & 1 \\ \bar{16} & 15 & 9 & 5 & \bar{13} \\ \bar{10} & 17 & \bar{18} & 3 & 8 \\ 19 & \bar{20} & 11 & \bar{14} & 4 \end{bmatrix}$ |
| $(3 \times 4) \quad \begin{bmatrix} 1 & \bar{6} & 2 & 3 \\ 8 & 11 & \bar{12} & \bar{7} \\ \bar{9} & \bar{5} & 10 & 4 \end{bmatrix}$ | $(5 \times 5) \quad \begin{bmatrix} 8 & 17 & \bar{22} & \bar{10} & 7 \\ 18 & 5 & 19 & \bar{15} & 24 \\ 4 & 20 & \bar{25} & 13 & \bar{12} \\ \bar{16} & 3 & \bar{21} & 11 & 23 \\ \bar{14} & 6 & \bar{2} & 1 & 9 \end{bmatrix}$ |
| $(3 \times 5) \quad \begin{bmatrix} 8 & \bar{12} & 10 & \bar{13} & 7 \\ 3 & 14 & \bar{15} & 4 & \bar{6} \\ \bar{11} & \bar{2} & 5 & 9 & \bar{1} \end{bmatrix}$ | $(5 \times 6) \quad \begin{bmatrix} 20 & \bar{21} & 5 & 27 & 26 & 4 \\ \bar{24} & 22 & \bar{14} & 11 & \bar{10} & 15 \\ 6 & \bar{7} & \bar{23} & \bar{1} & 9 & 16 \\ 30 & 8 & 19 & \bar{12} & \bar{28} & \bar{17} \\ 29 & \bar{2} & 13 & \bar{25} & 3 & \bar{18} \end{bmatrix}$ |
| $(3 \times 6) \quad \begin{bmatrix} 2 & 16 & 14 & 3 & 13 & \bar{11} \\ 17 & \bar{10} & \bar{15} & 9 & \bar{5} & 4 \\ 18 & \bar{6} & 1 & \bar{12} & \bar{8} & 7 \end{bmatrix}$ | |

Table 2.2: Small Heffter arrays

Later, we will see that portions of some of these arrays can be shifted, so that they can be used to construct larger arrays, often with different moduli. The arrays that result from this partial shifting will be called *seeds*, and can be found in Table 2.3.

2.5 Short Heffter Arrays of Odd Height

In this section we discuss the construction of Heffter arrays with 3 or 5 rows. These constructions depend entirely upon a generalization of Skolem sequences. Given a set K of integers, a K -near Skolem sequence of order n is a sequence $S = x_1, x_2, \dots, x_{2(n-|K|)}$ of integers satisfying

1. every number $1 \leq j \leq n$, $j \notin K$ appears exactly twice, and
2. for all $j \notin K$, $r(j) - \ell(j) = j$, where $x_{r(j)} = x_{\ell(j)} = j$ and $r(j) > \ell(j)$.

An example of a $\{1, 4\}$ -near Skolem sequence of order 7 is 6375326257, corresponding to the pairs $\{(1, 7), (2, 5), (3, 10), (4, 9), (6, 8)\}$ which is a partition of $[1, 10]$ into the differences $\{2, 3, 5, 6, 7\}$.

2.5.1 Constructing Heffter Systems From Near Skolem Sequences

In this section, we will find four small Heffter systems; two triple systems, and two quintuple systems, with two purposes. The first is to provide motivation for finding K -near Skolem sequences for each $K \subseteq \{1, 2\}$, and the second is to show how such sequences will be used to construct Heffter systems in general. We only bother with finding Heffter systems here, and not Heffter arrays, because it's clearer to see what we're up to. The particular cases we need to solve allow us to start simple, and add one complication at a time.

Constructions for K -near Skolem sequences are discussed in detail in Appendix A. Statements made in this section about the existence and nonexistence of certain orders of K -near Skolem sequences are supported in that appendix.

First up, we construct a Heffter triple system with n triples from a Skolem sequence of order N . These exist when $N \equiv 0, 1 \pmod{4}$. For example, we use the sequence 497841156798536232 to partition $[10, 27]$ and obtain 3-sets $\{d, a_d, \bar{b}_d\}$ for $d \in [1, 9]$,

$$\begin{array}{cccccccccc} 1 & 2 & 3 & 4 & 5 & 6 & 7 & 8 & 9 & \\ 15 & 25 & 23 & 10 & 17 & 18 & 12 & 13 & 11 & \\ \bar{16} & \bar{27} & \bar{26} & \bar{14} & \bar{22} & \bar{24} & \bar{19} & \bar{21} & \bar{20} & \end{array}$$

These are used to produce Heffter arrays of dimension $3 \times 4n$ in Sections 2.7.1.2 and 2.7.1.6, and of dimension $3 \times (4n + 1)$ in Sections 2.7.1.3 and 2.7.1.7. The $3 \times 4n$ arrays we construct are integer Heffter arrays, so can be stacked atop shifttable $4m \times 4n$ arrays, but we'll need

something else for the $(4m+3) \times (4n+1)$ case, which we describe at a high level in Section 2.6 and in more detail in Section 2.7.3.5.

Next, we construct a Heffter triple system with N triples from a $\{2\}$ -near Skolem sequence of order N . These exist when $N \equiv 2, 3 \pmod{4}$. For example, we use the sequence 746354376511 to partition $[8, 19]$ and obtain 3-sets $\{d, a_d, \overline{b_d}\}$ for $d \in [1, 7] \setminus 2$, together with one extra triple shown in boldface, $(2, 3n, 3n - 1)$ whose sum is $6n + 1$,

| | | | | | | |
|-----------------|-----------|-----------------|-----------------|-----------------|-----------------|-------------------|
| 1 | 2 | 3 | 4 | 5 | 6 | 7 |
| 18 | 20 | 11 | 9 | 22 | 10 | 8 |
| $\overline{19}$ | 21 | $\overline{14}$ | $\overline{13}$ | $\overline{27}$ | $\overline{16}$ | $\overline{15}$. |

These are used to produce Heffter arrays of dimension $3 \times (4n + 2)$ in Sections 2.7.1.4 and 2.7.1.8, and of dimension $3 \times (4n + 3)$ in Sections 2.7.1.1 and 2.7.1.5. The $3 \times (4n + 2)$ arrays cannot be integer Heffter arrays, so we'll need something else for the $(4m + 3) \times (4n + 2)$ and $(4m + 3) \times (4n + 3)$ cases, which we describe at a high level in Section 2.6 and in more detail in Section 2.7.3.2 and Section 2.7.3.3, respectively.

Next, we construct a Heffter quintuple system with N quintuples from a $\{1\}$ -near Skolem sequence of order $N + 1$. These exist when $N \equiv 0, 3 \pmod{4}$. For example, we use the sequence 68347364582725 to partition $[8, 21]$ into differences $[2, 8]$. To make 5-sets, we associate the pair (a_d, b_d) with the difference $d - 1$, and then patch things up with pairs $(\overline{x}, x + 1)$ covering $[22, 35]$ to bring the sum back to zero:

| | | | | | | |
|-----------------|-----------------|-----------------|-----------------|-----------------|-----------------|-----------------|
| 1 | 2 | 3 | 4 | 5 | 6 | 7 |
| 18 | 10 | 11 | 16 | 8 | 12 | 9 |
| $\overline{20}$ | $\overline{13}$ | $\overline{15}$ | $\overline{21}$ | $\overline{14}$ | $\overline{19}$ | $\overline{17}$ |
| $\overline{22}$ | $\overline{24}$ | $\overline{26}$ | $\overline{28}$ | $\overline{30}$ | $\overline{32}$ | $\overline{34}$ |
| 23 | 25 | 27 | 29 | 31 | 33 | 35. |

These are used to produce Heffter arrays of dimension $5 \times 4n$ in Sections 2.7.2.2 and 2.7.2.6, and of dimension $5 \times (4n + 3)$ in Sections 2.7.2.1 and 2.7.2.5. The $5 \times 4n$ arrays we construct are integer Heffter arrays, so can be stacked atop shifttable $4m \times 4n$ arrays, but we'll need something else for the $(4m+1) \times (4n+3)$ case, which we describe at a high level in Section 2.6 and in more detail in Section 2.7.3.5.

Finally, we construct a Heffter quintuple system with N quintuples from a $\{1, 2\}$ -near Skolem sequence of order $N + 1$. These exist when $N \equiv 1, 2 \pmod{4}$. For example, we use the sequence 5673453647 to partition $[7, 28]$ into differences $[3, 7]$. We make 5-sets as above, together with one extra quintuple shown in boldface, $(1, \overline{5N - 3}, 5N - 2, 5N - 1, 5N)$ whose

sum is $10N + 1$,

| | | | | | |
|-----------------------------------|-----------------|-----------------|-----------------|-----------------|-----------------|
| 1 | 2 | 3 | 4 | 5 | 6 |
| $\overline{27}$ | 10 | 11 | 7 | 8 | 9 |
| 28 | $\overline{13}$ | $\overline{15}$ | $\overline{12}$ | $\overline{14}$ | $\overline{16}$ |
| 29 | $\overline{17}$ | $\overline{19}$ | $\overline{21}$ | $\overline{23}$ | $\overline{25}$ |
| 30 | 18 | 20 | 22 | 24 | 26. |

These are used to produce Heffter arrays of dimension $5 \times (4n + 1)$ in Sections 2.7.2.3 and 2.7.2.7, and of dimension $5 \times (4n + 2)$ in Sections 2.7.2.4 and 2.7.2.8. The $5 \times (4n + 2)$ arrays cannot be integer Heffter arrays, so we'll need something else for the $(4m + 1) \times (4n + 2)$ and $(4m + 1) \times (4n + 1)$ cases, which we describe at a high level in Section 2.6 and in more detail in Section 2.7.3.1 and Section 2.7.3.4, respectively.

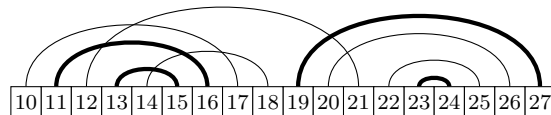
At this point, we have demonstrated the existence of Heffter triple systems and Heffter quintuple systems in all groups \mathbb{Z}_{6n+1} and \mathbb{Z}_{10n+1} , respectively, though we haven't really slogged through all the details. Together with the method of "growing" Heffter systems presented in Section 2.2.1, we can prove that Heffter m -systems exist in all groups \mathbb{Z}_{2mn+1} : simply observe that the extra triple can be replaced with $(1, \mathfrak{D}-1, \mathfrak{D})$ and the extra quintuple can be replaced with $(1, \overline{\mathfrak{D}} - 3, \mathfrak{D} - 2, \mathfrak{D} - 1, \mathfrak{D})$.

The specific constructions of K -near Skolem sequences we use have a special form, from which we produce a set of tiles which assemble into Heffter arrays. The next section will discuss that special form. The constructions themselves are described, together with a method to find them, in Appendix A.

2.5.2 Constructions of Skolem Sequences

This section provides a description of what is meant by a construction of a K -near Skolem sequence. Methods to produce Skolem sequences and their generalizations are manifold, which is touched upon briefly in Appendix A which also contains significantly more detail about the constructions that we use. This section features a construction of Skolem sequences of length $4n + 5$ for $n \geq 0$ which appears in the second row of Table A.1.

Consider the Skolem sequence of order 9: 759242574869311368. We can use this Skolem sequence to partition the interval $[10, 27]$ into the differences $[1, 9]$. In the following figure, we visualize the partition by drawing lines between paired integers.

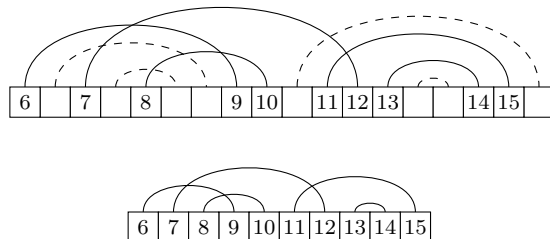


The above Skolem sequence has been chosen in part because four of its pairs can be *thickened* to produce larger Skolem sequences. The lines demarking the chosen pairs have been drawn thicker. To thicken a set of pairs

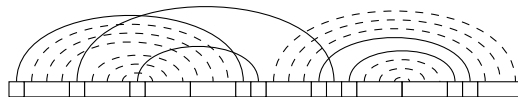
- replace the paired elements with intervals of a fixed length m , to produce paired intervals,
- among the paired intervals, pair the elements in one interval taken in increasing order with the elements in the other interval taken in decreasing order, and then
- adjust the values of all endpoints so that they form an interval and their relative ordering is the same as the original Skolem sequence.

This process is described more formally in Appendix A. It is not obvious when the final step of this process will produce a Skolem sequence, and this must be checked rigorously.

There is a degenerate case of thickening where $m = 0$ and the thickened pairs are simply deleted. As setting $m = 0$ results in a Skolem sequence of order 5, it is natural to use it to partition the interval $[6, 15]$.



pairs by replacing their endpoints with intervals of length $m = 3$. Here the interval to be partitioned has been omitted from the figure, and the pairs resulting from the thickening process are drawn as dashed lines.



Thickening by a variable amount, we obtain a description of a family of Skolem sequences. The constructions that appear in Appendix A are all of the form below.

- Between three and eight sporadic pairs, $(x_1, y_1), \dots, (x_k, y_k)$,
- the pairs $(a_1 + r, b_1 + 4m - r)$ for $0 \leq r < m$,
- the pairs $(a_2 + m + r, b_2 + 3m - r)$ for $0 \leq r < m$,
- the pairs $(a_3 + 4m + r, b_3 + 8m - r)$ for $0 \leq r < m$, and
- the pairs $(a_4 + 5m + r, b_4 + 7m - r)$ for $0 \leq r < m$.

In the next section, we will show how to make sets of 3×8 and 5×8 tiles from the thickened pairs in our near Skolem sequences.

2.5.3 Long Lines of Short Tiles

Crucial to the Heffter array constructions are 3×8 and 5×8 tiles whose row and column sums are zero in \mathbb{Z} . To make 3×8 tiles, we first construct a 3×4 tile by taking the columns *à la* Section 2.5.1 corresponding to the pairs for a single value of r , and applying our favorite sign sequence to each row,

$$B_r = \begin{bmatrix} b_1 - a_1 + 4m - 2r & \overline{b_2 - a_2 + 2m - 2r} & \overline{b_3 - a_3 + 4m - 2r} & b_4 - a_4 + 2m - 2r \\ a_1 + r & \overline{a_2 + m + r} & \overline{a_3 + 4m + r} & a_4 + 5m + r \\ \overline{b_1 + 4m - r} & b_2 + 3m - r & b_3 + 8m - r & \overline{b_4 + 7m - r} \end{bmatrix}$$

whence the column sums are zero and row sums are the constants

$$\begin{aligned} b_1 - a_1 - b_2 + a_2 - b_3 + a_3 + b_4 - a_4 \\ a_1 - a_2 - a_3 + a_4 \\ -b_1 + b_2 + b_3 - b_4 \end{aligned}$$

so that the 3×8 tile $[B_r | \overline{B_{r+1}}]$ has row sums and column sums zero.

The same trick makes 5×8 tiles. Here, we use the interval $[x + 8r + 1, x + 8r + 8]$ for the distance 1 pairs, though our constructions may differ. For each r ,

$$B_r = \begin{bmatrix} b_1 - a_1 + 4m - 2r - 1 & \overline{b_2 - a_2 + 2m - 2r - 1} & \overline{b_3 - a_3 + 4m - 2r - 1} & b_4 - a_4 + 2m - 2r - 1 \\ a_1 + r & \overline{a_2 + m + r} & \overline{a_3 + 4m + r} & a_4 + 5m + r \\ \overline{b_1 + 4m - r} & b_2 + 3m - r & b_3 + 8m - r & \overline{b_4 + 7m - r} \\ \overline{x + 8r + 1} & x + 8r + 3 & x + 8r + 5 & \overline{x + 8r + 7} \\ x + 8r + 2 & \overline{x + 8r + 4} & \overline{x + 8r + 6} & x + 8r + 8 \end{bmatrix}$$

has the same column sums as above for the first three rows, and zero for the final two, hence the 5×8 tile $[B_r | \overline{B_{r+1}}]$ has row sums and column sums zero.

2.5.4 The Final Short Tile

In the previous section, we described how to use almost all of the pairs in a K -near Heffter sequence to produce a very large collection of 3×8 or 5×8 tiles whose row and column sums are zero. Here, we'll describe how we finish off the construction of our Heffter arrays with a single *sporadic* tile.

Let q be 3 or 5. We have a pile of leftover entries from which to make this sporadic tile:

- we used pairs of $q \times 4$ tiles $[B_r | \overline{B_{r+1}}]$ which means that the tile B_{m-1} was not used if m is odd,
- the q -sets corresponding to sporadic differences were not used, and

- when applicable (where no integer Heffter system exists), we haven't used the extra q -set.

Let $Q = \{A_1, \dots, A_\ell\}$ be the collection of q -sets. We can represent these q -sets in a computer as polynomials in $\mathbb{Z}[m]$. For each of sixteen cases, we found matrices $H = h_{ij}$ such that

- $\{|h_{ij}| : 1 \leq i \leq q, 1 \leq j \leq \ell\} = \{|a| : a \in A, A \in Q\}$ (all entries are used),
- $\sum_{i=1}^q h_{ij} = 0 \pmod{2q(8m+t)+1}$ for all $1 \leq j \leq \ell$ (row sums are zero), and
- $\sum_{j=1}^\ell h_{ij} = 0 \pmod{2q(8m+t)+1}$ for all $1 \leq i \leq q$ (column sums are zero),

where our goal is to construct a $q \times (8m+t)$ Heffter array.

2.6 The Last Five Cases

At this point, we have described how we found constructions of Heffter arrays for all but the cases $(4n+u) \times (4m+v)$, where both m and n are large, $u, v \in \{1, 2, 3\}$ and at least one of (u, v) is odd. In this section, we describe the construction of large $(4m+3) \times (4n+1)$ Heffter arrays for $m \geq 1$ and $n \geq 2$. This is the most complex case of the above, and the rest are accomplished with the same approach. This has all gone on for far too long, so we'll omit the remaining cases and leave that to Section 2.7. As in the previous sections, we will describe our discovery process in broad strokes. The actual construction differs by a very small amount.

The layout of the construction follows:

$$\left[\begin{array}{c|ccc} A & B_0 & \cdots & B_{n-2} \\ \hline C_0 & & & \\ \hline \vdots & & & \\ \hline C_{m-3} & & & \\ \hline \end{array} \right] E$$

where

- A is a 9×7 tile called a *germ* with row and column sums $\equiv 0 \pmod{2\mathfrak{D}+1}$,
- the tiles B_i are 7×4 with row and column sums zero,
- the tiles C_i are 4×9 with row and column sums zero, and
- E is an even-dimension shiftable array.

We'll talk about seeds, which are used to make germs, walk through the construction of a 9×4 tile, present a 7×4 tile, and then wave our hands about how to germinate a seed.

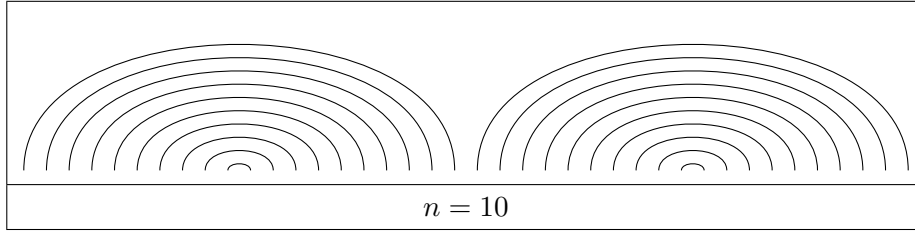
In Section 2.4, we mentioned the existence of *seeds*: Heffter-like arrays whose entries constitute two intervals, $[1, \alpha]$ and $[\mathfrak{D} - \beta, \mathfrak{D}]$ in absolute value, and whose row and column sums are all 0 or $2\mathfrak{D} + 1$. This reduces our quest from using each element in $[1, \mathfrak{D}]$ to using each in $(\alpha, \mathfrak{D} - \beta)$. We will chop the remaining interval $(\alpha, \mathfrak{D} - \beta)$ into subintervals of length 4 to use in $k \times 4$ tiles. These seed we need are found in Table 2.3.

Now, we'll describe how to construct an arbitrary number of 7×4 and 9×4 arrays. Let's assume that we've used the elements $[1, \alpha]$ in a seed for some $\alpha \in \{5, 6, 7\}$. As we've seen several times, the most convenient first step is to start with the sequence

$$\left[\alpha + 1 \quad \overline{\alpha + 2} \quad \overline{\alpha + 3} \quad \alpha + 4 \right].$$

Next, we want to use some sort of Skolem-like sequence, but we'd like to keep things simple. The *double rainbow* partition,

$$\begin{aligned} & \{(i, 2n - i + 1) : i \in [1, n]\} \cup \{(2n + i, 4n - i + 1) : i \in [1, n]\} \\ &= \{(a_{2i-1}, b_{2i-1}) : i \in [1, n]\} \cup \{(c_{2i-1}, d_{2i-1}) : i \in [1, n]\}, \end{aligned}$$



is a partition of $[1, 4n]$ into the multiset of differences $\{2i - 1 : i \in [1, n]\} \cup \{2i - 1 : i \in [1, n]\}$ which we shift by some amount. We can put these two ingredients together to produce a 3×4 array,

$$\begin{bmatrix} \alpha + 4r + 1 & \overline{\alpha + 4r + 2} & \overline{\alpha + 4r + 3} & \alpha + 4r + 4 \\ a_{4r+1} & \overline{c_{4r+1}} & \overline{a_{4r+3}} & c_{4r+3} \\ \overline{b_{4r+1}} & c_{4r+1} & b_{4r+3} & \overline{d_{4r+3}} \end{bmatrix}$$

with row sums zero and column sums $[\alpha, \overline{\alpha + 1}, \overline{\alpha}, \alpha + 1]$.

For example, we'll consider the case when $\alpha = 6$. We will assemble three 2×4 blocks, which collectively have column sums $[\overline{6}, 7, 6, \overline{7}]$. For x, y, z , and r arbitrary,

$$\begin{bmatrix} x + 4r + 1 & \overline{x + 4r + 3} & \overline{x + 4r + 5} & x + 4r + 7 \\ \overline{x + 4r + 2} & x + 4r + 4 & x + 4r + 6 & \overline{x + 4r + 8} \end{bmatrix}$$

has row sums all 0 and column sums $[\overline{1}, 1, 1, \overline{1}]$,

$$\begin{bmatrix} y + 4r + 1 & \overline{y + 4r + 2} & \overline{y + 4r + 5} & y + 4r + 6 \\ \overline{y + 4r + 3} & y + 4r + 4 & y + 4r + 7 & \overline{y + 4r + 8} \end{bmatrix}$$

$$(3 \times 3) \quad \begin{bmatrix} \mathfrak{D} - 3 & \mathfrak{D} & 4 \\ \mathfrak{D} - 1 & \overline{\mathfrak{D} - 2} & \overline{1} \\ 5 & \overline{2} & \overline{3} \end{bmatrix}$$

$$(5 \times 3) \quad \begin{bmatrix} \mathfrak{D} - 7 & 3 & \overline{\mathfrak{D} - 4} \\ \overline{\mathfrak{D} - 3} & \mathfrak{D} - 1 & \overline{2} \\ \mathfrak{D} - 5 & \overline{\mathfrak{D}} & 5 \\ \overline{\mathfrak{D} - 2} & 4 & \mathfrak{D} - 6 \\ 7 & \overline{6} & \overline{1} \end{bmatrix}$$

$$(6 \times 3) \quad \begin{bmatrix} 2 & \mathfrak{D} - 1 & \mathfrak{D} \\ \mathfrak{D} - 2 & \overline{\mathfrak{D} - 8} & \overline{6} \\ \mathfrak{D} - 4 & \overline{\mathfrak{D} - 3} & 1 \\ 3 & \mathfrak{D} - 9 & \overline{\mathfrak{D} - 6} \\ \mathfrak{D} - 5 & \overline{5} & \overline{\mathfrak{D} - 10} \\ \overline{\mathfrak{D} - 7} & 4 & \mathfrak{D} - 11 \end{bmatrix}$$

$$(5 \times 5) \quad \begin{bmatrix} \mathfrak{D} - 2 & \overline{\mathfrak{D} - 7} & \mathfrak{D} - 9 & 5 & \mathfrak{D} \\ \overline{4} & 7 & 3 & \overline{\mathfrak{D} - 4} & \mathfrak{D} - 10 \\ \overline{\mathfrak{D} - 13} & \mathfrak{D} - 11 & \overline{\mathfrak{D} - 14} & \mathfrak{D} - 17 & 1 \\ \mathfrak{D} - 5 & \overline{\mathfrak{D} - 12} & \mathfrak{D} - 16 & 6 & \overline{\mathfrak{D} - 3} \\ \mathfrak{D} - 1 & \mathfrak{D} - 15 & \overline{\mathfrak{D} - 8} & 2 & \overline{\mathfrak{D} - 6} \end{bmatrix}$$

$$(6 \times 5) \quad \begin{bmatrix} \mathfrak{D} - 10 & \overline{\mathfrak{D} - 6} & 6 & \mathfrak{D} & \mathfrak{D} - 1 \\ \overline{\mathfrak{D} - 9} & \mathfrak{D} - 8 & \overline{\mathfrak{D} - 23} & \mathfrak{D} - 22 & \overline{2} \\ 5 & \overline{\mathfrak{D} - 16} & \overline{\mathfrak{D} - 7} & \mathfrak{D} - 11 & \mathfrak{D} - 17 \\ \mathfrak{D} - 3 & \mathfrak{D} - 19 & \overline{1} & \overline{\mathfrak{D} - 18} & \overline{\mathfrak{D} - 5} \\ \mathfrak{D} - 4 & \overline{\mathfrak{D} - 20} & \mathfrak{D} - 21 & \overline{\mathfrak{D} - 2} & 3 \\ 4 & \mathfrak{D} - 15 & \mathfrak{D} - 14 & \overline{\mathfrak{D} - 13} & \overline{\mathfrak{D} - 12} \end{bmatrix}$$

Table 2.3: Five seeds to be used in creating Heffter arrays with at least one odd dimension, and both dimensions at least 7.

has row sums all 0 and column sums $[\overline{2}, 2, 2, \overline{2}]$, and

$$\begin{bmatrix} z + 4r + 1 & \overline{z + 4r + 2} & z + 4r + 8 & \overline{z + 4r + 7} \\ \overline{z + 4r + 4} & z + 4r + 6 & \overline{z + 4r + 5} & z + 4r + 3 \end{bmatrix}$$

has row sums all 0 and column sums $[\overline{3}, 4, 3, \overline{4}]$. Stacking the whole lot together, we have a 9×4 tile whose row and column sums are all zero:

$$\begin{bmatrix} 3 + 4r + 1 & \overline{3 + 4r + 2} & \overline{3 + 4r + 3} & 3 + 4r + 4 \\ a_{4r+1} & \overline{c_{4r+1}} & \overline{a_{4r+3}} & c_{4r+3} \\ \overline{b_{4r+1}} & c_{4r+1} & b_{4r+3} & \overline{d_{4r+3}} \\ x + 4r + 1 & \overline{x + 4r + 3} & \overline{x + 4r + 5} & x + 4r + 7 \\ \overline{x + 4r + 2} & x + 4r + 4 & x + 4r + 6 & \overline{x + 4r + 8} \\ y + 4r + 1 & \overline{y + 4r + 2} & \overline{y + 4r + 5} & y + 4r + 6 \\ \overline{y + 4r + 3} & y + 4r + 4 & y + 4r + 7 & \overline{y + 4r + 8} \\ z + 4r + 1 & \overline{z + 4r + 2} & z + 4r + 8 & \overline{z + 4r + 7} \\ \overline{z + 4r + 4} & z + 4r + 6 & \overline{z + 4r + 5} & z + 4r + 3. \end{bmatrix}$$

Likewise, we can construct a 7×4 tile whose row and column sums are all zero,

$$\begin{bmatrix} 3 + 4r + 1 & \overline{3 + 4r + 2} & \overline{3 + 4r + 3} & 3 + 4r + 4 \\ a_{4r+1} & \overline{c_{4r+1}} & \overline{a_{4r+3}} & c_{4r+3} \\ \overline{b_{4r+1}} & c_{4r+1} & b_{4r+3} & \overline{d_{4r+3}} \\ x + 4r + 1 & \overline{x + 4r + 2} & \overline{x + 4r + 3} & x + 4r + 4 \\ \overline{x + 4r + 5} & x + 4r + 6 & x + 4r + 7 & \overline{x + 4r + 8} \\ \overline{y + 4r + 7} & y + 4r + 8 & \overline{y + 4r + 2} & y + 4r + 1 \\ y + 4r + 6 & \overline{y + 4r + 4} & y + 4r + 3 & \overline{y + 4r + 5}. \end{bmatrix}$$

In the end, we found the needed tiles of this sort with computer assistance. In Appendix B, we have listed one shifttable 2×4 tile for each possible column sum under the requirement that row sums are zero, up to equivalence (permutations of column sums and negation). Using this table, it is easy to come up with the 9×4 and 7×4 tiles we need for the remaining cases.

The nice thing about all of this is that we can make 7×4 and 9×4 tiles whose entries partition intervals. This was difficult when we used the Skolem approach, and even with a solution in hand, we would have a huge number of cases to work through because of the unwieldy 3×8 and 5×8 tiles. Finally, we would be left with a very difficult problem of what to put in the corner (large Heffter arrays are, in practice, *very* difficult to find with brute force). Fortunately, we're now on easy street.

Finally, we mention how we find a 9×7 germ from a 5×3 seed, without really defining germs (germs contain seeds, the non-seed entries span unspecified intervals, row and column

sums are predictably nice). We have a 3×5 seed,

$$\begin{bmatrix} \mathfrak{D} - 7 & \overline{\mathfrak{D} - 3} & \mathfrak{D} - 5 & \overline{\mathfrak{D} - 2} & 7 \\ 3 & \mathfrak{D} - 1 & \overline{\mathfrak{D}} & 4 & \overline{6} \\ \overline{\mathfrak{D} - 4} & \overline{2} & 5 & \overline{1} & \mathfrak{D} - 6 \end{bmatrix}$$

which we can use our double rainbow to fill in the top three rows and leftmost three columns,

$$\begin{bmatrix} \mathfrak{D} - 7 & \overline{\mathfrak{D} - 3} & \mathfrak{D} - 5 & \overline{\mathfrak{D} - 2} & 7 & 8 & \overline{9} & \overline{10} & 11 \\ 3 & \mathfrak{D} - 1 & \overline{\mathfrak{D}} & 4 & \overline{6} & a_1 & \overline{c_1} & \overline{a_3} & c_3 \\ \overline{\mathfrak{D} - 4} & \overline{2} & 5 & \overline{1} & \mathfrak{D} - 6 & \overline{b_1} & d_1 & b_3 & \overline{d_3} \\ 12 & a_5 & \overline{b_5} & & & & & & \\ \overline{13} & \overline{c_5} & d_5 & & & & & & \\ \overline{14} & \overline{a_7} & b_7 & & & & & & \\ 15 & d_7 & \overline{d_7} & & & & & & \end{bmatrix}$$

which we fill in with a 4×6 shiftable array with row sums $[6, \overline{7}, \overline{6}, 7]$ and column sums $[0, 0, 6, \overline{7}, \overline{6}, 7]$. As always, precise details can be found in Section 2.7. And again, germs are conceptually simple because they play nicely with our 7×4 and 9×4 tiles.

We have, more or less, completely described the methods we used to obtain our constructions. Without further ado, we will present the precise constructions and prove that they produce Heffter arrays.

2.7 Complete Description of Heffter Arrays and Proofs That They Are Heffter Arrays: The Section That My Computer Wrote

In this section, we present a full description of the Heffter arrays with at least one dimension odd (less a few small dimension arrays, found in Section 2.4). Prior to writing this paper, we first found the constructions, and then wrote a program in Python to construct them for arbitrary dimensions. Later, we repurposed that code to use Sage to generate symbolic expressions for the block constructions that it produced. With a little more work, we enhanced that Sage code to produce the \LaTeX source for the subsections which follow. We think that the output is rather nicer than one expects of a computer generated proof.

Here, we describe how the code generates this output, so that the reader may verify the result. First, the code generates two or three small blocks, and computes their row and column sums as polynomials in several variables (modulo $2MN + 1$ if and only if $MN \equiv 1, 2 \pmod{4}$). Most of these blocks will have row and column sums all zero. Then, it examines the entries in each block.

- We assume the polynomial variables have a nonnegative value (else the constructions are invalid), and find their symbolic absolute value.
- For each entry e , we look for the entry $e + 1$ in the block, and $[e, e + 1]$ is an interval covered by the block. Continue this process until all entries in the block are used in an interval, and there are as few intervals as possible.
- Certain blocks have entries which are nonconstant polynomials in a variable r . We call these *variable blocks*.
- Suppose a sequence of variable blocks B_0, \dots, B_f are constructed. As we did with the individual entries, we assemble intervals $[a(r), b(r)]$ into long intervals $[a(0), b(f)]$ if $b(r) + 1 = a(r + 1)$ or $[a(f), b(0)]$ if $b(r) + 1 = a(r - 1)$.
 - In a few cases, a few variable intervals don't tie together nicely. We regroup these intervals into four sequences $(a_i(r), a_i(r) + 4, a_i(r) + 8, \dots, b_i(r))$. These sequences interlace to produce a whole interval $[a_1(0), b_2(f)]$ together with two sporadic entries, $\{a_0(0)\}$ and $\{b_3(f)\}$. These are tossed onto the pile of long intervals.

Next, we take a large Heffter array whose dimensions are both even. We know these to be shiftable, and the entries form a known interval. We add that shifted interval to the collection. Finally, we have some collection of intervals $I_0 = [a_0, b_0], I_1 = [a_1, b_1], \dots, I_q = [a_q, b_q]$. Then, we assemble these long intervals: if $b_i + 1 = a_j$, then we write $[a_i, b_j] = I_i \cup I_j = I_i I_j$, where adjacency denotes interval concatenation.

Since the proof is typeset by computer, we are able to retroactively relabel the intervals such that $[1, MN] = I_0 I_1 I_2 \dots I_f$. Putting all of this together, we see that each entry in the interval $[1, MN]$ is used precisely once, and since the row and column sums are zero, we have indeed produced a Heffter array of the claimed dimensions.

2.7.1 Constructions of $3 \times n$ Heffter Arrays

2.7.1.1 $3 \times (8n + 7)$ Heffter Arrays

Let $n \geq 0$, and

$$A = \begin{bmatrix} 2 & 24n+21 & 24n+20 \\ \frac{16n+15}{4n+3} & \frac{8n+7}{12n+12} & \frac{8n+8}{8n+9} \\ \frac{10n+10}{1} & \frac{4n+4}{20n+17} & \frac{14n+14}{20n+18} \\ \frac{20n+16}{22n+19} & \frac{12n+11}{8n+6} & \frac{8n+5}{14n+13} \end{bmatrix},$$

a block with row sums

$$[2\mathcal{D} + 1, 0, 0, 0, 0, 0, 0]$$

and column sums

$$[0, 0, 2\mathcal{D} + 1].$$

The entries in A cover the intervals $I_0 = [1, 2]$, $I_2 = [4n + 3, 4n + 4]$, $I_4 = [8n + 5, 8n + 9]$, $I_{17} = \{22n + 19\}$, $I_6 = \{10n + 10\}$, $I_{12} = \{16n + 15\}$, $I_{19} = [24n + 20, 24n + 21]$, $I_{15} = [20n + 16, 20n + 18]$, $I_8 = [12n + 11, 12n + 12]$ and $I_{10} = [14n + 13, 14n + 14]$. For $0 \leq r \leq n - 1$,

$$A_r = \begin{bmatrix} \overline{8n-4r+4} & \overline{8n+2r+10} & \overline{16n-2r+14} \\ \overline{8n-4r+3} & \overline{16n+2r+16} & \overline{24n-2r+19} \\ \overline{4n-4r+2} & \overline{18n+2r+16} & \overline{22n-2r+18} \\ \overline{4n-4r+1} & \overline{10n+2r+11} & \overline{14n-2r+12} \\ \overline{8n-4r+2} & \overline{8n+2r+11} & \overline{16n-2r+13} \\ \overline{8n-4r+1} & \overline{16n+2r+17} & \overline{24n-2r+18} \\ \overline{4n-4r} & \overline{18n+2r+17} & \overline{22n-2r+17} \\ \overline{4n-4r-1} & \overline{10n+2r+12} & \overline{14n-2r+11} \end{bmatrix},$$

a variable block with all row and column sums zero. The entries in A_r cover the intervals $[8n - 4r + 1, 8n - 4r + 4]$, $[4n - 4r - 1, 4n - 4r + 2]$, $[8n + 2r + 10, 8n + 2r + 11]$, $[18n + 2r + 16, 18n + 2r + 17]$, $[24n - 2r + 18, 24n - 2r + 19]$, $[16n - 2r + 13, 16n - 2r + 14]$, $[16n + 2r + 16, 16n + 2r + 17]$, $[14n - 2r + 11, 14n - 2r + 12]$, $[10n + 2r + 11, 10n + 2r + 12]$ and $[22n - 2r + 17, 22n - 2r + 18]$. Considering $0 \leq r \leq n - 1$, these blocks cover the intervals $I_3 = [4n + 5, 8n + 4]$, $I_1 = [3, 4n + 2]$, $I_5 = [8n + 10, 10n + 9]$, $I_{14} = [18n + 16, 20n + 15]$, $I_{18} = [22n + 20, 24n + 19]$, $I_{11} = [14n + 15, 16n + 14]$, $I_{13} = [16n + 16, 18n + 15]$, $I_9 = [12n + 13, 14n + 12]$, $I_7 = [10n + 11, 12n + 10]$ and $I_{16} = [20n + 19, 22n + 18]$.

Concatenating these intervals, we have covered $[1, 24n + 21] = I_0 I_1 \cdots I_{19}$. Therefore, the block construction $[A^T | A_0^T | \cdots | A_{n-1}^T]$ is a $3 \times (8n + 7)$ Heffter array.

2.7.1.2 $3 \times (8n + 8)$ Heffter Arrays

Let $n \geq 0$, and

$$A = \begin{bmatrix} \overline{8n+9} & \overline{1} & \overline{8n+10} \\ \overline{8n+8} & \overline{10n+12} & \overline{18n+20} \\ \overline{12n+14} & \overline{16n+18} & \overline{4n+4} \\ \overline{20n+22} & \overline{8n+7} & \overline{12n+15} \\ \overline{22n+23} & \overline{18n+21} & \overline{4n+2} \\ \overline{8n+5} & \overline{24n+24} & \overline{16n+19} \\ \overline{14n+16} & \overline{4n+3} & \overline{10n+13} \\ \overline{8n+11} & \overline{8n+6} & \overline{16n+17} \end{bmatrix},$$

a block with all row and column sums zero. The entries in A cover the intervals $I_0 = \{1\}$, $I_2 = [4n + 2, 4n + 4]$, $I_4 = [8n + 5, 8n + 11]$, $I_6 = [10n + 12, 10n + 13]$, $I_{14} = [18n + 20, 18n + 21]$, $I_{20} = \{24n + 24\}$, $I_{12} = [16n + 17, 16n + 19]$, $I_8 = [12n + 14, 12n + 15]$, $I_{18} = \{22n + 23\}$, $I_{16} = \{20n + 22\}$ and $I_{10} = \{14n + 16\}$. For $0 \leq r \leq n - 1$,

$$A_r = \begin{bmatrix} \overline{4n-4r} & \overline{18n+2r+22} & \overline{22n-2r+22} \\ \overline{8n-4r+3} & \overline{16n+2r+20} & \overline{24n-2r+23} \\ \overline{4n-4r+1} & \overline{10n+2r+14} & \overline{14n-2r+15} \\ \overline{8n-4r+4} & \overline{8n+2r+12} & \overline{16n-2r+16} \\ \overline{4n-4r-2} & \overline{18n+2r+23} & \overline{22n-2r+21} \\ \overline{8n-4r+1} & \overline{16n+2r+21} & \overline{24n-2r+22} \\ \overline{4n-4r-1} & \overline{10n+2r+15} & \overline{14n-2r+14} \\ \overline{8n-4r+2} & \overline{8n+2r+13} & \overline{16n-2r+15} \end{bmatrix},$$

a variable block with all row and column sums zero. The entries in A_r cover the intervals $[4n - 4r - 2, 4n - 4r + 1]$, $[8n - 4r + 1, 8n - 4r + 4]$, $[8n + 2r + 12, 8n + 2r + 13]$, $[16n +$

$2r + 20, 16n + 2r + 21], [22n - 2r + 21, 22n - 2r + 22], [18n + 2r + 22, 18n + 2r + 23], [16n - 2r + 15, 16n - 2r + 16], [10n + 2r + 14, 10n + 2r + 15], [24n - 2r + 22, 24n - 2r + 23]$ and $[14n - 2r + 14, 14n - 2r + 15]$. Considering $0 \leq r \leq n - 1$, these blocks cover the intervals $I_1 = [2, 4n + 1], I_3 = [4n + 5, 8n + 4], I_5 = [8n + 12, 10n + 11], I_{13} = [16n + 20, 18n + 19], I_{17} = [20n + 23, 22n + 22], I_{15} = [18n + 22, 20n + 21], I_{11} = [14n + 17, 16n + 16], I_7 = [10n + 14, 12n + 13], I_{19} = [22n + 24, 24n + 23]$ and $I_9 = [12n + 16, 14n + 15]$.

Concatenating these intervals, we have covered $[1, 24n + 24] = I_0 I_1 \cdots I_{20}$. Therefore, the block construction $[A^T | A_0^T | \cdots | A_{n-1}^T]$ is a $3 \times (8n + 8)$ Heffter array.

2.7.1.3 $3 \times (8n + 9)$ Heffter Arrays

Let $n \geq 0$, and

$$A = \begin{bmatrix} 8n+7 & 8n+10 & \overline{16n+17} \\ 18n+21 & \overline{10n+12} & 8n+9 \\ \overline{12n+14} & \overline{16n+18} & 4n+4 \\ \overline{4n+6} & \overline{18n+20} & 22n+26 \\ \overline{18n+22} & 4n+3 & 22n+25 \\ 8n+5 & 16n+16 & 8n+11 \\ 14n+15 & 4n+2 & \overline{10n+13} \\ \overline{16n+19} & 8n+8 & \overline{24n+27} \\ \overline{18n+23} & 4n+1 & \overline{22n+24} \end{bmatrix},$$

a block with all row and column sums zero. The entries in A cover the intervals $I_3 = \{4n+6\}$, $I_5 = \{8n + 5\}$, $I_1 = [4n + 1, 4n + 4]$, $I_7 = [8n + 7, 8n + 11]$, $I_9 = [10n + 12, 10n + 13]$, $I_{20} = [22n + 24, 22n + 26]$, $I_{22} = \{24n + 27\}$, $I_{17} = [18n + 20, 18n + 23]$, $I_{13} = \{14n + 15\}$, $I_{11} = \{12n + 14\}$ and $I_{15} = [16n + 16, 16n + 19]$. For $0 \leq r \leq n - 1$,

$$A_r = \begin{bmatrix} 8n-4r+3 & 8n+2r+12 & \overline{16n-2r+15} \\ 4n-4r & \overline{10n+2r+14} & 14n-2r+14 \\ 8n-4r+6 & 16n+2r+20 & \overline{24n-2r+26} \\ \overline{4n-4r-1} & \overline{18n+2r+24} & 22n-2r+23 \\ 8n-4r+1 & 8n+2r+13 & \overline{16n-2r+14} \\ 4n-4r-2 & 10n+2r+15 & \overline{14n-2r+13} \\ 8n-4r+4 & \overline{16n+2r+21} & 24n-2r+25 \\ \overline{4n-4r-3} & 18n+2r+25 & \overline{22n-2r+22} \end{bmatrix},$$

a variable block with all row and column sums zero. The entries in A_r cover the intervals $[4n - 4r - 3, 4n - 4r]$, $\{8n - 4r + 1\}$, $[8n - 4r + 3, 8n - 4r + 4]$, $\{8n - 4r + 6\}$, $[8n + 2r + 12, 8n + 2r + 13]$, $[16n + 2r + 20, 16n + 2r + 21]$, $[24n - 2r + 25, 24n - 2r + 26]$, $[16n - 2r + 14, 16n - 2r + 15]$, $[22n - 2r + 22, 22n - 2r + 23]$, $[10n + 2r + 14, 10n + 2r + 15]$, $[14n - 2r + 13, 14n - 2r + 14]$ and $[18n + 2r + 24, 18n + 2r + 25]$. Considering $0 \leq r \leq n - 1$, these blocks cover the intervals $I_0 = [1, 4n]$, $I_{14} = [8n + 12, 10n + 11]$, $I_{19} = [16n + 20, 18n + 19]$, $I_{10} = [22n + 27, 24n + 26]$, $I_{12} = [14n + 16, 16n + 15]$, $I_{18} = [20n + 24, 22n + 23]$, $I_2 = [10n + 14, 12n + 13]$, $I_4 = [12n + 15, 14n + 14]$ and $I_6 = [18n + 24, 20n + 23]$. Additionally, we split the intervals $\{8n - 4r + 1\}$, $[8n - 4r + 3, 8n - 4r + 4]$ and $\{8n - 4r + 6\}$ into the sequences

$$(4n + 5, 4n + 9, \dots, 8n + 1),$$

$$(4n + 7, 4n + 11, \dots, 8n + 3),$$

$$(4n + 8, 4n + 12, \dots, 8n + 4),$$

and

$$(4n + 10, 4n + 14, \dots, 8n + 6),$$

and rejoin them into the intervals $I_2 = \{4n + 5\}$, $I_4 = [4n + 7, 8n + 4]$ and $I_6 = \{8n + 6\}$.

Concatenating these intervals, we have covered $[1, 24n + 27] = I_0 I_1 \cdots I_{22}$. Therefore, the block construction $[A^T | A_0^T | \cdots | A_{n-1}^T]$ is a $3 \times (8n + 9)$ Heffter array.

2.7.1.4 $3 \times (8n + 10)$ Heffter Arrays

Let $n \geq 0$, and

$$A = \begin{bmatrix} 2 & 24n+29 & 24n+30 \\ \frac{8n+10}{8n+10} & \frac{8n+11}{8n+11} & \frac{16n+21}{16n+21} \\ \bar{1} & \frac{10n+13}{10n+13} & \frac{10n+14}{10n+14} \\ \frac{8n+8}{8n+8} & \frac{12n+16}{12n+16} & \frac{20n+24}{20n+24} \\ \frac{16n+20}{16n+20} & \frac{20n+25}{20n+25} & \frac{4n+5}{4n+5} \\ \frac{20n+26}{20n+26} & \frac{8n+9}{8n+9} & \frac{12n+17}{12n+17} \\ \frac{8n+7}{8n+7} & \frac{8n+12}{8n+12} & \frac{16n+19}{16n+19} \\ \frac{10n+15}{10n+15} & \frac{4n+3}{4n+3} & \frac{14n+18}{14n+18} \\ \frac{22n+27}{22n+27} & \frac{18n+23}{18n+23} & \frac{4n+4}{4n+4} \\ \frac{8n+6}{8n+6} & \frac{24n+28}{24n+28} & \frac{16n+22}{16n+22} \end{bmatrix},$$

a block with row sums

$$[2\mathfrak{D} + 1, 0, 0, 0, 0, 0, 0, 0, 0, 0, 0]$$

and column sums

$$[0, \overline{2\mathfrak{D} + 1}, 4\mathfrak{D} + 2].$$

The entries in A cover the intervals $I_0 = [1, 2]$, $I_2 = [4n + 3, 4n + 5]$, $I_4 = [8n + 6, 8n + 12]$, $I_{14} = \{18n + 23\}$, $I_8 = [12n + 16, 12n + 17]$, $I_{10} = \{14n + 18\}$, $I_{12} = [16n + 19, 16n + 22]$, $I_6 = [10n + 13, 10n + 15]$, $I_{20} = [24n + 28, 24n + 30]$, $I_{18} = \{22n + 27\}$ and $I_{16} = [20n + 24, 20n + 26]$. For $0 \leq r \leq n - 1$,

$$A_r = \begin{bmatrix} \frac{8n-4r+5}{8n-4r+5} & \frac{8n+2r+13}{8n+2r+13} & \frac{16n-2r+18}{16n-2r+18} \\ \frac{4n-4r+1}{4n-4r+1} & \frac{10n+2r+16}{10n+2r+16} & \frac{14n-2r+17}{14n-2r+17} \\ \frac{4n-4r+2}{4n-4r+2} & \frac{18n+2r+24}{18n+2r+24} & \frac{22n-2r+26}{22n-2r+26} \\ \frac{8n-4r+4}{8n-4r+4} & \frac{16n+2r+23}{16n+2r+23} & \frac{24n-2r+27}{24n-2r+27} \\ \frac{8n-4r+3}{8n-4r+3} & \frac{8n+2r+14}{8n+2r+14} & \frac{16n-2r+17}{16n-2r+17} \\ \frac{4n-4r-1}{4n-4r-1} & \frac{10n+2r+17}{10n+2r+17} & \frac{14n-2r+16}{14n-2r+16} \\ \frac{4n-4r}{4n-4r} & \frac{18n+2r+25}{18n+2r+25} & \frac{22n-2r+25}{22n-2r+25} \\ \frac{8n-4r+2}{8n-4r+2} & \frac{16n+2r+24}{16n+2r+24} & \frac{24n-2r+26}{24n-2r+26} \end{bmatrix},$$

a variable block with all row and column sums zero. The entries in A_r cover the intervals $[4n - 4r - 1, 4n - 4r + 2]$, $[8n - 4r + 2, 8n - 4r + 5]$, $[8n + 2r + 13, 8n + 2r + 14]$, $[10n + 2r + 16, 10n + 2r + 17]$, $[18n + 2r + 24, 18n + 2r + 25]$, $[16n - 2r + 17, 16n - 2r + 18]$, $[16n + 2r + 23, 16n + 2r + 24]$, $[22n - 2r + 25, 22n - 2r + 26]$, $[14n - 2r + 16, 14n - 2r + 17]$ and $[24n - 2r + 26, 24n - 2r + 27]$. Considering $0 \leq r \leq n - 1$, these blocks cover the intervals $I_1 = [3, 4n + 2]$, $I_3 = [4n + 6, 8n + 5]$, $I_5 = [8n + 13, 10n + 12]$, $I_7 = [10n + 16, 12n + 15]$, $I_{15} = [18n + 24, 20n + 23]$, $I_{11} = [14n + 19, 16n + 18]$, $I_{13} = [16n + 23, 18n + 22]$, $I_{17} = [20n + 27, 22n + 26]$, $I_9 = [12n + 18, 14n + 17]$ and $I_{19} = [22n + 28, 24n + 27]$.

Concatenating these intervals, we have covered $[1, 24n + 30] = I_0 I_1 \cdots I_{20}$. Therefore, the block construction $[A^T | A_0^T | \cdots | A_{n-1}^T]$ is a $3 \times (8n + 10)$ Heffter array.

2.7.1.5 $3 \times (8n + 11)$ Heffter Arrays

Let $n \geq 0$, and

$$A = \begin{bmatrix} 2 & \overline{24n+33} & \overline{24n+32} \\ \overline{8n+11} & \overline{8n+12} & \overline{16n+23} \\ \overline{4n+5} & \overline{12n+18} & \overline{8n+13} \\ \overline{4n+6} & \overline{10n+15} & \overline{14n+21} \\ \overline{1} & \overline{20n+27} & \overline{20n+28} \\ \overline{8n+9} & \overline{12n+17} & \overline{20n+26} \\ \overline{22n+30} & \overline{8n+10} & \overline{14n+20} \\ \overline{8n+8} & \overline{16n+22} & \overline{8n+14} \\ \overline{16n+24} & \overline{24n+31} & \overline{8n+7} \\ \overline{22n+29} & \overline{4n+4} & \overline{18n+25} \\ \overline{4n+3} & \overline{14n+19} & \overline{10n+16} \end{bmatrix},$$

a block with row sums

$$[2\mathfrak{D} + 1, 0, 0, 0, 0, 0, 0, 0, 0, 0, 0]$$

and column sums

$$[0, 0, 2\mathfrak{D} + 1].$$

The entries in A cover the intervals $I_0 = [1, 2]$, $I_2 = [4n + 3, 4n + 6]$, $I_4 = [8n + 7, 8n + 14]$, $I_{20} = [24n + 31, 24n + 33]$, $I_{10} = [14n + 19, 14n + 21]$, $I_8 = [12n + 17, 12n + 18]$, $I_{12} = [16n + 22, 16n + 24]$, $I_{18} = [22n + 29, 22n + 30]$, $I_6 = [10n + 15, 10n + 16]$, $I_{14} = \{18n + 25\}$ and $I_{16} = [20n + 26, 20n + 28]$. For $0 \leq r \leq n - 1$,

$$A_r = \begin{bmatrix} \overline{8n-4r+6} & \overline{8n+2r+15} & \overline{16n-2r+21} \\ \overline{8n-4r+5} & \overline{16n+2r+25} & \overline{24n-2r+30} \\ \overline{4n-4r+2} & \overline{18n+2r+26} & \overline{22n-2r+28} \\ \overline{4n-4r+1} & \overline{10n+2r+17} & \overline{14n-2r+18} \\ \overline{8n-4r+4} & \overline{8n+2r+16} & \overline{16n-2r+20} \\ \overline{8n-4r+3} & \overline{16n+2r+26} & \overline{24n-2r+29} \\ \overline{4n-4r} & \overline{18n+2r+27} & \overline{22n-2r+27} \\ \overline{4n-4r-1} & \overline{10n+2r+18} & \overline{14n-2r+17} \end{bmatrix},$$

a variable block with all row and column sums zero. The entries in A_r cover the intervals $[4n - 4r - 1, 4n - 4r + 2]$, $[8n - 4r + 3, 8n - 4r + 6]$, $[8n + 2r + 15, 8n + 2r + 16]$, $[10n + 2r + 17, 10n + 2r + 18]$, $[18n + 2r + 26, 18n + 2r + 27]$, $[16n - 2r + 20, 16n - 2r + 21]$, $[24n - 2r + 29, 24n - 2r + 30]$, $[14n - 2r + 17, 14n - 2r + 18]$, $[16n + 2r + 25, 16n + 2r + 26]$ and $[22n - 2r + 27, 22n - 2r + 28]$. Considering $0 \leq r \leq n - 1$, these blocks cover the intervals $I_1 = [3, 4n + 2]$, $I_3 = [4n + 7, 8n + 6]$, $I_5 = [8n + 15, 10n + 14]$, $I_7 = [10n + 17, 12n + 16]$, $I_{15} = [18n + 26, 20n + 25]$, $I_{11} = [14n + 22, 16n + 21]$, $I_{19} = [22n + 31, 24n + 30]$, $I_9 = [12n + 19, 14n + 18]$, $I_{13} = [16n + 25, 18n + 24]$ and $I_{17} = [20n + 29, 22n + 28]$.

Concatenating these intervals, we have covered $[1, 24n + 33] = I_0 I_1 \cdots I_{20}$. Therefore, the block construction $[A^T | A_0^T | \cdots | A_{n-1}^T]$ is a $3 \times (8n + 11)$ Heffter array.

2.7.1.6 $3 \times (8n + 12)$ Heffter Arrays

Let $n \geq 0$, and

$$A = \begin{bmatrix} 1 & 8n+13 & \overline{8n+14} \\ \frac{8n+12}{4n+6} & \frac{10n+17}{16n+26} & \frac{18n+29}{12n+20} \\ \frac{8n+11}{22n+34} & \frac{12n+21}{18n+30} & \frac{20n+32}{4n+4} \\ \frac{16n+27}{4n+5} & \frac{24n+36}{10n+18} & \frac{8n+9}{14n+23} \\ \frac{8n+15}{22n+33} & \frac{8n+10}{4n+2} & \frac{16n+25}{18n+31} \\ \frac{24n+35}{4n+3} & \frac{8n+7}{14n+22} & \frac{16n+28}{10n+19} \\ \frac{16n+24}{8n+8} & & \frac{8n+16}{8n+16} \end{bmatrix},$$

a block with all row and column sums zero. The entries in A cover the intervals $I_0 = \{1\}$, $I_2 = [4n+2, 4n+6]$, $I_4 = [8n+7, 8n+16]$, $I_{14} = [18n+29, 18n+31]$, $I_8 = [12n+20, 12n+21]$, $I_{18} = [22n+33, 22n+34]$, $I_{16} = \{20n+32\}$, $I_6 = [10n+17, 10n+19]$, $I_{12} = [16n+24, 16n+28]$, $I_{20} = [24n+35, 24n+36]$ and $I_{10} = [14n+22, 14n+23]$. For $0 \leq r \leq n-1$,

$$A_r = \begin{bmatrix} 4n-4r & 18n+2r+32 & \overline{22n-2r+32} \\ \frac{8n-4r+5}{4n-4r+1} & \frac{16n+2r+29}{10n+2r+20} & \frac{24n-2r+34}{14n-2r+21} \\ \frac{8n-4r+6}{4n-4r-2} & \frac{8n+2r+17}{18n+2r+33} & \frac{16n-2r+23}{22n-2r+31} \\ \frac{8n-4r+3}{4n-4r-1} & \frac{16n+2r+30}{10n+2r+21} & \frac{24n-2r+33}{14n-2r+20} \\ \frac{8n-4r+4}{8n-4r+4} & \frac{8n+2r+18}{8n+2r+18} & \frac{16n-2r+22}{16n-2r+22} \end{bmatrix},$$

a variable block with all row and column sums zero. The entries in A_r cover the intervals $[4n-4r-2, 4n-4r+1]$, $[8n-4r+3, 8n-4r+6]$, $[8n+2r+17, 8n+2r+18]$, $[18n+2r+32, 18n+2r+33]$, $[14n-2r+20, 14n-2r+21]$, $[10n+2r+20, 10n+2r+21]$, $[16n+2r+29, 16n+2r+30]$, $[22n-2r+31, 22n-2r+32]$, $[24n-2r+33, 24n-2r+34]$ and $[16n-2r+22, 16n-2r+23]$. Considering $0 \leq r \leq n-1$, these blocks cover the intervals $I_1 = [2, 4n+1]$, $I_3 = [4n+7, 8n+6]$, $I_5 = [8n+17, 10n+16]$, $I_{15} = [18n+32, 20n+31]$, $I_9 = [12n+22, 14n+21]$, $I_7 = [10n+20, 12n+19]$, $I_{13} = [16n+29, 18n+28]$, $I_{17} = [20n+33, 22n+32]$, $I_{19} = [22n+35, 24n+34]$ and $I_{11} = [14n+24, 16n+23]$.

Concatenating these intervals, we have covered $[1, 24n+36] = I_0 I_1 \cdots I_{20}$. Therefore, the block construction $[A^T | A_0^T | \cdots | A_{n-1}^T]$ is a $3 \times (8n+12)$ Heffter array.

2.7.1.7 $3 \times (8n + 13)$ Heffter Arrays

Let $n \geq 0$, and

$$A = \begin{bmatrix} 8n+11 & 8n+14 & \overline{16n+25} \\ 18n+30 & 8n+13 & \overline{10n+17} \\ \overline{4n+6} & \overline{16n+26} & \overline{12n+20} \\ \overline{4n+8} & \overline{18n+29} & \overline{22n+37} \\ \overline{4n+5} & \overline{18n+31} & \overline{22n+36} \\ \overline{8n+9} & \overline{16n+24} & \overline{8n+15} \\ \overline{10n+18} & \overline{4n+4} & \overline{14n+22} \\ \overline{24n+39} & \overline{16n+27} & \overline{8n+12} \\ \overline{4n+3} & \overline{22n+35} & \overline{18n+32} \\ \overline{8n+16} & \overline{8n+7} & \overline{16n+23} \\ \overline{10n+19} & \overline{14n+21} & \overline{4n+2} \\ \overline{24n+38} & \overline{8n+10} & \overline{16n+28} \\ \overline{22n+34} & \overline{4n+1} & \overline{18n+33} \end{bmatrix},$$

a block with all row and column sums zero. The entries in A cover the intervals $I_5 = \{8n+7\}$, $I_3 = \{4n+8\}$, $I_1 = [4n+1, 4n+6]$, $I_7 = [8n+9, 8n+16]$, $I_{22} = [24n+38, 24n+39]$, $I_{11} = \{12n+20\}$, $I_{15} = [16n+23, 16n+28]$, $I_{13} = [14n+21, 14n+22]$, $I_9 = [10n+17, 10n+19]$, $I_{20} = [22n+34, 22n+37]$ and $I_{17} = [18n+29, 18n+33]$. For $0 \leq r \leq n-1$,

$$A_r = \begin{bmatrix} 8n-4r+5 & 8n+2r+17 & \overline{16n-2r+22} \\ \overline{4n-4r} & \overline{10n+2r+20} & \overline{14n-2r+20} \\ 8n-4r+8 & 16n+2r+29 & \overline{24n-2r+37} \\ \overline{4n-4r-1} & \overline{18n+2r+34} & \overline{22n-2r+33} \\ 8n-4r+3 & 8n+2r+18 & \overline{16n-2r+21} \\ \overline{4n-4r-2} & \overline{10n+2r+21} & \overline{14n-2r+19} \\ 8n-4r+6 & \overline{16n+2r+30} & \overline{24n-2r+36} \\ \overline{4n-4r-3} & \overline{18n+2r+35} & \overline{22n-2r+32} \end{bmatrix},$$

a variable block with all row and column sums zero. The entries in A_r cover the intervals $[4n-4r-3, 4n-4r]$, $[8n-4r+5, 8n-4r+6]$, $\{8n-4r+3\}$, $\{8n-4r+8\}$, $[8n+2r+17, 8n+2r+18]$, $[24n-2r+36, 24n-2r+37]$, $[16n-2r+21, 16n-2r+22]$, $[10n+2r+20, 10n+2r+21]$, $[16n+2r+29, 16n+2r+30]$, $[18n+2r+34, 18n+2r+35]$, $[14n-2r+19, 14n-2r+20]$ and $[22n-2r+32, 22n-2r+33]$. Considering $0 \leq r \leq n-1$, these blocks cover the intervals $I_0 = [1, 4n]$, $I_{10} = [8n+17, 10n+16]$, $I_{16} = [22n+38, 24n+37]$, $I_{18} = [14n+23, 16n+22]$, $I_{12} = [10n+20, 12n+19]$, $I_{19} = [16n+29, 18n+28]$, $I_2 = [18n+34, 20n+33]$, $I_4 = [12n+21, 14n+20]$ and $I_6 = [20n+34, 22n+33]$. Additionally, we split the intervals $[8n-4r+5, 8n-4r+6]$, $\{8n-4r+3\}$ and $\{8n-4r+8\}$ into the sequences

$$(4n+7, 4n+11, \dots, 8n+3),$$

$$(4n+9, 4n+13, \dots, 8n+5),$$

$$(4n+10, 4n+14, \dots, 8n+6),$$

and

$$(4n+12, 4n+16, \dots, 8n+8),$$

and rejoin them into the intervals $I_2 = \{4n+7\}$, $I_4 = [4n+9, 8n+6]$ and $I_6 = \{8n+8\}$.

Concatenating these intervals, we have covered $[1, 24n + 39] = I_0 I_1 \cdots I_{22}$. Therefore, the block construction $[A^T | A_0^T | \cdots | A_{n-1}^T]$ is a $3 \times (8n + 13)$ Heffter array.

2.7.1.8 $3 \times (8n + 14)$ Heffter Arrays

Let $n \geq 0$, and

$$A = \begin{bmatrix} 2 & 24n+41 & 24n+42 \\ \frac{8n+14}{1} & \frac{8n+15}{10n+19} & \frac{16n+29}{10n+18} \\ \frac{8n+12}{4n+7} & \frac{20n+34}{16n+28} & \frac{12n+22}{20n+35} \\ \frac{8n+13}{4n+5} & \frac{20n+36}{14n+25} & \frac{12n+23}{10n+20} \\ \frac{8n+11}{4n+5} & \frac{8n+16}{14n+25} & \frac{16n+27}{10n+20} \\ 22n+38 & \frac{4n+6}{18n+32} & \frac{16n+27}{10n+20} \\ 24n+40 & \frac{8n+10}{16n+30} & \frac{16n+27}{10n+20} \\ \frac{16n+26}{4n+3} & \frac{8n+17}{14n+24} & \frac{8n+9}{10n+21} \\ 22n+37 & 18n+33 & 4n+4 \\ 8n+8 & 16n+31 & \frac{24n+39}{1} \end{bmatrix},$$

a block with row sums

$$[2\mathfrak{D} + 1, 0, 0, 0, 0, 0, 0, 0, 0, 0, 0, 0, 0, 0, 0]$$

and column sums

$$[2\mathfrak{D} + 1, 2\mathfrak{D} + 1, \overline{2\mathfrak{D} + 1}].$$

The entries in A cover the intervals $I_0 = [1, 2]$, $I_2 = [4n + 3, 4n + 7]$, $I_4 = [8n + 8, 8n + 17]$, $I_{10} = [14n + 24, 14n + 25]$, $I_{20} = [24n + 39, 24n + 42]$, $I_{14} = [18n + 32, 18n + 33]$, $I_{12} = [16n + 26, 16n + 31]$, $I_6 = [10n + 18, 10n + 21]$, $I_8 = [12n + 22, 12n + 23]$, $I_{18} = [22n + 37, 22n + 38]$ and $I_{16} = [20n + 34, 20n + 36]$. For $0 \leq r \leq n - 1$,

$$A_r = \begin{bmatrix} \frac{8n-4r+7}{4n-4r+1} & \frac{8n+2r+18}{10n+2r+22} & \frac{16n-2r+25}{14n-2r+23} \\ \frac{4n-4r+2}{8n-4r+6} & \frac{18n+2r+34}{16n+2r+32} & \frac{22n-2r+36}{24n-2r+38} \\ \frac{8n-4r+5}{4n-4r-1} & \frac{8n+2r+19}{10n+2r+23} & \frac{16n-2r+24}{14n-2r+22} \\ \frac{4n-4r-1}{4n-4r} & \frac{10n+2r+23}{18n+2r+35} & \frac{14n-2r+22}{22n-2r+35} \\ \frac{8n-4r+4}{16n+2r+33} & \frac{16n+2r+32}{24n-2r+37} & \frac{16n-2r+25}{14n-2r+23} \end{bmatrix},$$

a variable block with all row and column sums zero. The entries in A_r cover the intervals $[8n - 4r + 4, 8n - 4r + 7]$, $[4n - 4r - 1, 4n - 4r + 2]$, $[8n + 2r + 18, 8n + 2r + 19]$, $[16n - 2r + 24, 16n - 2r + 25]$, $[10n + 2r + 22, 10n + 2r + 23]$, $[24n - 2r + 37, 24n - 2r + 38]$, $[18n + 2r + 34, 18n + 2r + 35]$, $[16n + 2r + 32, 16n + 2r + 33]$, $[14n - 2r + 22, 14n - 2r + 23]$ and $[22n - 2r + 35, 22n - 2r + 36]$. Considering $0 \leq r \leq n - 1$, these blocks cover the intervals $I_3 = [4n + 8, 8n + 7]$, $I_1 = [3, 4n + 2]$, $I_5 = [8n + 18, 10n + 17]$, $I_{11} = [14n + 26, 16n + 25]$, $I_7 = [10n + 22, 12n + 21]$, $I_{19} = [22n + 39, 24n + 38]$, $I_{15} = [18n + 34, 20n + 33]$, $I_{13} = [16n + 32, 18n + 31]$, $I_9 = [12n + 24, 14n + 23]$ and $I_{17} = [20n + 37, 22n + 36]$.

Concatenating these intervals, we have covered $[1, 24n + 42] = I_0 I_1 \cdots I_{20}$. Therefore, the block construction $[A^T | A_0^T | \cdots | A_{n-1}^T]$ is a $3 \times (8n + 14)$ Heffter array.

2.7.2 Constructions of $5 \times n$ Heffter Arrays

2.7.2.1 $5 \times (8n + 7)$ Heffter Arrays

Let $n \geq 0$, and

$$A = \begin{bmatrix} \overline{8n+9} & \overline{10n+11} & \overline{18n+19} & \overline{1} & \overline{2} \\ \overline{4n+5} & \overline{16n+17} & \overline{12n+13} & \overline{24n+24} & \overline{24n+25} \\ \overline{24n+27} & \overline{24n+26} & \overline{8n+8} & \overline{20n+21} & \overline{12n+14} \\ \overline{4n+3} & \overline{22n+22} & \overline{24n+29} & \overline{18n+20} & \overline{24n+28} \\ \overline{24n+31} & \overline{24n+23} & \overline{8n+6} & \overline{16n+18} & \overline{24n+30} \\ \overline{24n+32} & \overline{24n+33} & \overline{14n+15} & \overline{10n+12} & \overline{4n+4} \\ \overline{24n+35} & \overline{24n+34} & \overline{8n+10} & \overline{16n+16} & \overline{8n+7} \end{bmatrix},$$

a block with all row and column sums zero. The entries in A cover the intervals $I_0 = [1, 2]$, $I_2 = [4n+3, 4n+5]$, $I_4 = [8n+6, 8n+10]$, $I_8 = [12n+13, 12n+14]$, $I_{20} = [24n+23, 24n+35]$, $I_6 = [10n+11, 10n+12]$, $I_{12} = [16n+16, 16n+18]$, $I_{10} = \{14n+15\}$, $I_{16} = \{20n+21\}$, $I_{14} = [18n+19, 18n+20]$ and $I_{18} = \{22n+22\}$. For $0 \leq r \leq n-1$,

$$A_r = \begin{bmatrix} \overline{4n-4r+1} & \overline{18n+2r+21} & \overline{22n-2r+21} & \overline{24n+2r+36} & \overline{24n+2r+37} \\ \overline{8n-4r+4} & \overline{16n+2r+19} & \overline{24n-2r+22} & \overline{26n+2r+36} & \overline{26n+2r+37} \\ \overline{4n-4r+2} & \overline{10n+2r+13} & \overline{14n-2r+14} & \overline{28n+2r+36} & \overline{28n+2r+37} \\ \overline{8n-4r+5} & \overline{8n+2r+11} & \overline{16n-2r+15} & \overline{30n+2r+36} & \overline{30n+2r+37} \\ \overline{4n-4r-1} & \overline{18n+2r+22} & \overline{22n-2r+20} & \overline{32n+2r+36} & \overline{32n+2r+37} \\ \overline{8n-4r+2} & \overline{16n+2r+20} & \overline{24n-2r+21} & \overline{34n+2r+36} & \overline{34n+2r+37} \\ \overline{4n-4r} & \overline{10n+2r+14} & \overline{14n-2r+13} & \overline{36n+2r+36} & \overline{36n+2r+37} \\ \overline{8n-4r+3} & \overline{8n+2r+12} & \overline{16n-2r+14} & \overline{38n+2r+36} & \overline{38n+2r+37} \end{bmatrix},$$

a variable block with all row and column sums zero. The entries in A_r cover the intervals $[4n-4r-1, 4n-4r+2]$, $[8n-4r+2, 8n-4r+5]$, $[8n+2r+11, 8n+2r+12]$, $[24n+2r+36, 24n+2r+37]$, $[36n+2r+36, 36n+2r+37]$, $[16n+2r+19, 16n+2r+20]$, $[10n+2r+13, 10n+2r+14]$, $[22n-2r+20, 22n-2r+21]$, $[26n+2r+36, 26n+2r+37]$, $[38n+2r+36, 38n+2r+37]$, $[24n-2r+21, 24n-2r+22]$, $[28n+2r+36, 28n+2r+37]$, $[30n+2r+36, 30n+2r+37]$, $[18n+2r+21, 18n+2r+22]$, $[14n-2r+13, 14n-2r+14]$, $[32n+2r+36, 32n+2r+37]$, $[16n-2r+14, 16n-2r+15]$ and $[34n+2r+36, 34n+2r+37]$. Considering $0 \leq r \leq n-1$, these blocks cover the intervals $I_1 = [3, 4n+2]$, $I_3 = [4n+6, 8n+5]$, $I_5 = [8n+11, 10n+10]$, $I_{21} = [24n+36, 26n+35]$, $I_{27} = [36n+36, 38n+35]$, $I_{13} = [16n+19, 18n+18]$, $I_7 = [10n+13, 12n+12]$, $I_{17} = [20n+22, 22n+21]$, $I_{22} = [26n+36, 28n+35]$, $I_{28} = [38n+36, 40n+35]$, $I_{19} = [22n+23, 24n+22]$, $I_{23} = [28n+36, 30n+35]$, $I_{24} = [30n+36, 32n+35]$, $I_{15} = [18n+21, 20n+20]$, $I_9 = [12n+15, 14n+14]$, $I_{25} = [32n+36, 34n+35]$, $I_{11} = [14n+16, 16n+15]$ and $I_{26} = [34n+36, 36n+35]$.

Concatenating these intervals, we have covered $[1, 40n+35] = I_0 I_1 \cdots I_{28}$. Therefore, the block construction $[A^T | A_0^T | \cdots | A_{n-1}^T]$ is a $5 \times (8n+7)$ Heffter array.

2.7.2.2 $5 \times (8n + 8)$ Heffter Arrays

Let $n \geq 0$, and

$$A = \begin{bmatrix} \overline{8n+10} & \overline{8n+11} & \overline{1} & \overline{2} & \overline{16n+20} \\ \overline{4n+5} & \overline{8n+12} & \overline{24n+28} & \overline{12n+16} & \overline{24n+27} \\ \overline{12n+15} & \overline{24n+30} & \overline{8n+9} & \overline{24n+29} & \overline{20n+23} \\ \overline{8n+8} & \overline{24n+31} & \overline{22n+25} & \overline{14n+18} & \overline{24n+32} \\ \overline{8n+13} & \overline{24n+33} & \overline{8n+7} & \overline{16n+19} & \overline{24n+34} \\ \overline{24n+35} & \overline{24n+36} & \overline{10n+14} & \overline{4n+4} & \overline{14n+17} \\ \overline{24n+26} & \overline{24n+38} & \overline{16n+21} & \overline{8n+6} & \overline{24n+37} \\ \overline{24n+40} & \overline{24n+39} & \overline{4n+3} & \overline{22n+24} & \overline{18n+22} \end{bmatrix},$$

a block with all row and column sums zero. The entries in A cover the intervals $I_0 = [1, 2]$, $I_2 = [4n+3, 4n+5]$, $I_4 = [8n+6, 8n+13]$, $I_{18} = [22n+24, 22n+25]$, $I_{20} = [24n+26, 24n+40]$, $I_{16} = \{20n+23\}$, $I_{12} = [16n+19, 16n+21]$, $I_{14} = \{18n+22\}$, $I_8 = [12n+15, 12n+16]$, $I_6 = \{10n+14\}$ and $I_{10} = [14n+17, 14n+18]$. For $0 \leq r \leq n-1$,

$$A_r = \begin{bmatrix} \overline{8n-4r+5} & \overline{8n+2r+14} & \overline{16n-2r+18} & \overline{24n+2r+41} & \overline{24n+2r+42} \\ \overline{4n-4r+2} & \overline{10n+2r+15} & \overline{14n-2r+16} & \overline{26n+2r+41} & \overline{26n+2r+42} \\ \overline{8n-4r+4} & \overline{16n+2r+22} & \overline{24n-2r+25} & \overline{28n+2r+41} & \overline{28n+2r+42} \\ \overline{4n-4r+1} & \overline{18n+2r+23} & \overline{22n-2r+23} & \overline{30n+2r+41} & \overline{30n+2r+42} \\ \overline{8n-4r+3} & \overline{8n+2r+15} & \overline{16n-2r+17} & \overline{32n+2r+41} & \overline{32n+2r+42} \\ \overline{4n-4r} & \overline{10n+2r+16} & \overline{14n-2r+15} & \overline{34n+2r+41} & \overline{34n+2r+42} \\ \overline{8n-4r+2} & \overline{16n+2r+23} & \overline{24n-2r+24} & \overline{36n+2r+41} & \overline{36n+2r+42} \\ \overline{4n-4r-1} & \overline{18n+2r+24} & \overline{22n-2r+22} & \overline{38n+2r+41} & \overline{38n+2r+42} \end{bmatrix},$$

a variable block with all row and column sums zero. The entries in A_r cover the intervals $[4n-4r-1, 4n-4r+2]$, $[8n-4r+2, 8n-4r+5]$, $[8n+2r+14, 8n+2r+15]$, $[30n+2r+41, 30n+2r+42]$, $[24n-2r+24, 24n-2r+25]$, $[16n-2r+17, 16n-2r+18]$, $[14n-2r+15, 14n-2r+16]$, $[28n+2r+41, 28n+2r+42]$, $[18n+2r+23, 18n+2r+24]$, $[32n+2r+41, 32n+2r+42]$, $[34n+2r+41, 34n+2r+42]$, $[38n+2r+41, 38n+2r+42]$, $[26n+2r+41, 26n+2r+42]$, $[24n+2r+41, 24n+2r+42]$, $[16n+2r+22, 16n+2r+23]$, $[36n+2r+41, 36n+2r+42]$, $[22n-2r+22, 22n-2r+23]$ and $[10n+2r+15, 10n+2r+16]$. Considering $0 \leq r \leq n-1$, these blocks cover the intervals $I_1 = [3, 4n+2]$, $I_3 = [4n+6, 8n+5]$, $I_5 = [8n+14, 10n+13]$, $I_{24} = [30n+41, 32n+40]$, $I_{19} = [22n+26, 24n+25]$, $I_{11} = [14n+19, 16n+18]$, $I_9 = [12n+17, 14n+16]$, $I_{23} = [28n+41, 30n+40]$, $I_{15} = [18n+23, 20n+22]$, $I_{25} = [32n+41, 34n+40]$, $I_{26} = [34n+41, 36n+40]$, $I_{28} = [38n+41, 40n+40]$, $I_{22} = [26n+41, 28n+40]$, $I_{21} = [24n+41, 26n+40]$, $I_{13} = [16n+22, 18n+21]$, $I_{27} = [36n+41, 38n+40]$, $I_{17} = [20n+24, 22n+23]$ and $I_7 = [10n+15, 12n+14]$.

Concatenating these intervals, we have covered $[1, 40n+40] = I_0 I_1 \cdots I_{28}$. Therefore, the block construction $[A^T | A_0^T | \cdots | A_{n-1}^T]$ is a $5 \times (8n+8)$ Heffter array.

2.7.2.3 $5 \times (8n + 9)$ Heffter Arrays

Let $n \geq 0$, and

$$A = \begin{bmatrix} 1 & \bar{2} & 3 & 40n+45 & 40n+44 \\ \overline{8n+11} & \overline{12n+14} & \overline{24n+28} & \overline{24n+29} & \overline{20n+24} \\ \overline{8n+10} & \overline{10n+13} & \overline{18n+22} & \overline{24n+30} & \overline{24n+31} \\ \overline{24n+33} & \overline{18n+20} & \overline{24n+32} & \overline{4n+7} & \overline{22n+26} \\ \overline{24n+34} & \overline{24n+27} & \overline{8n+9} & \overline{16n+19} & \overline{24n+35} \\ \overline{4n+5} & \overline{24n+37} & \overline{18n+21} & \overline{24n+36} & \overline{22n+25} \\ \overline{20n+23} & \overline{24n+39} & \overline{12n+16} & \overline{8n+8} & \overline{24n+38} \\ \overline{24n+40} & \overline{8n+12} & \overline{8n+6} & \overline{24n+41} & \overline{16n+17} \\ \overline{24n+43} & \overline{24n+42} & \overline{4n+4} & \overline{12n+15} & \overline{16n+18} \end{bmatrix},$$

a block with row sums

$$[2\mathfrak{D} + 1, 0, 0, 0, 0, 0, 0, 0, 0]$$

and column sums

$$[0, 0, \overline{2\mathfrak{D} + 1}, 0, 4\mathfrak{D} + 2].$$

The entries in A cover the intervals $I_0 = [1, 3]$, $I_4 = \{4n + 7\}$, $I_2 = [4n + 4, 4n + 5]$, $I_6 = \{8n+6\}$, $I_8 = [8n+8, 8n+12]$, $I_{19} = [20n+23, 20n+24]$, $I_{15} = [16n+17, 16n+19]$, $I_{17} = [18n + 20, 18n + 22]$, $I_{12} = [12n + 14, 12n + 16]$, $I_{10} = \{10n + 13\}$, $I_{23} = [24n + 27, 24n + 43]$, $I_{32} = [40n + 44, 40n + 45]$ and $I_{21} = [22n + 25, 22n + 26]$. For $0 \leq r \leq n - 1$,

$$A_r = \begin{bmatrix} \overline{8n-4r+7} & \overline{16n+2r+20} & \overline{24n-2r+26} & \overline{24n+2r+44} & \overline{24n+2r+45} \\ \overline{4n-4r+2} & \overline{18n+2r+23} & \overline{22n-2r+24} & \overline{26n+2r+44} & \overline{26n+2r+45} \\ \overline{4n-4r+3} & \overline{10n+2r+14} & \overline{14n-2r+16} & \overline{28n+2r+44} & \overline{28n+2r+45} \\ \overline{8n-4r+4} & \overline{8n+2r+13} & \overline{16n-2r+16} & \overline{30n+2r+44} & \overline{30n+2r+45} \\ \overline{8n-4r+5} & \overline{16n+2r+21} & \overline{24n-2r+25} & \overline{32n+2r+44} & \overline{32n+2r+45} \\ \overline{4n-4r} & \overline{18n+2r+24} & \overline{22n-2r+23} & \overline{34n+2r+44} & \overline{34n+2r+45} \\ \overline{4n-4r+1} & \overline{10n+2r+15} & \overline{14n-2r+15} & \overline{36n+2r+44} & \overline{36n+2r+45} \\ \overline{8n-4r+2} & \overline{8n+2r+14} & \overline{16n-2r+15} & \overline{38n+2r+44} & \overline{38n+2r+45} \end{bmatrix},$$

a variable block with all row and column sums zero. The entries in A_r cover the intervals $[4n - 4r, 4n - 4r + 3]$, $\{8n - 4r + 7\}$, $\{8n - 4r + 2\}$, $[8n - 4r + 4, 8n - 4r + 5]$, $[8n + 2r + 13, 8n + 2r + 14]$, $[28n + 2r + 44, 28n + 2r + 45]$, $[22n - 2r + 23, 22n - 2r + 24]$, $[16n + 2r + 20, 16n + 2r + 21]$, $[30n + 2r + 44, 30n + 2r + 45]$, $[34n + 2r + 44, 34n + 2r + 45]$, $[24n - 2r + 25, 24n - 2r + 26]$, $[16n - 2r + 15, 16n - 2r + 16]$, $[24n + 2r + 44, 24n + 2r + 45]$, $[26n + 2r + 44, 26n + 2r + 45]$, $[10n + 2r + 14, 10n + 2r + 15]$, $[36n + 2r + 44, 36n + 2r + 45]$, $[32n + 2r + 44, 32n + 2r + 45]$, $[14n - 2r + 15, 14n - 2r + 16]$, $[38n + 2r + 44, 38n + 2r + 45]$ and $[18n + 2r + 23, 18n + 2r + 24]$. Considering $0 \leq r \leq n - 1$, these blocks cover the intervals $I_1 = [4, 4n+3]$, $I_{16} = [8n+13, 10n+12]$, $I_{27} = [28n+44, 30n+43]$, $I_{29} = [20n+25, 22n+24]$, $I_{22} = [16n + 20, 18n + 19]$, $I_{14} = [30n + 44, 32n + 43]$, $I_{24} = [34n + 44, 36n + 43]$, $I_{25} = [22n + 27, 24n + 26]$, $I_{11} = [14n + 17, 16n + 16]$, $I_{30} = [24n + 44, 26n + 43]$, $I_{28} = [26n + 44, 28n + 43]$, $I_{13} = [10n + 14, 12n + 13]$, $I_{31} = [36n + 44, 38n + 43]$, $I_{18} = [32n + 44, 34n + 43]$, $I_3 = [12n+17, 14n+16]$, $I_5 = [38n+44, 40n+43]$ and $I_7 = [18n+23, 20n+22]$. Additionally, we split the intervals $\{8n - 4r + 7\}$, $\{8n - 4r + 2\}$ and $[8n - 4r + 4, 8n - 4r + 5]$ into the sequences

$$(4n + 6, 4n + 10, \dots, 8n + 2),$$

$$(4n + 8, 4n + 12, \dots, 8n + 4),$$

$$(4n + 9, 4n + 13, \dots, 8n + 5),$$

and

$$(4n + 11, 4n + 15, \dots, 8n + 7),$$

and rejoin them into the intervals $I_3 = \{4n + 6\}$, $I_5 = [4n + 8, 8n + 5]$ and $I_7 = \{8n + 7\}$.

Concatenating these intervals, we have covered $[1, 40n + 45] = I_0 I_1 \cdots I_{32}$. Therefore, the block construction $[A^T | A_0^T | \cdots | A_{n-1}^T]$ is a $5 \times (8n + 9)$ Heffter array.

2.7.2.4 $5 \times (8n + 10)$ Heffter Arrays

Let $n \geq 0$, and

$$A = \begin{bmatrix} 1 & \bar{2} & 3 & \overline{40n+49} & \overline{40n+50} \\ \overline{8n+12} & \overline{12n+15} & \overline{24n+32} & \overline{24n+31} & \overline{20n+26} \\ \overline{8n+11} & \overline{14n+19} & \overline{22n+29} & \overline{24n+33} & \overline{24n+34} \\ \overline{12n+16} & \overline{20n+25} & \overline{24n+35} & \overline{8n+10} & \overline{24n+36} \\ \overline{24n+38} & \overline{20n+27} & \overline{4n+7} & \overline{24n+37} & \overline{16n+21} \\ \overline{24n+40} & \overline{14n+18} & \overline{4n+6} & \overline{18n+23} & \overline{24n+39} \\ \overline{16n+20} & \overline{24n+42} & \overline{24n+41} & \overline{8n+13} & \overline{8n+8} \\ \overline{8n+9} & \overline{24n+43} & \overline{24n+44} & \overline{16n+22} & \overline{24n+30} \\ \overline{4n+4} & \overline{24n+45} & \overline{10n+14} & \overline{24n+46} & \overline{14n+17} \\ \overline{24n+47} & \overline{24n+48} & \overline{4n+5} & \overline{22n+28} & \overline{18n+24} \end{bmatrix},$$

a block with row sums

$$[2\mathfrak{D} + 1, 0, 0, 0, 0, 0, 0, 0, 0, 0, 0]$$

and column sums

$$[0, 0, 0, 0, 2\mathfrak{D} + 1].$$

The entries in A cover the intervals $I_0 = [1, 3]$, $I_2 = [4n + 4, 4n + 7]$, $I_4 = [8n + 8, 8n + 13]$, $I_{10} = [14n + 17, 14n + 19]$, $I_{29} = [40n + 49, 40n + 50]$, $I_{14} = [18n + 23, 18n + 24]$, $I_{20} = [24n + 30, 24n + 48]$, $I_{16} = [20n + 25, 20n + 27]$, $I_8 = [12n + 15, 12n + 16]$, $I_{12} = [16n + 20, 16n + 22]$, $I_{18} = [22n + 28, 22n + 29]$ and $I_6 = \{10n + 14\}$. For $0 \leq r \leq n - 1$,

$$A_r = \begin{bmatrix} \overline{8n-4r+6} & \overline{8n+2r+14} & \overline{16n-2r+19} & \overline{24n+2r+49} & \overline{24n+2r+50} \\ \overline{8n-4r+7} & \overline{16n+2r+23} & \overline{24n-2r+29} & \overline{26n+2r+49} & \overline{26n+2r+50} \\ \overline{4n-4r+2} & \overline{10n+2r+15} & \overline{14n-2r+16} & \overline{28n+2r+49} & \overline{28n+2r+50} \\ \overline{4n-4r+3} & \overline{18n+2r+25} & \overline{22n-2r+27} & \overline{30n+2r+49} & \overline{30n+2r+50} \\ \overline{8n-4r+4} & \overline{8n+2r+15} & \overline{16n-2r+18} & \overline{32n+2r+49} & \overline{32n+2r+50} \\ \overline{8n-4r+5} & \overline{16n+2r+24} & \overline{24n-2r+28} & \overline{34n+2r+49} & \overline{34n+2r+50} \\ \overline{4n-4r} & \overline{10n+2r+16} & \overline{14n-2r+15} & \overline{36n+2r+49} & \overline{36n+2r+50} \\ \overline{4n-4r+1} & \overline{18n+2r+26} & \overline{22n-2r+26} & \overline{38n+2r+49} & \overline{38n+2r+50} \end{bmatrix},$$

a variable block with all row and column sums zero. The entries in A_r cover the intervals $[4n - 4r, 4n - 4r + 3]$, $[8n - 4r + 4, 8n - 4r + 7]$, $[8n + 2r + 14, 8n + 2r + 15]$, $[26n + 2r + 49, 26n + 2r + 50]$, $[18n + 2r + 25, 18n + 2r + 26]$, $[16n - 2r + 18, 16n - 2r + 19]$, $[34n + 2r + 49, 34n + 2r + 50]$, $[14n - 2r + 15, 14n - 2r + 16]$, $[24n + 2r + 49, 24n + 2r + 50]$, $[36n + 2r + 49, 36n + 2r + 50]$, $[30n + 2r + 49, 30n + 2r + 50]$, $[28n + 2r + 49, 28n + 2r + 50]$, $[22n - 2r + 26, 22n - 2r + 27]$, $[32n + 2r + 49, 32n + 2r + 50]$, $[24n - 2r + 28, 24n - 2r + 29]$, $[16n + 2r + 23, 16n + 2r + 24]$,

$[10n + 2r + 15, 10n + 2r + 16]$ and $[38n + 2r + 49, 38n + 2r + 50]$. Considering $0 \leq r \leq n - 1$, these blocks cover the intervals $I_1 = [4, 4n + 3]$, $I_3 = [4n + 8, 8n + 7]$, $I_5 = [8n + 14, 10n + 13]$, $I_{22} = [26n + 49, 28n + 48]$, $I_{15} = [18n + 25, 20n + 24]$, $I_{11} = [14n + 20, 16n + 19]$, $I_{26} = [34n + 49, 36n + 48]$, $I_9 = [12n + 17, 14n + 16]$, $I_{21} = [24n + 49, 26n + 48]$, $I_{27} = [36n + 49, 38n + 48]$, $I_{24} = [30n + 49, 32n + 48]$, $I_{23} = [28n + 49, 30n + 48]$, $I_{17} = [20n + 28, 22n + 27]$, $I_{25} = [32n + 49, 34n + 48]$, $I_{19} = [22n + 30, 24n + 29]$, $I_{13} = [16n + 23, 18n + 22]$, $I_7 = [10n + 15, 12n + 14]$ and $I_{28} = [38n + 49, 40n + 48]$.

Concatenating these intervals, we have covered $[1, 40n + 50] = I_0 I_1 \cdots I_{29}$. Therefore, the block construction $[A^T | A_0^T | \cdots | A_{n-1}^T]$ is a $5 \times (8n + 10)$ Heffter array.

2.7.2.5 $5 \times (8n + 11)$ Heffter Arrays

Let $n \geq 0$, and

$$A = \begin{bmatrix} \overline{8n+13} & \overline{10n+16} & \overline{18n+28} & \overline{2} & \overline{1} \\ \overline{4n+7} & \overline{12n+19} & \overline{16n+25} & \overline{24n+36} & \overline{24n+37} \\ \overline{8n+12} & \overline{12n+20} & \overline{24n+38} & \overline{20n+31} & \overline{24n+39} \\ \overline{4n+5} & \overline{22n+33} & \overline{24n+40} & \overline{24n+41} & \overline{18n+29} \\ \overline{16n+26} & \overline{8n+10} & \overline{24n+35} & \overline{24n+43} & \overline{24n+42} \\ \overline{4n+6} & \overline{24n+45} & \overline{10n+17} & \overline{24n+44} & \overline{14n+22} \\ \overline{16n+24} & \overline{24n+46} & \overline{24n+47} & \overline{8n+14} & \overline{8n+11} \\ \overline{22n+32} & \overline{24n+48} & \overline{18n+30} & \overline{4n+3} & \overline{24n+49} \\ \overline{24n+50} & \overline{16n+27} & \overline{24n+34} & \overline{24n+51} & \overline{8n+8} \\ \overline{10n+18} & \overline{24n+53} & \overline{14n+21} & \overline{24n+52} & \overline{4n+4} \\ \overline{24n+55} & \overline{16n+23} & \overline{8n+9} & \overline{8n+15} & \overline{24n+54} \end{bmatrix},$$

a block with all row and column sums zero. The entries in A cover the intervals $I_0 = [1, 2]$, $I_2 = [4n + 3, 4n + 7]$, $I_4 = [8n + 8, 8n + 15]$, $I_{18} = [22n + 32, 22n + 33]$, $I_6 = [10n + 16, 10n + 18]$, $I_8 = [12n + 19, 12n + 20]$, $I_{14} = [18n + 28, 18n + 30]$, $I_{10} = [14n + 21, 14n + 22]$, $I_{16} = \{20n + 31\}$, $I_{12} = [16n + 23, 16n + 27]$ and $I_{20} = [24n + 34, 24n + 55]$. For $0 \leq r \leq n - 1$,

$$A_r = \begin{bmatrix} \overline{4n-4r+1} & \overline{18n+2r+31} & \overline{22n-2r+31} & \overline{24n+2r+56} & \overline{24n+2r+57} \\ \overline{8n-4r+6} & \overline{16n+2r+28} & \overline{24n-2r+33} & \overline{26n+2r+56} & \overline{26n+2r+57} \\ \overline{4n-4r+2} & \overline{10n+2r+19} & \overline{14n-2r+20} & \overline{28n+2r+56} & \overline{28n+2r+57} \\ \overline{8n-4r+7} & \overline{8n+2r+16} & \overline{16n-2r+22} & \overline{30n+2r+56} & \overline{30n+2r+57} \\ \overline{4n-4r-1} & \overline{18n+2r+32} & \overline{22n-2r+30} & \overline{32n+2r+56} & \overline{32n+2r+57} \\ \overline{8n-4r+4} & \overline{16n+2r+29} & \overline{24n-2r+32} & \overline{34n+2r+56} & \overline{34n+2r+57} \\ \overline{4n-4r} & \overline{10n+2r+20} & \overline{14n-2r+19} & \overline{36n+2r+56} & \overline{36n+2r+57} \\ \overline{8n-4r+5} & \overline{8n+2r+17} & \overline{16n-2r+21} & \overline{38n+2r+56} & \overline{38n+2r+57} \end{bmatrix},$$

a variable block with all row and column sums zero. The entries in A_r cover the intervals $[8n - 4r + 4, 8n - 4r + 7]$, $[4n - 4r - 1, 4n - 4r + 2]$, $[8n + 2r + 16, 8n + 2r + 17]$, $[30n + 2r + 56, 30n + 2r + 57]$, $[16n + 2r + 28, 16n + 2r + 29]$, $[24n - 2r + 32, 24n - 2r + 33]$, $[14n - 2r + 19, 14n - 2r + 20]$, $[28n + 2r + 56, 28n + 2r + 57]$, $[18n + 2r + 31, 18n + 2r + 32]$, $[32n + 2r + 56, 32n + 2r + 57]$, $[16n - 2r + 21, 16n - 2r + 22]$, $[26n + 2r + 56, 26n + 2r + 57]$, $[24n + 2r + 56, 24n + 2r + 57]$, $[22n - 2r + 30, 22n - 2r + 31]$, $[34n + 2r + 56, 34n + 2r + 57]$, $[10n + 2r + 19, 10n + 2r + 20]$, $[36n + 2r + 56, 36n + 2r + 57]$ and $[38n + 2r + 56, 38n + 2r + 57]$. Considering $0 \leq r \leq n - 1$, these blocks cover the intervals $I_3 = [4n + 8, 8n + 7]$, $I_1 = [3, 4n + 2]$, $I_5 = [8n + 16, 10n + 15]$, $I_{24} = [30n + 56, 32n + 55]$, $I_{13} = [16n + 28, 18n + 27]$, $I_{19} = [22n + 34, 24n + 33]$, $I_9 = [12n + 21, 14n + 20]$, $I_{23} = [28n + 56, 30n + 55]$, $I_{15} = [18n + 31, 20n + 30]$, $I_{25} = [32n + 56, 34n + 55]$,

$I_{11} = [14n + 23, 16n + 22]$, $I_{22} = [26n + 56, 28n + 55]$, $I_{21} = [24n + 56, 26n + 55]$, $I_{17} = [20n + 32, 22n + 31]$, $I_{26} = [34n + 56, 36n + 55]$, $I_7 = [10n + 19, 12n + 18]$, $I_{27} = [36n + 56, 38n + 55]$ and $I_{28} = [38n + 56, 40n + 55]$.

Concatenating these intervals, we have covered $[1, 40n + 55] = I_0 I_1 \cdots I_{28}$. Therefore, the block construction $[A^T | A_0^T | \cdots | A_{n-1}^T]$ is a $5 \times (8n + 11)$ Heffter array.

2.7.2.6 $5 \times (8n + 12)$ Heffter Arrays

Let $n \geq 0$, and

$$A = \begin{bmatrix} \frac{8n+14}{4n+7} & \frac{8n+15}{8n+16} & \frac{16n+28}{12n+22} & \frac{1}{24n+39} & \frac{2}{24n+40} \\ \frac{8n+13}{8n+12} & \frac{12n+21}{14n+25} & \frac{24n+41}{22n+36} & \frac{24n+42}{24n+44} & \frac{20n+33}{24n+43} \\ \frac{8n+17}{14n+24} & \frac{16n+27}{10n+19} & \frac{24n+45}{24n+48} & \frac{8n+11}{24n+47} & \frac{24n+46}{4n+6} \\ \frac{24n+49}{24n+51} & \frac{24n+50}{4n+5} & \frac{24n+38}{24n+52} & \frac{16n+29}{22n+35} & \frac{8n+10}{18n+31} \\ \frac{8n+9}{14n+23} & \frac{24n+54}{24n+56} & \frac{24n+53}{24n+55} & \frac{8n+18}{4n+4} & \frac{16n+26}{10n+20} \\ \frac{24n+37}{24n+60} & \frac{24n+57}{24n+59} & \frac{24n+58}{18n+32} & \frac{8n+8}{22n+34} & \frac{16n+30}{4n+3} \end{bmatrix},$$

a block with all row and column sums zero. The entries in A cover the intervals $I_0 = [1, 2]$, $I_2 = [4n + 3, 4n + 7]$, $I_4 = [8n + 8, 8n + 18]$, $I_{10} = [14n + 23, 14n + 25]$, $I_8 = [12n + 21, 12n + 22]$, $I_{16} = \{20n + 33\}$, $I_{14} = [18n + 31, 18n + 32]$, $I_{12} = [16n + 26, 16n + 30]$, $I_6 = [10n + 19, 10n + 20]$, $I_{18} = [22n + 34, 22n + 36]$ and $I_{20} = [24n + 37, 24n + 60]$. For $0 \leq r \leq n - 1$,

$$A_r = \begin{bmatrix} \frac{8n-4r+7}{4n-4r+2} & \frac{8n+2r+19}{10n+2r+21} & \frac{16n-2r+25}{14n-2r+22} & \frac{24n+2r+61}{26n+2r+61} & \frac{24n+2r+62}{26n+2r+62} \\ \frac{8n-4r+6}{4n-4r+1} & \frac{16n+2r+31}{18n+2r+33} & \frac{24n-2r+36}{22n-2r+33} & \frac{28n+2r+61}{30n+2r+61} & \frac{28n+2r+62}{30n+2r+62} \\ \frac{8n-4r+5}{4n-4r} & \frac{8n+2r+20}{10n+2r+22} & \frac{16n-2r+24}{14n-2r+21} & \frac{32n+2r+61}{34n+2r+61} & \frac{32n+2r+62}{34n+2r+62} \\ \frac{8n-4r+4}{4n-4r-1} & \frac{16n+2r+32}{18n+2r+34} & \frac{24n-2r+35}{22n-2r+32} & \frac{36n+2r+61}{38n+2r+61} & \frac{36n+2r+62}{38n+2r+62} \end{bmatrix},$$

a variable block with all row and column sums zero. The entries in A_r cover the intervals $[8n - 4r + 4, 8n - 4r + 7]$, $[4n - 4r - 1, 4n - 4r + 2]$, $[8n + 2r + 19, 8n + 2r + 20]$, $[28n + 2r + 61, 28n + 2r + 62]$, $[36n + 2r + 61, 36n + 2r + 62]$, $[18n + 2r + 33, 18n + 2r + 34]$, $[14n - 2r + 21, 14n - 2r + 22]$, $[16n - 2r + 24, 16n - 2r + 25]$, $[30n + 2r + 61, 30n + 2r + 62]$, $[34n + 2r + 61, 34n + 2r + 62]$, $[24n + 2r + 61, 24n + 2r + 62]$, $[10n + 2r + 21, 10n + 2r + 22]$, $[16n + 2r + 31, 16n + 2r + 32]$, $[26n + 2r + 61, 26n + 2r + 62]$, $[38n + 2r + 61, 38n + 2r + 62]$, $[22n - 2r + 32, 22n - 2r + 33]$, $[24n - 2r + 35, 24n - 2r + 36]$ and $[32n + 2r + 61, 32n + 2r + 62]$. Considering $0 \leq r \leq n - 1$, these blocks cover the intervals $I_3 = [4n + 8, 8n + 7]$, $I_1 = [3, 4n + 2]$, $I_5 = [8n + 19, 10n + 18]$, $I_{23} = [28n + 61, 30n + 60]$, $I_{27} = [36n + 61, 38n + 60]$, $I_{15} = [18n + 33, 20n + 32]$, $I_9 = [12n + 23, 14n + 22]$, $I_{11} = [14n + 26, 16n + 25]$, $I_{24} = [30n + 61, 32n + 60]$, $I_{26} = [34n + 61, 36n + 60]$, $I_{21} = [24n + 61, 26n + 60]$, $I_7 = [10n + 21, 12n + 20]$, $I_{13} = [16n + 31, 18n + 30]$, $I_{22} = [26n + 61, 28n + 60]$, $I_{28} = [38n + 61, 40n + 60]$, $I_{17} = [20n + 34, 22n + 33]$, $I_{19} = [22n + 37, 24n + 36]$ and $I_{25} = [32n + 61, 34n + 60]$.

Concatenating these intervals, we have covered $[1, 40n + 60] = I_0 I_1 \cdots I_{28}$. Therefore, the block construction $[A^T | A_0^T | \cdots | A_{n-1}^T]$ is a $5 \times (8n + 12)$ Heffter array.

2.7.2.7 $5 \times (8n + 13)$ Heffter Arrays

Let $n \geq 0$, and

$$A = \begin{bmatrix} \overline{1} & \overline{2} & \overline{3} & \overline{40n+65} & \overline{40n+64} \\ \overline{8n+15} & \overline{12n+20} & \overline{20n+34} & \overline{24n+40} & \overline{24n+41} \\ \overline{8n+14} & \overline{10n+18} & \overline{18n+31} & \overline{24n+42} & \overline{24n+43} \\ \overline{4n+9} & \overline{18n+29} & \overline{24n+44} & \overline{24n+45} & \overline{22n+37} \\ \overline{8n+13} & \overline{16n+27} & \overline{24n+47} & \overline{24n+39} & \overline{24n+46} \\ \overline{4n+7} & \overline{18n+30} & \overline{24n+49} & \overline{24n+48} & \overline{22n+36} \\ \overline{20n+33} & \overline{24n+50} & \overline{8n+12} & \overline{12n+22} & \overline{24n+51} \\ \overline{16n+25} & \overline{24n+52} & \overline{8n+16} & \overline{8n+10} & \overline{24n+53} \\ \overline{24n+55} & \overline{4n+6} & \overline{12n+21} & \overline{24n+54} & \overline{16n+26} \\ \overline{24n+57} & \overline{24n+56} & \overline{16n+28} & \overline{8n+11} & \overline{24n+38} \\ \overline{18n+32} & \overline{22n+35} & \overline{24n+58} & \overline{24n+59} & \overline{4n+4} \\ \overline{10n+19} & \overline{24n+61} & \overline{14n+23} & \overline{4n+5} & \overline{24n+60} \\ \overline{24n+62} & \overline{24n+63} & \overline{8n+8} & \overline{16n+24} & \overline{8n+17} \end{bmatrix},$$

a block with row sums

$$[2\mathfrak{D} + 1, 0, 0, 0, 0, 0, 0, 0, 0, 0, 0, 0, 0, 0]$$

and column sums

$$[0, \overline{2\mathfrak{D} + 1}, 0, 0, 4\mathfrak{D} + 2].$$

The entries in A cover the intervals $I_0 = [1, 3]$, $I_6 = \{8n + 8\}$, $I_2 = [4n + 4, 4n + 7]$, $I_4 = \{4n + 9\}$, $I_8 = [8n + 10, 8n + 17]$, $I_{10} = [10n + 18, 10n + 19]$, $I_{14} = \{14n + 23\}$, $I_{33} = [40n + 64, 40n + 65]$, $I_{22} = [22n + 35, 22n + 37]$, $I_{18} = [18n + 29, 18n + 32]$, $I_{16} = [16n + 24, 16n + 28]$, $I_{20} = [20n + 33, 20n + 34]$, $I_{24} = [24n + 38, 24n + 63]$ and $I_{12} = [12n + 20, 12n + 22]$. For $0 \leq r \leq n - 1$,

$$A_r = \begin{bmatrix} \overline{8n-4r+9} & \overline{16n+2r+29} & \overline{24n-2r+37} & \overline{24n+2r+64} & \overline{24n+2r+65} \\ \overline{4n-4r+2} & \overline{18n+2r+33} & \overline{22n-2r+34} & \overline{26n+2r+64} & \overline{26n+2r+65} \\ \overline{4n-4r+3} & \overline{10n+2r+20} & \overline{14n-2r+22} & \overline{28n+2r+64} & \overline{28n+2r+65} \\ \overline{8n-4r+6} & \overline{8n+2r+18} & \overline{16n-2r+23} & \overline{30n+2r+64} & \overline{30n+2r+65} \\ \overline{8n-4r+7} & \overline{16n+2r+30} & \overline{24n-2r+36} & \overline{32n+2r+64} & \overline{32n+2r+65} \\ \overline{4n-4r} & \overline{18n+2r+34} & \overline{22n-2r+33} & \overline{34n+2r+64} & \overline{34n+2r+65} \\ \overline{4n-4r+1} & \overline{10n+2r+21} & \overline{14n-2r+21} & \overline{36n+2r+64} & \overline{36n+2r+65} \\ \overline{8n-4r+4} & \overline{8n+2r+19} & \overline{16n-2r+22} & \overline{38n+2r+64} & \overline{38n+2r+65} \end{bmatrix},$$

a variable block with all row and column sums zero. The entries in A_r cover the intervals $[4n - 4r, 4n - 4r + 3]$, $\{8n - 4r + 9\}$, $[8n - 4r + 6, 8n - 4r + 7]$, $\{8n - 4r + 4\}$, $[8n + 2r + 18, 8n + 2r + 19]$, $[34n + 2r + 64, 34n + 2r + 65]$, $[18n + 2r + 33, 18n + 2r + 34]$, $[32n + 2r + 64, 32n + 2r + 65]$, $[14n - 2r + 21, 14n - 2r + 22]$, $[24n - 2r + 36, 24n - 2r + 37]$, $[28n + 2r + 64, 28n + 2r + 65]$, $[38n + 2r + 64, 38n + 2r + 65]$, $[10n + 2r + 20, 10n + 2r + 21]$, $[22n - 2r + 33, 22n - 2r + 34]$, $[36n + 2r + 64, 36n + 2r + 65]$, $[16n + 2r + 29, 16n + 2r + 30]$, $[16n - 2r + 22, 16n - 2r + 23]$, $[30n + 2r + 64, 30n + 2r + 65]$, $[24n + 2r + 64, 24n + 2r + 65]$ and $[26n + 2r + 64, 26n + 2r + 65]$. Considering $0 \leq r \leq n - 1$, these blocks cover the intervals $I_1 = [4, 4n + 3]$, $I_{29} = [8n + 18, 10n + 17]$, $I_{13} = [34n + 64, 36n + 63]$, $I_{23} = [18n + 33, 20n + 32]$,

$I_{27} = [32n + 64, 34n + 63]$, $I_{32} = [12n + 23, 14n + 22]$, $I_{11} = [22n + 38, 24n + 37]$, $I_{21} = [28n + 64, 30n + 63]$, $I_{31} = [38n + 64, 40n + 63]$, $I_{17} = [10n + 20, 12n + 19]$, $I_{15} = [20n + 35, 22n + 34]$, $I_{28} = [36n + 64, 38n + 63]$, $I_{25} = [16n + 29, 18n + 28]$, $I_{26} = [14n + 24, 16n + 23]$, $I_3 = [30n + 64, 32n + 63]$, $I_5 = [24n + 64, 26n + 63]$ and $I_7 = [26n + 64, 28n + 63]$. Additionally, we split the intervals $\{8n - 4r + 9\}$, $[8n - 4r + 6, 8n - 4r + 7]$ and $\{8n - 4r + 4\}$ into the sequences

$$(4n + 8, 4n + 12, \dots, 8n + 4),$$

$$(4n + 10, 4n + 14, \dots, 8n + 6),$$

$$(4n + 11, 4n + 15, \dots, 8n + 7),$$

and

$$(4n + 13, 4n + 17, \dots, 8n + 9),$$

and rejoin them into the intervals $I_3 = \{4n + 8\}$, $I_5 = [4n + 10, 8n + 7]$ and $I_7 = \{8n + 9\}$.

Concatenating these intervals, we have covered $[1, 40n + 65] = I_0 I_1 \cdots I_{33}$. Therefore, the block construction $[A^T | A_0^T | \cdots | A_{n-1}^T]$ is a $5 \times (8n + 13)$ Heffter array.

2.7.2.8 $5 \times (8n + 14)$ Heffter Arrays

Let $n \geq 0$, and

$$A = \begin{bmatrix} 1 & \bar{2} & 3 & 40n+70 & 40n+69 \\ \overline{8n+16} & \overline{12n+21} & \overline{20n+36} & \overline{24n+44} & \overline{24n+43} \\ \overline{8n+15} & \overline{14n+26} & \overline{22n+40} & \overline{24n+45} & \overline{24n+46} \\ \overline{8n+14} & \overline{12n+22} & \overline{20n+35} & \overline{24n+47} & \overline{24n+48} \\ \overline{4n+9} & \overline{16n+29} & \overline{20n+37} & \overline{24n+49} & \overline{24n+50} \\ \overline{4n+8} & \overline{14n+25} & \overline{18n+32} & \overline{24n+51} & \overline{24n+52} \\ \overline{8n+12} & \overline{8n+17} & \overline{16n+28} & \overline{24n+53} & \overline{24n+54} \\ \overline{8n+13} & \overline{16n+30} & \overline{24n+56} & \overline{24n+42} & \overline{24n+55} \\ \overline{4n+6} & \overline{24n+57} & \overline{10n+19} & \overline{24n+58} & \overline{14n+24} \\ \overline{4n+7} & \overline{24n+60} & \overline{24n+59} & \overline{18n+33} & \overline{22n+39} \\ \overline{8n+10} & \overline{16n+27} & \overline{24n+62} & \overline{8n+18} & \overline{24n+61} \\ \overline{16n+31} & \overline{24n+63} & \overline{8n+11} & \overline{24n+64} & \overline{24n+41} \\ \overline{24n+66} & \overline{4n+4} & \overline{24n+65} & \overline{14n+23} & \overline{10n+20} \\ \overline{24n+67} & \overline{24n+68} & \overline{18n+34} & \overline{4n+5} & \overline{22n+38} \end{bmatrix},$$

a block with row sums

$$[2\mathfrak{D} + 1, 0, 0, 0, 0, 0, 0, 0, 0, 0, 0, 0, 0, 0]$$

and column sums

$$[\overline{2\mathfrak{D} + 1}, \overline{2\mathfrak{D} + 1}, 2\mathfrak{D} + 1, 0, 4\mathfrak{D} + 2].$$

The entries in A cover the intervals $I_0 = [1, 3]$, $I_2 = [4n + 4, 4n + 9]$, $I_4 = [8n + 10, 8n + 18]$, $I_8 = [12n + 21, 12n + 22]$, $I_{10} = [14n + 23, 14n + 26]$, $I_{18} = [22n + 38, 22n + 40]$, $I_{29} = [40n + 69, 40n + 70]$, $I_{12} = [16n + 27, 16n + 31]$, $I_{14} = [18n + 32, 18n + 34]$, $I_6 = [10n + 19, 10n + 20]$,

$I_{20} = [24n + 41, 24n + 68]$ and $I_{16} = [20n + 35, 20n + 37]$. For $0 \leq r \leq n - 1$,

$$A_r = \begin{bmatrix} \overline{8n-4r+8} & \overline{8n+2r+19} & \overline{16n-2r+26} & \overline{24n+2r+69} & \overline{24n+2r+70} \\ \overline{8n-4r+9} & \overline{16n+2r+32} & \overline{24n-2r+40} & \overline{26n+2r+69} & \overline{26n+2r+70} \\ \overline{4n-4r+2} & \overline{10n+2r+21} & \overline{14n-2r+22} & \overline{28n+2r+69} & \overline{28n+2r+70} \\ \overline{4n-4r+3} & \overline{18n+2r+35} & \overline{22n-2r+37} & \overline{30n+2r+69} & \overline{30n+2r+70} \\ \overline{8n-4r+6} & \overline{8n+2r+20} & \overline{16n-2r+25} & \overline{32n+2r+69} & \overline{32n+2r+70} \\ \overline{8n-4r+7} & \overline{16n+2r+33} & \overline{24n-2r+39} & \overline{34n+2r+69} & \overline{34n+2r+70} \\ \overline{4n-4r} & \overline{10n+2r+22} & \overline{14n-2r+21} & \overline{36n+2r+69} & \overline{36n+2r+70} \\ \overline{4n-4r+1} & \overline{18n+2r+36} & \overline{22n-2r+36} & \overline{38n+2r+69} & \overline{38n+2r+70} \end{bmatrix},$$

a variable block with all row and column sums zero. The entries in A_r cover the intervals $[4n - 4r, 4n - 4r + 3]$, $[8n - 4r + 6, 8n - 4r + 9]$, $[8n + 2r + 19, 8n + 2r + 20]$, $[32n + 2r + 69, 32n + 2r + 70]$, $[14n - 2r + 21, 14n - 2r + 22]$, $[24n + 2r + 69, 24n + 2r + 70]$, $[16n + 2r + 32, 16n + 2r + 33]$, $[16n - 2r + 25, 16n - 2r + 26]$, $[22n - 2r + 36, 22n - 2r + 37]$, $[34n + 2r + 69, 34n + 2r + 70]$, $[30n + 2r + 69, 30n + 2r + 70]$, $[24n - 2r + 39, 24n - 2r + 40]$, $[36n + 2r + 69, 36n + 2r + 70]$, $[10n + 2r + 21, 10n + 2r + 22]$, $[38n + 2r + 69, 38n + 2r + 70]$, $[26n + 2r + 69, 26n + 2r + 70]$, $[18n + 2r + 35, 18n + 2r + 36]$ and $[28n + 2r + 69, 28n + 2r + 70]$. Considering $0 \leq r \leq n - 1$, these blocks cover the intervals $I_1 = [4, 4n + 3]$, $I_3 = [4n + 10, 8n + 9]$, $I_5 = [8n + 19, 10n + 18]$, $I_{25} = [32n + 69, 34n + 68]$, $I_9 = [12n + 23, 14n + 22]$, $I_{21} = [24n + 69, 26n + 68]$, $I_{13} = [16n + 32, 18n + 31]$, $I_{11} = [14n + 27, 16n + 26]$, $I_{17} = [20n + 38, 22n + 37]$, $I_{26} = [34n + 69, 36n + 68]$, $I_{24} = [30n + 69, 32n + 68]$, $I_{19} = [22n + 41, 24n + 40]$, $I_{27} = [36n + 69, 38n + 68]$, $I_7 = [10n + 21, 12n + 20]$, $I_{28} = [38n + 69, 40n + 68]$, $I_{22} = [26n + 69, 28n + 68]$, $I_{15} = [18n + 35, 20n + 34]$ and $I_{23} = [28n + 69, 30n + 68]$.

Concatenating these intervals, we have covered $[1, 40n + 70] = I_0 I_1 \cdots I_{29}$. Therefore, the block construction $[A^T | A_0^T | \cdots | A_{n-1}^T]$ is a $5 \times (8n + 14)$ Heffter array.

2.7.3 Constructions For m and n Large

2.7.3.1 Large $(4m + 1) \times (4n + 2)$ Construction

See Section 2.7.2 for the description of Heffter arrays of dimension $5 \times (4n + 2)$. In this section, we will describe the construction of $(4m + 1) \times (4n + 2)$ Heffter arrays where $m \geq 2$ and $n \geq 1$. Let

$$A = \begin{bmatrix} \overline{\mathfrak{D}-10} & \overline{\mathfrak{D}-9} & \overline{5} & \overline{\mathfrak{D}-3} & \overline{\mathfrak{D}-4} & \overline{4} \\ \overline{\mathfrak{D}-6} & \overline{\mathfrak{D}-8} & \overline{\mathfrak{D}-16} & \overline{\mathfrak{D}-19} & \overline{\mathfrak{D}-20} & \overline{\mathfrak{D}-15} \\ \overline{6} & \overline{\mathfrak{D}-23} & \overline{\mathfrak{D}-7} & \overline{1} & \overline{\mathfrak{D}-21} & \overline{\mathfrak{D}-14} \\ \overline{\mathfrak{D}} & \overline{\mathfrak{D}-22} & \overline{\mathfrak{D}-11} & \overline{\mathfrak{D}-18} & \overline{\mathfrak{D}-2} & \overline{\mathfrak{D}-13} \\ \overline{\mathfrak{D}-1} & \overline{2} & \overline{\mathfrak{D}-17} & \overline{\mathfrak{D}-5} & \overline{3} & \overline{\mathfrak{D}-12} \\ \overline{\mathfrak{D}-47} & \overline{\mathfrak{D}-46} & \overline{\mathfrak{D}-45} & \overline{\mathfrak{D}-44} & \overline{\mathfrak{D}-37} & \overline{\mathfrak{D}-39} \\ \overline{\mathfrak{D}-41} & \overline{\mathfrak{D}-40} & \overline{\mathfrak{D}-36} & \overline{\mathfrak{D}-38} & \overline{\mathfrak{D}-43} & \overline{\mathfrak{D}-42} \\ \overline{\mathfrak{D}-35} & \overline{\mathfrak{D}-34} & \overline{\mathfrak{D}-33} & \overline{\mathfrak{D}-32} & \overline{\mathfrak{D}-25} & \overline{\mathfrak{D}-27} \\ \overline{\mathfrak{D}-29} & \overline{\mathfrak{D}-28} & \overline{\mathfrak{D}-24} & \overline{\mathfrak{D}-26} & \overline{\mathfrak{D}-31} & \overline{\mathfrak{D}-30} \end{bmatrix},$$

a block with row sums

$$[2\mathfrak{D} + 1, 0, 0, 0, 0, 0, 0, 0, 0]$$

and column sums

$$[2\mathfrak{D} + 1, 0, 0, 0, 0, 0, 0].$$

The entries in A cover the intervals $I_0 = [1, 6]$ and $I_8 = [16mn + 8m + 4n - 45, 16mn + 8m + 4n + 2]$. For $0 \leq r \leq n - 2$,

$$A_r = \begin{bmatrix} \overline{4r+7} & \overline{4r+8} & \overline{4r+9} & \overline{4r+10} \\ \overline{6n-2r} & \overline{10n-2r-4} & \overline{6n-2r-1} & \overline{10n-2r-5} \\ \overline{6n+2r+1} & \overline{10n+2r-3} & \overline{6n+2r+2} & \overline{10n+2r-2} \\ \overline{12n+24r-5} & \overline{12n+24r-3} & \overline{12n+24r-1} & \overline{12n+24r+1} \\ \overline{12n+24r-4} & \overline{12n+24r-2} & \overline{12n+24r} & \overline{12n+24r+2} \\ \overline{12n+24r+3} & \overline{12n+24r+4} & \overline{12n+24r+7} & \overline{12n+24r+8} \\ \overline{12n+24r+5} & \overline{12n+24r+6} & \overline{12n+24r+9} & \overline{12n+24r+10} \\ \overline{12n+24r+11} & \overline{12n+24r+12} & \overline{12n+24r+18} & \overline{12n+24r+17} \\ \overline{12n+24r+14} & \overline{12n+24r+16} & \overline{12n+24r+15} & \overline{12n+24r+13} \end{bmatrix},$$

a variable block with all row and column sums zero. The entries in A_r cover the intervals $[4r + 7, 4r + 10]$, $[6n - 2r - 1, 6n - 2r]$, $[6n + 2r + 1, 6n + 2r + 2]$, $[10n - 2r - 5, 10n - 2r - 4]$, $[10n + 2r - 3, 10n + 2r - 2]$ and $[12n + 24r - 5, 12n + 24r + 18]$. Considering $0 \leq r \leq n - 2$, these blocks cover the intervals $I_1 = [7, 4n + 2]$, $I_2 = [4n + 3, 6n]$, $I_3 = [6n + 1, 8n - 2]$, $I_4 = [8n - 1, 10n - 4]$, $I_5 = [10n - 3, 12n - 6]$ and $I_6 = [12n - 5, 36n - 30]$. Additionally, let E_0 be a $(4m - 8) \times (4n + 2)$ shiftable Heffter array and $E = E_0 + 36n - 30$, covering the interval $I_7 = [36n - 29, 8(2n + 1)(m - 2) + 36n - 30]$. Concatenating these intervals, we have covered $[1, 16mn + 8m + 4n + 2] = I_0 I_1 \cdots I_8$. Therefore, the block construction below is a $(4m + 1) \times (4n + 2)$ Heffter array.

$$\left[\begin{array}{c|c|c|c} A & A_0 & \cdots & A_{n-2} \\ \hline & E & & \end{array} \right]$$

2.7.3.2 Large $(4m + 3) \times (4n + 2)$ Construction

See Section 2.7.1 for the description of Heffter arrays of dimension $3 \times (4n + 2)$. In this section, we will describe the construction of $(4m + 3) \times (4n + 2)$ Heffter arrays where $m \geq 1$ and $n \geq 1$. Let

$$A = \begin{bmatrix} 2 & \overline{\mathfrak{D}-2} & \overline{\mathfrak{D}-4} & 3 & \overline{\mathfrak{D}-5} & \overline{\mathfrak{D}-7} \\ \overline{\mathfrak{D}-1} & \overline{\mathfrak{D}-8} & \overline{\mathfrak{D}-3} & \overline{\mathfrak{D}-9} & \overline{5} & 4 \\ \overline{\mathfrak{D}} & \overline{6} & 1 & \overline{\mathfrak{D}-6} & \overline{\mathfrak{D}-10} & \overline{\mathfrak{D}-11} \\ \overline{\mathfrak{D}-35} & \overline{\mathfrak{D}-34} & \overline{\mathfrak{D}-33} & \overline{\mathfrak{D}-32} & \overline{\mathfrak{D}-25} & \overline{\mathfrak{D}-27} \\ \overline{\mathfrak{D}-29} & \overline{\mathfrak{D}-28} & \overline{\mathfrak{D}-24} & \overline{\mathfrak{D}-26} & \overline{\mathfrak{D}-31} & \overline{\mathfrak{D}-30} \\ \overline{\mathfrak{D}-23} & \overline{\mathfrak{D}-22} & \overline{\mathfrak{D}-21} & \overline{\mathfrak{D}-20} & \overline{\mathfrak{D}-13} & \overline{\mathfrak{D}-15} \\ \overline{\mathfrak{D}-17} & \overline{\mathfrak{D}-16} & \overline{\mathfrak{D}-12} & \overline{\mathfrak{D}-14} & \overline{\mathfrak{D}-19} & \overline{\mathfrak{D}-18} \end{bmatrix},$$

a block with row sums

$$[2\mathfrak{D} + 1, 0, 0, 0, 0, 0, 0]$$

and column sums

$$[2\mathfrak{D} + 1, 0, 0, 0, 0, 0, 0].$$

The entries in A cover the intervals $I_0 = [1, 6]$ and $I_8 = [16mn + 8m + 12n - 29, 16mn + 8m + 12n + 6]$. and for $0 \leq r \leq n - 2$,

$$A_r = \begin{bmatrix} \frac{4r+7}{6n+2r+1} & \frac{\overline{4r+8}}{10n+2r-3} & \frac{\overline{4r+9}}{6n+2r+2} & \frac{4r+10}{10n+2r-2} \\ \frac{12n+16r-5}{12n+16r-3} & \frac{12n+16r-4}{12n+16r-1} & \frac{12n+16r+2}{12n+16r} & \frac{12n+16r+1}{12n+16r-2} \\ \frac{12n+16r+3}{12n+16r+7} & \frac{12n+16r+4}{12n+16r+8} & \frac{12n+16r+5}{12n+16r+9} & \frac{12n+16r+6}{12n+16r+10} \end{bmatrix},$$

a variable block with all row and column sums zero. The entries in A_r cover the intervals $[4r + 7, 4r + 10]$, $[6n - 2r - 1, 6n - 2r]$, $[6n + 2r + 1, 6n + 2r + 2]$, $[10n - 2r - 5, 10n - 2r - 4]$, $[10n + 2r - 3, 10n + 2r - 2]$ and $[12n + 16r - 5, 12n + 16r + 10]$. Considering $0 \leq r \leq n - 2$, these blocks cover the intervals $I_1 = [7, 4n + 2]$, $I_2 = [4n + 3, 6n]$, $I_3 = [6n + 1, 8n - 2]$, $I_4 = [8n - 1, 10n - 4]$, $I_5 = [10n - 3, 12n - 6]$ and $I_6 = [12n - 5, 28n - 22]$. Additionally, let E_0 be a $(4m - 4) \times (4n + 2)$ shiftable Heffter array and $E = E_0 + 28n - 22$, covering the interval $I_7 = [28n - 21, 8(2n + 1)(m - 1) + 28n - 22]$. Concatenating these intervals, we have covered $[1, 16mn + 8m + 12n + 6] = I_0 I_1 \cdots I_8$. Then, the block construction below is a $(4m + 3) \times (4n + 2)$ Heffter array.

$$\left[\begin{array}{c|c|c|c} A & A_0 & \cdots & A_{n-2} \\ \hline & E & & \end{array} \right]$$

2.7.3.3 Large $(4m + 3) \times (4n + 3)$ Construction

See Section 2.7.1 for the description of Heffter arrays of dimension $3 \times (4n + 3)$. In this section, we will describe the construction of $(4m + 3) \times (4n + 3)$ Heffter arrays where $m \geq 1$ and $n \geq 1$. Let $y = m + n$,

$$A = \begin{bmatrix} \overline{\mathfrak{D}-3} & \overline{\mathfrak{D}-1} & \overline{5} & \overline{6} & \overline{7} & \overline{8} & \overline{9} \\ \overline{\mathfrak{D}} & \overline{\mathfrak{D}-2} & \overline{2} & \overline{6y+5} & \overline{10y+5} & \overline{6y+4} & \overline{10y+4} \\ 4 & \overline{1} & \overline{3} & \overline{6y+6} & \overline{10y+6} & \overline{6y+7} & \overline{10y+7} \\ 10 & \overline{6y+3} & \overline{6y+8} & \overline{12y+14} & \overline{12y+21} & \overline{12y+9} & \overline{12y+7} \\ \overline{11} & \overline{10y+3} & \overline{10y+8} & \overline{12y+16} & \overline{12y+20} & \overline{12y+19} & \overline{12y+17} \\ \overline{12} & \overline{6y+2} & \overline{6y+9} & \overline{12y+15} & \overline{12y+6} & \overline{12y+12} & \overline{12y+8} \\ 13 & \overline{10y+2} & \overline{10y+9} & \overline{12y+18} & \overline{12y+13} & \overline{12y+11} & \overline{12y+10} \end{bmatrix},$$

a block with row sums

$$[2\overline{\mathfrak{D}} + 1, 0, 0, 0, 0, 0, 0]$$

and column sums

$$[2\overline{\mathfrak{D}} + 1, 0, 0, 0, 0, 0, 0].$$

The entries in A cover the intervals $I_0 = [1, 13]$, $I_3 = [6m + 6n + 2, 6m + 6n + 9]$, $I_6 = [10m + 10n + 2, 10m + 10n + 9]$, $I_8 = [12m + 12n + 6, 12m + 12n + 21]$ and $I_{11} = [16mn +$

$12m + 12n + 6, 16mn + 12m + 12n + 9]$. For $0 \leq r \leq m + n - 3$, let

$$B_r = \begin{bmatrix} \frac{4r+14}{6m+6n-2r+1} & \frac{4r+15}{10m+10n-2r+1} & \frac{4r+16}{6m+6n-2r} & \frac{4r+17}{10m+10n-2r} \\ \frac{6m+6n+2r+10}{12m+12n+16r+22} & \frac{6m+6n+2r+11}{12m+12n+16r+23} & \frac{6m+6n+2r+12}{12m+12n+16r+24} & \frac{6m+6n+2r+13}{12m+12n+16r+25} \\ \frac{10m+10n+2r+10}{12m+12n+16r+26} & \frac{10m+10n+2r+11}{12m+12n+16r+27} & \frac{10m+10n+2r+12}{12m+12n+16r+28} & \frac{10m+10n+2r+13}{12m+12n+16r+29} \\ \frac{12m+12n+16r+30}{12m+12n+16r+31} & \frac{12m+12n+16r+31}{12m+12n+16r+32} & \frac{12m+12n+16r+32}{12m+12n+16r+33} & \frac{12m+12n+16r+33}{12m+12n+16r+34} \\ \frac{12m+12n+16r+34}{12m+12n+16r+35} & \frac{12m+12n+16r+35}{12m+12n+16r+36} & \frac{12m+12n+16r+36}{12m+12n+16r+37} & \frac{12m+12n+16r+37}{12m+12n+16r+38} \end{bmatrix},$$

a variable block with all row and column sums zero. The entries in B_r cover the intervals $[4r + 14, 4r + 17]$, $[6m + 6n - 2r, 6m + 6n - 2r + 1]$, $[10m + 10n - 2r, 10m + 10n - 2r + 1]$, $[6m + 6n + 2r + 10, 6m + 6n + 2r + 11]$, $[10m + 10n + 2r + 10, 10m + 10n + 2r + 11]$ and $[12m + 12n + 16r + 22, 12m + 12n + 16r + 37]$. Considering $0 \leq r \leq m + n - 3$, these blocks cover the intervals $I_1 = [14, 4m + 4n + 5]$, $I_2 = [4m + 4n + 6, 6m + 6n + 1]$, $I_5 = [8m + 8n + 6, 10m + 10n + 1]$, $I_4 = [6m + 6n + 10, 8m + 8n + 5]$, $I_7 = [10m + 10n + 10, 12m + 12n + 5]$ and $I_9 = [12m + 12n + 22, 28m + 28n - 11]$. Additionally, let E_0 be a $(4m - 4) \times (4n - 4)$ shiftable Heffter array and $E = E_0 + 28m + 28n - 11$, covering the interval $I_{10} = [28m + 28n - 10, 16(n - 1)(m - 1) + 28m + 28n - 11]$. Concatenating these intervals, we have covered $[1, 16mn + 12m + 12n + 9] = I_0 I_1 \cdots I_{11}$. Then, the block construction below is a $(4m + 1) \times (4n + 3)$ Heffter array.

$$\begin{bmatrix} A & B_0 & \cdots & B_{n-2} \\ B_{n-1}^T & & & \\ \vdots & & & \\ B_{m+n-3}^T & & & E \end{bmatrix}$$

2.7.3.4 Large $(4m + 1) \times (4n + 1)$ Construction

See Section 2.7.2 for the description of Heffter arrays of dimension $5 \times (4n + 1)$. In this section, we will describe the construction of $(4m + 1) \times (4n + 1)$ Heffter arrays where $m \geq 2$ and $n \geq 2$. Let $y = m + n$, and

$$A = \begin{bmatrix} \mathfrak{D}-17 & \mathfrak{D}-8 & \overline{\mathfrak{D}-3} & \overline{\mathfrak{D}-15} & 7 & 8 & \overline{9} & \overline{10} & 11 \\ \mathfrak{D}-7 & 5 & \mathfrak{D}-6 & \overline{\mathfrak{D}-10} & \mathfrak{D}-1 & 6y-5 & \overline{10y-13} & \overline{6y-6} & 10y-14 \\ 4 & \mathfrak{D}-5 & \overline{\mathfrak{D}} & \mathfrak{D}-12 & \overline{\mathfrak{D}-13} & \overline{6y-4} & 10y-12 & \overline{6y-3} & \overline{10y-11} \\ \overline{\mathfrak{D}-9} & 3 & \overline{\mathfrak{D}-4} & \mathfrak{D}-14 & \mathfrak{D}-2 & \overline{12y-16} & \overline{12y-15} & \overline{12y-12} & 12y-11 \\ \overline{\mathfrak{D}-11} & 6 & \overline{2} & 1 & \mathfrak{D}-16 & \overline{12y-14} & 12y-13 & 12y-10 & \overline{12y-9} \\ 12 & 6y-7 & \overline{6y-2} & 12y-8 & \overline{12y-6} & 12y+8 & \overline{12y+15} & 12y+3 & \overline{12y+1} \\ 13 & \overline{10y-15} & 10y-10 & \overline{12y-7} & 12y-5 & \overline{12y+10} & 12y+14 & 12y+13 & \overline{12y+11} \\ 14 & 6y-8 & \overline{6y-1} & 12y-4 & 12y-2 & 12y+9 & 12y & \overline{12y+6} & 12y+2 \\ 15 & 10y-16 & \overline{10y-9} & 12y-3 & \overline{12y-1} & \overline{12y+12} & 12y+7 & \overline{12y+5} & 12y+4 \end{bmatrix},$$

a block with row sums

$$[0, 2\mathfrak{D} + 1, 0, 0, 0, 0, 0, 0, 0]$$

and column sums

$$[0, 2\mathfrak{D} + 1, \overline{2\mathfrak{D} + 1}, 0, 2\mathfrak{D} + 1, 0, 0, 0, 0].$$

The entries in A cover the intervals $I_0 = [1, 15]$, $I_3 = [6m + 6n - 8, 6m + 6n - 1]$, $I_6 = [10m + 10n - 16, 10m + 10n - 9]$, $I_8 = [12m + 12n - 16, 12m + 12n + 15]$ and $I_{11} = [16mn + 4m + 4n - 16, 16mn + 4m + 4n + 1]$. For $0 \leq r \leq m + n - 5$, let

$$B_r = \begin{bmatrix} \overline{4r+16} & \overline{4r+17} & \overline{4r+18} & \overline{4r+19} \\ \overline{6m+6n-2r-9} & \overline{10m+10n-2r-17} & \overline{6m+6n-2r-10} & \overline{10m+10n-2r-18} \\ \overline{6m+6n+2r} & \overline{10m+10n+2r-8} & \overline{6m+6n+2r+1} & \overline{10m+10n+2r-7} \\ \overline{12m+12n+24r+16} & \overline{12m+12n+24r+17} & \overline{12m+12n+24r+20} & \overline{12m+12n+24r+21} \\ \overline{12m+12n+24r+18} & \overline{12m+12n+24r+19} & \overline{12m+12n+24r+22} & \overline{12m+12n+24r+23} \\ \overline{12m+12n+24r+24} & \overline{12m+12n+24r+25} & \overline{12m+12n+24r+28} & \overline{12m+12n+24r+29} \\ \overline{12m+12n+24r+26} & \overline{12m+12n+24r+27} & \overline{12m+12n+24r+30} & \overline{12m+12n+24r+31} \\ \overline{12m+12n+24r+32} & \overline{12m+12n+24r+33} & \overline{12m+12n+24r+39} & \overline{12m+12n+24r+38} \\ \overline{12m+12n+24r+35} & \overline{12m+12n+24r+37} & \overline{12m+12n+24r+36} & \overline{12m+12n+24r+34} \end{bmatrix},$$

a variable block with all row and column sums zero. The entries in B_r cover the intervals $[4r + 16, 4r + 19]$, $[6m + 6n + 2r, 6m + 6n + 2r + 1]$, $[6m + 6n - 2r - 10, 6m + 6n - 2r - 9]$, $[10m + 10n + 2r - 8, 10m + 10n + 2r - 7]$, $[10m + 10n - 2r - 18, 10m + 10n - 2r - 17]$ and $[12m + 12n + 24r + 16, 12m + 12n + 24r + 39]$. Considering $0 \leq r \leq m + n - 5$, these blocks cover the intervals $I_1 = [16, 4m + 4n - 1]$, $I_4 = [6m + 6n, 8m + 8n - 9]$, $I_2 = [4m + 4n, 6m + 6n - 9]$, $I_7 = [10m + 10n - 8, 12m + 12n - 17]$, $I_5 = [8m + 8n - 8, 10m + 10n - 17]$ and $I_9 = [12m + 12n + 16, 36m + 36n - 81]$. Additionally, let E_0 be a $(4m - 8) \times (4n - 8)$ shiftable Heffter array and $E = E_0 + 36m + 36n - 81$, covering the interval $I_{10} = [36m + 36n - 80, 16(n - 2)(m - 2) + 36m + 36n - 81]$. Concatenating these intervals, we have covered $[1, 16mn + 4m + 4n + 1] = I_0 I_1 \cdots I_{11}$. Then, the block construction below is a $(4m + 1) \times (4n + 3)$ Heffter array.

$$\begin{bmatrix} A & B_0 & \cdots & B_{n-3} \\ \hline B_{n-2}^T & & & \\ \vdots & & E & \\ \hline B_{m+n-5}^T & & & \end{bmatrix}$$

2.7.3.5 Large $(4m + 3) \times (4n + 1)$ Construction

See Sections 2.7.1 and 2.7.2 for the description of Heffter arrays of dimension $3 \times (4n + 1)$ and $(4m + 3) \times 5$ respectively. In this section, we will describe the construction of $(4m + 3) \times (4n + 1)$ Heffter arrays where $m \geq 1$ and $n \geq 2$. Let $y = m + n$, and

$$A = \begin{bmatrix} \overline{\mathfrak{D}-7} & 3 & \overline{\mathfrak{D}-4} & 8 & \overline{9} & \overline{10} & 11 \\ \overline{\mathfrak{D}-3} & \overline{\mathfrak{D}-1} & \overline{2} & \overline{6y+1} & \overline{10y-3} & \overline{6y} & \overline{10y-4} \\ \overline{\mathfrak{D}-5} & \overline{\mathfrak{D}} & 5 & \overline{6y+2} & \overline{10y-2} & \overline{6y+3} & \overline{10y-1} \\ \overline{\mathfrak{D}-2} & 4 & \overline{\mathfrak{D}-6} & \overline{12y-4} & \overline{12y-3} & \overline{12y} & \overline{12y+1} \\ 7 & \overline{6} & \overline{1} & \overline{12y-2} & \overline{12y-1} & \overline{12y+2} & \overline{12y+3} \\ 12 & \overline{6y-1} & \overline{6y+4} & \overline{12y+17} & \overline{12y+4} & \overline{12y+10} & \overline{12y+18} \\ 13 & \overline{10y-5} & 10y & \overline{12y+13} & \overline{12y+19} & \overline{12y+12} & \overline{12y+14} \\ 14 & \overline{6y-2} & \overline{6y+5} & \overline{12y+6} & \overline{12y+8} & \overline{12y+16} & \overline{12y+7} \\ 15 & \overline{10y-6} & \overline{10y+1} & \overline{12y+15} & \overline{12y+9} & \overline{12y+11} & \overline{12y+5} \end{bmatrix},$$

2.7.3.6 $(4m) \times (4n + 1)$ Heffter Arrays

Let $m \geq 1$ and $n \geq 1$. See Section 2.7.2 for the description of Heffter arrays of dimension $5 \times (4m)$, and let A be such an array. Recall that the row and column sums of A are zero over the integers. Additionally, let B be a shifttable $(4m \times 4(n - 1))$ Heffter array.

Then, the block construction $[A^T|B + 20m]$ is a $(4m) \times (4n + 1)$ Heffter array.

2.7.3.7 $(4m) \times (4n + 3)$ Heffter Arrays

Let $m \geq 1$ and $n \geq 0$. See Section 2.7.1 for the description of Heffter arrays of dimension $3 \times (4m)$, and let A be such an array. Recall that the row and column sums of A are zero over the integers. Additionally, let B be a shifttable $(4m) \times (4n)$ Heffter array.

Then, the block construction $[A^T|B + 12m]$ is a $(4m) \times (4n + 3)$ Heffter array.

2.8 Future Work

The ultimate goal for these constructions was to find simple Heffter arrays for all dimensions $m, n > 2$. Mattern succeeded for the $3 \times n$ arrays, and she was able to find simple orderings of three out of five rows for the $5 \times n$ arrays. The last two rows are made up of pairs at distance 1, which was convenient for the purpose of finding our $5 \times n$ constructions. However, it is possible to construct $5 \times n$ Heffter arrays with a rather different approach.

We propose such an approach here. Consider the Skolem sequences of order 4 and 8, 41134232 and 5673853627248114. We use the Skolem sequence of order 4 to generate a Heffter system,

$$\begin{array}{cccc} 1 & 2 & 3 & 4 \\ 2 & 6 & 4 & 1 \\ \bar{3} & \bar{8} & \bar{7} & \bar{5} \end{array}$$

and the Skolem sequence of order 8 to produce a partition of $[5, 20]$ into differences $[1, 8]$,

$$\begin{array}{cccccccc} 1 & 2 & 3 & 4 & 5 & 6 & 7 & 8 \\ \hline 18 & 13 & 8 & 16 & 5 & 6 & 7 & 9 \\ 19 & 15 & 11 & 20 & 10 & 12 & 14 & 17. \end{array}$$

Then, we expand the last two rows of the Heffter triple system using our Skolem partition,

$$\begin{array}{cccc} 1 & 2 & 3 & 4 \\ \bar{13} & \bar{6} & \bar{16} & \bar{18} \\ 15 & 12 & 20 & 19 \\ 8 & 9 & 7 & 5 \\ \bar{11} & \bar{17} & \bar{14} & \bar{10} \end{array}$$

and obtain a Heffter quintuple system. Since Skolem sequences exist for all $m \equiv 0 \pmod{4}$, this approach can be used to produce Heffter quintuple systems for \mathbb{Z}_{20n+1} for all n , giving hope that we can find alternate constructions for $5 \times 4n$ Heffter arrays. The author suspects that Mattern's approach to finding simple orderings of these constructions will be more fruitful.

Chapter 3

A Step Beyond DeVos When One Set is Two Cosets

This chapter is joint work with Matt DeVos, who provided the general outline of the proof, portions of the classification of 4-regular graphs with girth 4, as well as significant editorial contributions. The contents of this chapter are being divided into three papers regarding the classification of 4-regular edge-transitive graphs with girth 4, the 6-regular edge-transitive graphs with girth 3, and Theorem 3.3.4 respectively.

3.1 History

In this chapter, we will be considering arbitrary, possibly nonabelian groups. Therefore, we will use multiplicative notation throughout. For every positive integer n , we let Z_n denote a cyclic group of order n . For subsets A, B of a group G , we define the *product set* $AB = \{ab : a \in A, b \in B\}$.

In 1813, Cauchy [13] proved the following theorem.

Theorem 3.1.1 (Cauchy-Davenport). *If p is a prime and A and B are nonempty subsets of the cyclic group Z_p , then either $AB = Z_p$ or $|AB| \geq |A| + |B| - 1$.*

This result was rediscovered by Davenport [17] in 1935. Davenport [16] noted that his result was not original in 1947, and the above is now known as the Cauchy-Davenport theorem. Davenport's rediscovery garnered significant interest in related problems.

In 1953, Kneser [32] proved a generalization to the Cauchy-Davenport theorem for abelian groups. Here, $\text{Stab}(X) = \text{Stab}_G(X) = \{g \in G : gX = X\}$ is the *stabilizer* of X .

Theorem 3.1.2 (Kneser). *If A and B are nonempty finite subsets of an abelian group G , either $AB = G$ or $|AB| \geq |A| + |B| - |\text{Stab}(AB)|$.*

Kneser's theorem implies the Cauchy-Davenport theorem since $\text{Stab}_G(X)$ is necessarily a subgroup of G and the only subgroups of Z_p are the trivial group and Z_p itself.

In 2005, Károlyi [28] noted a corollary of Kneser’s theorem, that if $p(G)$ denotes the smallest prime divisor of $|G|$ then $|AB| \geq \min\{p(G), |A| + |B| - 1\}$. He proved that the same statement holds true in the setting of finite (possibly nonabelian) groups. In 2006, Wheeler [46] independently proved Károlyi’s theorem, having been given the problem by Károlyi prior to 2005.

Theorem 3.1.3 (Károlyi-Wheeler). *If A and B are nonempty subsets of a finite group G and $p(G) > |A| + |B| - 1$, then $|AB| \geq |A| + |B| - 1$.*

Both describe the theorem as the Cauchy-Davenport theorem for finite groups. This seems to be a bit of a misnomer, as it is easy to construct nontrivial examples where Károlyi’s theorem fails to capture Kneser’s.

In 2013, DeVos [18] proved what could properly be called the Cauchy-Davenport theorem for arbitrary groups.

Theorem 3.1.4 (DeVos). *Let A and B be nonempty finite subsets of a group G . Then, there exists a subgroup $H \leq G$ so that $|AB| \geq |A| + |B| - |H|$ and for every $y \in AB$, there exists $x \in G$ so that $y(x^{-1}Hx) \subseteq AB$.*

One can show that in the abelian case, there is a unique maximal subgroup H that satisfies the above, and that $H = \text{Stab}(AB)$, so Kneser’s theorem is a corollary of DeVos’s.

Parallel to this history is a study of inverse problems. In 1956, Vosper [44] proved that

Theorem 3.1.5 (Vosper). *If p is prime and $A, B \subseteq Z_p$ are nonempty, then $|AB| < |A| + |B|$ if and only if*

1. $|A| + |B| > p$,
2. $|A| = 1$ or $|B| = 1$,
3. $B = c(G \setminus A^{-1})$ for some $c \in G$, or
4. A and B are geometric progressions with the same ratio.

In 1960, Kemperman found a similar *structural* theorem for the case of abelian groups, classifying those sets A, B for which $|AB| < |A| + |B|$. DeVos broke tradition by proving his structural theorem, and then unwinding that structure to find the appropriate bounding theorem.

We will not describe DeVos’s structural theorem, as it takes eleven pages for him to do so, culminating in the rather terse Theorem 4.7 (all terms deliberately left undefined; see [18] for details).

Theorem 3.1.6 (DeVos). *A nontrivial trio is maximal and critical if and only if it is a song.*

In 2009, Gryniewicz [25] classifies those subsets A, B of an abelian group for which $|AB| = |A| + |B|$ in a paper entitled “A Step Beyond Kemperman’s Structure Theorem”, and we make progress towards taking that step beyond DeVos’s structural theorem. The ultimate goal here would be to classify those subsets A, B of an arbitrary group for which $|AB| = |A| + |B|$, but this chapter addresses a more modest problem where $B = xH \cup yH$ for some subgroup $H < G$. This special case is of particular interest since it exhibits all of the exceptional structures in DeVos’s Theorem.

3.2 Introduction

The vast majority of this chapter is graph theoretic in nature. In the next section, we’ll introduce the notation we’ll be using to describe graphs. Following that, we’ll provide the motivation for studying graphs.

3.2.1 Notation for Graphs

Notation abounds in this chapter. Most of the notation is fairly standard and the reader may refer to [20] for any undefined terms.

We define a graph $X = (V, E)$ to have a finite number of *vertices* V and *edges* E , a set of two-element subsets of V . That is, graphs are simple. In several proofs, we will describe graphs by describing graphs derived from those original graphs – we can’t guarantee these derived graphs to be simple, in fact, a few will have multiple edges. We call graphs that have multiple edges *multigraphs*. We never allow loops.

We will write edges like $uv \in E$, with $u \in V$ and $v \in V$, whenever possible. Otherwise, we will use the notation $\{u, v\}$. In a directed graph, we will use the notation (u, v) to denote the *arc* from u to v . A vertex $v \in V$ is *incident* to an edge $e \in E$ if $v \in e$, and two vertices u and v are *adjacent* if $uv \in E$ and we sometimes write $u \sim v$ to denote adjacency. If v is incident to exactly d edges, then we say that v has *degree* $\deg(v) = d$. If $\deg(u) = \deg(v) = d$ for all $u, v \in V$, then we say that X is *d-regular*. We define $N(v)$ to be the set of *neighbors* of v , $N(v) = \{u \in V : u \sim v\}$. For directed graphs, we define the *in-degree* and *out-degree* to be $d^+(v) = |\{(u, v) \in E\}|$ and $d^-(v) = |\{(v, u) \in E\}|$ respectively.

For a subset $A \subset V$, we will write $X[A]$ to denote the *induced subgraph* with vertex set A and edges $\{uv \in E : u \in A \text{ and } v \in A\}$. When it is ambiguous which graph a vertex belongs to, we will write $\deg_X(v)$ to denote the degree of v in the graph X . Most frequently, we will be interested in the degree of v in the induced subgraph $X[A]$, and we write $\deg_A(v)$ as a shorthand for $\deg_{X[A]}(v)$.

Given two graphs $X = (V, E)$ and $Y = (W, F)$, we say that X and Y are *isomorphic* or write $X \cong Y$ if there exists an *isomorphism* between X and Y – a bijection $\phi : V \rightarrow W$ such that $\phi(E) = \{\{\phi(u), \phi(v)\} : uv \in E\} = F$. Given a graph X , we write $\text{Aut}(X)$ to be the *automorphism group* of X : the set of isomorphisms between X and itself.

The *orbit* of $G \leq \text{Aut}(X)$ on a subgraph z of X is $G(z) = \{\phi(z) : \phi \in G\}$. If the family of similar subgraphs is Z and $Z = G(z)$, then we say that $\text{Aut}(X)$ *acts transitively* on Z , or that X is *Z-transitive*. For example, if $uv \in E$ and $G(uv) = E$, then we say that X is *edge transitive*.

Our main theorem concerns *edge cuts*. Given a graph $X = (V, E)$ and a subset $A \subset V$ of its vertices, we define the *edge boundary* of A to be the edges between A and $V \setminus A$ which we denote $\partial(A) = \{uv \in E : u \in A, v \notin A\}$. The set $\partial(A)$ is an edge cut, in that there are no edges between A and $V \setminus A$ in the graph $(V, E \setminus \partial(A))$. We denote the size of an edge cut by $c(A) = |\partial(A)|$. Similar to the boundary, we sometimes need to refer to the edges interior to A , denoted $E_A = E(X[A])$. If X is a d -regular graph and $|c(A)| \leq 2d$ we will call $\partial(A)$ a *small edge cut*.

We call a subgraph C of X a *cycle* if it consists of vertices (v_1, \dots, v_ℓ) and edges $v_i v_{i+1}$ for all $1 \leq i < \ell$ and $v_\ell v_1$. We sometimes specify cycles by their vertices, or by their edges, and ℓ is the *length* of the cycle. The *girth* g of a graph X is the minimum length attained by a cycle in X , and $g = \infty$ in the case that X is a forest. In a graph of girth g , we say that a cycle (v_1, \dots, v_g) of length g is a *girth cycle*. If a graph is edge transitive, every edge belongs to the same number of girth cycles. We say that X has *frequency* k if every edge belongs to exactly k girth cycles.

If a graph is both edge transitive and vertex transitive, then we say that it is *double transitive*¹ – the majority of this chapter is devoted to double transitive graphs. Particularly, we classify double transitive graphs whose degree and girth are specified. To that end, we say that X is a (d, g) -*graph* if it is d -regular, double transitive and has girth g . Frequency is a useful parameter to refine the classification, and we say that X is a (d, g, k) -*graph* if it is a (d, g) -graph with frequency k .

3.2.1.1 Definitions of Graphs

In this chapter, we find a large number of exceptional graphs, and a few families of graphs. In the interest of collecting all graph notation, we list them all here.

We define three *toroidal families*: 1-skeletons of tilings of the torus by triangles, squares, and hexagons. We will denote these families $\mathcal{T}_3, \mathcal{T}_4$, and \mathcal{T}_6 and refer to them as *triangulations, quadrangulations* and *hexangulations of the torus* respectively.

We also define families of graphs constructed by gluing copies of a fixed graph together at vertices. Let \mathcal{V} be a graph and $m \in \mathbb{N}$. The notation $[\mathcal{V}]_m$ denotes the family of connected graphs $X = (V, E)$ for which the set of all induced subgraphs of X which are isomorphic to \mathcal{V} covers every $v \in V$ exactly m times, and covers every $e \in E$ exactly once. Three graphs \tilde{v}

¹Sadly, the term *half-transitive* is used in the literature to refer to those double transitive graphs which are not arc-transitive. Some authors use *symmetric* to describe the graphs we call double transitive, whereas others insist that symmetric is arc-transitive.

appear in this paper: K_3, K_4 and C_4 which we denote by \triangle, \boxtimes and \square respectively. Brackets will be omitted from the notation for those families. For example, $\triangle_3 := [K_3]_3$.

Additionally, we use a fair bit of notation to compactly describe the exceptional graphs.

1. For $n \in \mathbb{N}$, the *cycle graph* C_n has $V = [1, n]$ and $E = \{\{v, v + 1 \pmod n\} : v \in V\}$.
2. For $n \in \mathbb{N}$, the *complete graph* K_n has $V = [1, n]$ and $E = \{ij : i, j \in [1, n], i \neq j\}$. We'll see K_n appear for $n \in [2, 7]$.
3. For $n_1, \dots, n_k \in \mathbb{N}$ the *complete multipartite graph* K_{n_1, \dots, n_k} has $\sum_{i=1}^k n_i$ vertices V partitioned into sets (V_1, \dots, V_k) of size $|V_i| = n_i$ for all $1 \leq i \leq k$, and edges $\{ab : a \in V_i, b \in V_j\}$ for all $i \neq j$. We need $K_{2,2}, K_{3,3}, K_{2,3}$ and some others we'll use special notation for.
4. Most of the complete multipartite graphs we see have $n_1 = \dots = n_k$. When this is the case, we use the notation $K_{n(k)} := K_{n, \dots, n}$. The graphs of this form that we see are $K_{3(3)}, K_{2(3)}$ (also known as the octahedron) and $K_{2(4)}$.
5. For $n \in \mathbb{N}$ and X a graph, the *n-fold clone graph* is $X^{(n)}$ with vertices $[1, n] \times V$ and edges $\{\{(i, u), (j, v)\} : uv \in E(X)\}$. In particular, we use this for the family $C_m^{(2)}$ for $m \geq 4$. An unfortunate consequence of this notation is that $(K_k)^{(m)} \cong K_{m, \dots, m} = K_{m(k)}$, which is why we prefer the $K_{m(k)}$ form.
6. For $n \in \mathbb{N}$ and X a graph, we use the notation nX to denote n *disjoint copies of* X , the graph with vertices $\{v_i : v \in V(X), i \in [1, n]\}$ and edges $\{u_i v_i : i \in [1, n], uv \in E\}$.
7. For $n \in \mathbb{N}$, the *n-dimensional cube* Q_n has vertices $V = \{0, 1\}^n$ and edges between vertices which differ in one coordinate. We only need Q_3 and Q_4 .
8. For $n \in \mathbb{N}$, we define a graph M_n to have vertices $V = \{1, 2\} \times [1, n]$ and edges $\{(1, i), (2, j) : i, j \in [1, n], i \neq j\}$. We only need M_5 , and incidentally, $Q_3 \cong M_4$.
9. For X a graph, we denote the *line graph of* X by $\mathcal{L}(X)$, which has vertex set $E(X)$ and edges $\{uv : u \in E, v \in E, |u \cap v| = 1\}$. We'll need the line graphs of $K_4, K_5, K_{3(2)}$, and Q_3 in addition to two infinite families which we don't consider exceptional.
10. For $n, m \in \mathbb{N}$, we denote the *generalized Petersen graph* by $GP(n, m)$ which has vertices $\{x_i, y_i : i \in Z_n\}$ and edges $\{x_i y_i, x_i x_{i+1}, y_i y_{i+m} : i \in Z_n\}$. We will need $GP(5, 2)$ also known as Petersen's graph or Pet, $GP(8, 3)$ also known as the Möbius-Kantor graph, and $GP(10, 3)$ also known as the Desargues graph.
11. For a family S of sets whose union is $P = \bigcup_{s \in S} s$, the *incidence structure of* S is a graph $\mathcal{I}(S)$ with vertex set $P \cup S$ and edges $\{ps : p \in s \in S\}$. We will specifically refer to the Heawood graph $\text{Hea} = \mathcal{I}(\{123, 345, 156, 147, 257, 367, 246\})$, where abc denotes the set

$\{a, b, c\}$, and the Pappus graph $\text{Pap} = \mathcal{I}(\{123, 456, 789, 147, 258, 369, 158, 348, 267\})$. Additionally, we classify the graphs Δ_3 by looking at $\mathcal{I}(T)$ where T is the set of triangles in a graph $X \in \Delta_3$. In Section 3.2.2, we discuss some more general incidence structures, and in particular consider $\mathcal{I}(E)$ where E is the set of edges of a graph.

12. Similarly, given S , we define the *co-incidence structure of S* to be $\mathcal{I}^c(S)$ with vertex set $P \cup S$ and edges $\{ps : p \in P \setminus s, s \in S\}$. Specifically, we need the co-Heawood graph, $\text{Hea}^c = \mathcal{I}^c(\{123, 345, 156, 147, 257, 367, 246\})$. This notation is motivated by the fact that Hea^c is the *bipartite complement* of Hea .
13. Finally, two platonic solids show up outside of the families: the dodecahedron Dod and icosahedron Ico . The others belong to previously-defined families. The tetrahedron is K_4 , the cube is Q_3 and the octahedron is $K_{2(3)}$.

In total, the collection of exceptional graphs is $K_4, K_5, K_6, K_7, K_{3,3}, K_{4,4}, K_{2(3)}, K_{3(3)}, K_{2(4)}, \mathcal{L}(K_5), \mathcal{L}(K_{3,3}), \mathcal{L}(Q_3), Q_3, Q_4, M_5, \text{Pet}, \text{GP}(8, 3), \text{GP}(10, 3), \text{Hea}, \text{Pap}, \text{Hea}^c, \text{Dod}$ and Ico . In Table C.1, the reader can find alternate characterizations, nice drawings and planar / toroidal embeddings of these graphs (with the sole exception of Hea^c , which does not embed on the torus).

3.2.2 Reduction to Classifying Graphs

In this section, we'll describe the reduction from classifying pairs A, B of nonempty subsets of a group G for which $|AB| \leq |A| + |B|$. We will define a graph called a *multiplication graph*, which will encode the group multiplication. Taking quotients of these multiplication graphs, we will obtain incidence structures of the edges of double transitive graphs. We define the multiplication graph $\mathcal{S} = \mathcal{S}(G, B)$ with vertex set $\{1, 2\} \times G$ and edges $\{(1, g), (2, gb)\}$ for every $b \in B$ and $g \in G$. Note that left-multiplication gives us a rich set of symmetries on \mathcal{S} : if $h \in G$, the map $(1, g) \mapsto (1, hg)$ and $(2, g) \mapsto (2, hg)$ is an automorphism of G , so $\text{Aut}(\mathcal{S})$ acts transitively on each $\{1\} \times G$ and $\{2\} \times G$. Furthermore, \mathcal{S} encodes multiplication by B in the sense that if $A \subseteq G$ then the set of neighbors of $\{1\} \times A$ in \mathcal{S} is precisely $\{2\} \times (AB)$. Note the similarity to Cayley graphs: if we identify $(1, g)$ with $(2, g)$ and orient the edges (g, bg) , then we obtain the Cayley digraph $\text{Cay}(G, B)$.

Now assume that $B = Hx \cup Hy$ for some $H \leq G, x \in G, y \in G$ and $y \notin xH$. Consider the neighbors of $(1, g)$ and $(1, gh)$ for $g \in G$ and $h \in H$. Since $gB = ghB$ the vertices $(1, g)$ and $(1, gh)$ have the same neighbors (are clones). Identifying these clones gives a quotient graph. More precisely, we consider the graph obtained by replacing $\{1\} \times G$ with left H cosets, $G/H = \{gH : g \in G\}$. Let $\mathcal{Q} = \mathcal{Q}(G, B)$ be the graph with vertex set $G \cup G/H$ and edges $\{(gH, gx) : g \in G\}$ and $\{(gH, gy) : g \in G\}$. Again, $\text{Aut}(\mathcal{Q})$ acts transitively on both G and G/H via left-multiplication. Next, we'll show that \mathcal{Q} is the incidence structure

associated with edges of a graph (possibly a multigraph) which we will call $\mathcal{X}(G, B)$ where G and G/H respectively correspond to the edges and vertices of \mathcal{X} .

By construction, every $g \in G$ has $\deg_{\mathcal{Q}}(g) = 2$. Now, we define the graph $\mathcal{X}(G, B)$ to have vertex set G/H and edges $\{\{gx^{-1}H, gy^{-1}H\} : g \in G\}$. Then, \mathcal{X} is the graph with vertices corresponding to cosets in G/H and edges corresponding to group elements $g \in G$, and a vertex $v \in \mathcal{X}$ is incident to an edge $uv \in \mathcal{X}$ whenever their correspondents in \mathcal{Q} are adjacent. Now, we see that G acts transitively on both the vertices and edges of \mathcal{X} , and by double-counting edges, we see that \mathcal{X} is $2|H|$ -regular. We will address the case that \mathcal{X} is the incidence graph for the edges of a multigraph in the next paragraph.

Now that we've got the graph \mathcal{X} , we'll rephrase the problem of finding small product sets involving B in terms of finding small edge cuts in \mathcal{X} . We note that \mathcal{X} is a d -regular graph for $d = |B| = 2|H|$. If A_0 is a nonempty subset of G and $|A_0B| \leq |A_0| + |B|$, then we note that $B = HB$ and so $A_0B = A_0HB$, so $|A_0HB| \leq |A_0H| + |B|$. We can realize A_0H as a union of H cosets, $A = \{a_1H, \dots, a_mH\}$, hence a set of vertices in \mathcal{X} , and A_0B as the set of edges incident to A . In terms of the graph, we count the edges incident to A in two ways to obtain

$$|A_0H| = \frac{d}{2}|A| = \frac{c(A)}{2} + |E_A| \text{ and } |A_0B| = c(A) + |E_A|.$$

Therefore,

$$\frac{1}{2}c(A) = |A_0B| - |A_0H| \leq |B| = d.$$

In the case that \mathcal{X} is a multigraph, every edge has the same multiplicity m by edge-transitivity. If X is the underlying simple graph (that is, the graph where the sets of m parallel edges in \mathcal{X} have been replaced with single edges) then X is a $d' = d/m$ -regular double transitive graph, and moreover, if $A \subset V(\mathcal{X})$ and $c_{\mathcal{X}} \leq 2d$, then $c_X(A) \leq 2d'$. In the next section, we will present a classification theorem for the d -regular double transitive graphs with small edge cuts.

3.3 Classification Theorem

3.3.1 Tindell's Theorem

Before we get started classifying edge cuts of size $\leq 2d$, we'll classify those of size $\leq d$. We do this right up front because it comes in handy rather soon, and because it gives us an opportunity to give a preview of the strategy that the proof of Theorem 3.3.4 will roughly follow.

The question of finding small edge cuts is generally an interesting problem to graph theorists, and insisting on a large amount of symmetry provides a certain amount of control over a graph. One of the more fundamental results in this area is due to Mader [34].

Theorem 3.3.1 (Mader). *Let (V, E) be a connected d -regular vertex-transitive graph. If $\emptyset \subsetneq A \subsetneq V$, then $c(A) \geq d$.*

In an unpublished manuscript, Tindell provides a classification theorem for the tight case of Mader's theorem. Lovasz and Plummer [33] independently prove a version of this theorem.

Theorem 3.3.2 (Tindell). *Let $X = (V, E)$ be a d -regular connected vertex-transitive graph with $d > 2$. If $A \subset V$ satisfies $|A| \leq |V \setminus A|$ and $c(A) = d$, then either $|A| = 1$ or $X[A] \cong K_d$.*

In the case of double transitive graphs, the theorem simplifies significantly. We state a natural corollary of Tindell's theorem, but we will prove it independently. We do this both to avoid sending the user hunting for an obscure manuscript, and because it showcases the primary tools of the proof of the main theorem. In particular, we will rely on the submodular inequality $c(A \cap B) + c(A \cup B) \leq c(A) + c(B)$ which holds for any two subsets $A, B \subseteq V(X)$ in a process called *uncrossing*, which we develop more fully in Lemma 3.6.4.

Lemma 3.3.3. *Let $X = (V, E)$ be a d -regular connected double transitive graph with $d \geq 3$. If $A \subset V$ with $|A| \leq |V \setminus A|$ and $c(A) = d$, then $|A| = 1$.*

Proof. Let A be a minimum size counterexample to this lemma. For a vertex $v \in A$, define $d_i(v) = |N(v) \cap A|$ and $d_e(v) = |N(v) \setminus A|$ to be the number of internal or external edges incident to v respectively.

In the case that $d_i(u) = d_i(v) = d_i$ for all $u, v \in A$, we write d as a sum $d = d_i + d_e$ and a product $d = c(A) = |A|d_e$. For a vertex $v \in A$, we have d_i neighbors of v contained in A , so $|A| \geq d_i + 1$, so $d_i = (|A| - 1)d_e \geq d_i d_e$. If $d_e = 0$, we have a connected component of X , a contradiction. If $d_i = 0$, then $|A| = 1$. Otherwise, $d_e = 1$, $d_i = d - 1$ and $|A| = d$, so $X[A] \cong K_d$.

In the case that $X[A] \cong K_d$, we note that an edge $ab \in \partial(A)$ incident to $a \in A$ is contained in a copy of K_d by edge-transitivity. Thus, b has at least $d - 2$ neighbors in common with a , which must be contained in A , hence $|\partial(A \cup \{b\})| \leq 2$. Since $d \geq 3$, Mader's theorem implies that $c(A \cup \{b\}) = 0$, so $A \cup \{b\}$ is a connected component of (hence all of) X , contradicting $|A| \leq |V \setminus A|$.

Since A is a minimum size counterexample, so $|A| > 1$ and by the above, there are two vertices u, v with $d_i(u) > d_i(v)$. Were there some $x \in A$ with $d_i(x) < d/2 < d_e(x) = d - d_i(x)$, we would have $c(A \setminus \{x\}) = c(A) - d_e(x) + d_i(x) < c(A) = d$, a contradiction to Mader's theorem. Hence, $d_i(x) \geq d/2$ for all $x \in A$. In particular, $d_i(u) > d_i(v) \geq d/2$.

Now, we consider the case when there are two vertices $u, v \in A$ with different internal degrees. Let $\phi \in \text{Aut}(X)$ such that $\phi(u) = v$. Note that $\phi(A) \neq A$ since $d_i(u) \neq d_i(v)$. Furthermore, since $d_i(u) > d/2$ and $d_i(v) \geq d/2$, there must exist $x \in A$ such that $ux \in E$ and $\phi(x) \in A$. Therefore, $\{u, x\} \subseteq A \cap \phi(A) \subset A$ so we count cut edges to find $c(A \cap \phi(A)) + c(A \cup \phi(A)) \leq c(A) + c(\phi(A)) = 2d$ so by Mader's theorem, $c(A \cap \phi(A)) = c(A \cup \phi(A)) = d$.

However, $|A \cap \phi(A)| \geq 2$ is a smaller counterexample, and this contradiction completes the proof. \square

3.3.2 The Main Theorem

In this section, we present the classification theorem for double transitive graphs with small edge cuts and consider its ramifications in terms of classifying $A, B \subset G$ with $|AB| \leq |A| + |B|$ when B is the union of two H -cosets. Our theorem is presented in a very compact manner, and we will prove it in several stages. In particular, Lemmas 3.6.1, 3.6.2 and 3.6.3 directly refer to a large number of cases covered by the theorem, as does the final proof. For convenience, Appendix C contains the following theorem so that the reader can tear it out for easy reference when considering these cases.

Theorem 3.3.4. *Let $X = (V, E)$ be a connected d -regular double transitive graph and $A \subset V$. If $c(A) \leq 2d$ and $|A| \leq |V|/2$ then $X[A]$ is isomorphic to one of the following:*

| d | $c(A)$ | $X[A]$ | X | d | $c(A)$ | $X[A]$ | X |
|-----|----------|---------------------------------------|---|-----|----------|---|-------------------------|
| any | $2d$ | $\cdot \cdot$ | any | 4 | $2d$ | \boxtimes | $\mathcal{L}(Q_3)$ |
| any | $2d - 2$ | \dashrightarrow | any | 4 | $2d$ | \diamond | $\mathcal{L}(Q_3)$ |
| any | d | \cdot | any | 4 | $2d$ | \boxtimes | $\mathcal{L}(Q_3)$ |
| 6 | $2d$ | \triangle | $\mathcal{T}_3, \triangle_3, \boxtimes_2$ | 4 | $2d - 2$ | \triangle | $\triangle_2, K_{2(3)}$ |
| 6 | $2d$ | \triangle | $\boxtimes_2, K_{2(4)}$ | 3 | $2d$ | \dashrightarrow | any |
| 5 | $2d$ | \diamond | Ico | 3 | $2d$ | \wedge | any |
| 5 | $2d$ | \star | Ico | 3 | $2d$ | \hexagon | \mathcal{T}_6 |
| 5 | $2d - 1$ | \triangle | Ico, K_6 | 3 | $2d$ | \pentagon | Dod |
| 4 | $2d$ | \dashrightarrow | any | 3 | $2d$ | $\diamond \diamond$ | Dod |
| 4 | $2d$ | \square | Q_4 | 3 | $2d$ | \star | Dod |
| 4 | $2d$ | \square | $\mathcal{T}_4, \square_2, \text{Hea}^c$ | 3 | $2d$ | \diamond | GP(10, 3) |
| 4 | $2d - 2$ | \diamond | M_5 | 3 | $2d$ | \diamond | GP(8, 3) |
| 4 | $2d$ | $\boxtimes \dashrightarrow \boxtimes$ | $C_m^{(2)}$ | 3 | $2d - 1$ | \dashrightarrow | any |
| 4 | $2d$ | $\boxtimes \dashrightarrow \boxtimes$ | $C_m^{(2)}$ | 3 | $2d - 1$ | \pentagon | Pet, Dod |
| 4 | $2d$ | $\boxtimes \dashrightarrow \boxtimes$ | $C_m^{(2)}$ | 3 | $2d - 2$ | \square | Q_3 |
| 4 | $2d$ | \boxtimes | \triangle_2 | 2 | $2d$ | $\dashrightarrow \dashrightarrow \dashrightarrow$ | any |
| 4 | $2d$ | ∇ | \triangle_2 | 2 | d | $\dashrightarrow \dashrightarrow \dashrightarrow$ | any |

Note that there are three large families of cuts in $C_m^{(2)}$. Some of the smaller members of those families, notably \diamond and \square , appear elsewhere on the table and we do not list $C_m^{(2)}$ there. Also, when an exceptional graph is known to belong to a particular family, it is not shown alongside that family. For example, $K_{2(4)}$ contains \triangle but is not listed since $K_{2(4)} \in \mathcal{T}_3$.

Our main theorem provides considerable information about sets A, B with $B = Hx \cup Hy$ for which $|AB| \leq |A| + |B|$. Although we will not explore all of those consequences here, we give the following corollary to give a taste.

Corollary 3.3.5. *Let A and B be nonempty subsets of a finite group G , and let $H < G$. Then, if $B = HB$, $|B| = 2|H|$, $A = AH$, $|A| \leq |G|/2$ and $|AB| \leq |A| + |B|$ then one of the following holds:*

- $|A| \leq 6|H|$,
- G has a proper normal subgroup K such that $|G/K| \leq 384$
- G has a proper normal subgroup K such that G/K is cyclic or dihedral.

Proof. Let X be the simple graph underlying $\mathcal{X}(G, B)$ as described in Section 3.2.2, which is double transitive by construction, and consider A_H , the set of left H -cosets contained in A , to be vertices in X . The action of G on X induces a group homomorphism $G \rightarrow \text{Aut}(X)$, and we let $K \triangleleft G$ denote the kernel of this homomorphism. Then G/K is isomorphic to a subgroup $H \leq \text{Aut}(X)$ which acts transitively on the vertices and edges of X .

Summarizing Theorem 3.3.4, we find that

- $|A_H| \leq 6$,
- X is one of $\mathcal{L}(Q_3)$, Q_4 , Dod, GP(8, 3) or GP(10, 3)
- $X \cong C_m$ or $C_m^{(2)}$, $m \geq 6$.

The first case captures almost all of the table, leaving us with those sets A with $|A| > 6$. The remaining instances appear in a small number of exceptional graphs (we refer to this notion as *stability*, which most of this chapter is devoted to), unless $X \cong C_m$ or $C_m^{(2)}$. We used Sage to compute the automorphism groups of these few exceptional graphs, and GAP to identify the structure of those groups for the interested reader.

| X | $\text{Aut}(X)$ | $ \text{Aut}(X) $ |
|--------------------|--|-------------------|
| Dod | $Z_2 \times A_5$ | 120 |
| $\mathcal{L}(Q_3)$ | $Z_2 \times S_4$ | 48 |
| Q_4 | $((((Z_2 \times D_4) \rtimes Z_2) \rtimes Z_3) \rtimes Z_2) \rtimes Z_2$ | 384 |
| GP(8, 3) | $GL(2, 3) \rtimes Z_2$ | 96 |
| GP(10, 3) | $Z_2 \times S_5$ | 240 |

For $m \geq 6$, the automorphism group of C_m is D_m , so G/K must be cyclic or dihedral. If $X \cong C_m^{(2)}$ then identifying clones gives an action of G on C_m and we again conclude that G/K is cyclic or dihedral. \square

We note that \bowtie appears in the line graph of every double-transitive cubic graph, so one cannot improve Corollary 3.3.5 beyond $|A_H| \leq 5$. To make that improvement, the only exceptional cuts that we would pick up are in Dod and Ico, resulting in no change. However, a 6-cycle gives a small cut for $X \in \mathcal{T}_6$, and the resulting corollary would necessitate a more careful look at the symmetry groups of hexangulations of the torus. We opted for succinctness, and direct the reader to Miller [35] to learn about those symmetries.

In the next section, we'll look at the properties of graphs which are double transitive. Primarily, we'll be making observations that will make the process of classifying such graphs easier.

3.4 Observations on Vertex- and Edge-Transitive Graphs

In this section, we'll examine some basic properties of double transitive graphs. The first lets us pass between frequency and what we might call vertex frequency. Since we study a few frequency-like parameters only once or twice apiece, we don't make them explicit to avoid bombarding the reader with definitions.

Observation 3.4.1. *Let X be a (d, g, k) -graph. Then every vertex belongs to $\frac{dk}{2}$ girth cycles.*

Proof. Let C_v denote the collection of girth cycles incident to $v \in V$. For each $c \in C_v$ there are two edges incident to v . On the other hand, for each $u \in N(v)$ there are k cycles in C_v containing the edge uv . Counting (edge, girth cycle) pairs (e, c) where $v \in e \in E(c)$, we find $2|C_v| = dk$. \square

Next, we look at how nearly edge-transitivity comes to implying arc-transitivity.

Observation 3.4.2. *If a graph $X = (V, E)$ is edge transitive, then either X is vertex-transitive or there is a bipartition $V = A \cup B$ for which $\text{Aut}(X)$ acts transitively on both A and B .*

If a graph $X = (V, E)$ is double transitive and d -regular, then either X is arc-transitive, or there is an arc-transitive orientation Y of X . In the case that X is not arc-transitive, then d is even and $d_Y^+(v) = d_Y^-(v) = d/2$ for all $v \in V$.

Proof. Let $x \sim y$, and consider the digraph $Y = (V, \text{Aut}(X) \cdot (x, y))$ where $E' = \text{Aut}(X) \cdot (x, y)$ is the orbit of the arc (x, y) . Since X is edge-transitive, every edge in E is represented by at least one arc. Furthermore, $\text{Aut}(X)$ acts transitively on the tails x of arcs (x, y) and likewise with heads. If X is not vertex-transitive, it follows that $V(X) = (\text{Aut}(X) \cdot x) \cup (\text{Aut}(X) \cdot y)$ and these two orbits are disjoint.

In the case that X is vertex-transitive, Y is also vertex transitive. Particularly, $d_Y^+(u) = d_Y^+(v)$ for all $u, v \in V$. Summing vertex-arc incidences, we find that $d_Y^+(u) = d_Y^-(u)$ for all

$u \in V$. If X is not arc-transitive, then $d_Y^+(v) + d_Y^-(v) = d$ for all $v \in V$, so $d_Y^+(v) = d_Y^-(v) = d/2$ and d must be even. \square

In the proof of Observation 3.4.2, we constructed a digraph whose edges were the orbit of an arc under $\text{Aut}(X)$. In future instances, we will denote this graph \vec{X} , an *arc-transitive orientation of X* .

We can use Observations 3.4.1 and 3.4.2 to learn even a little more about the induced graph $X[N(v)]$ in the case where the girth is 3.

Lemma 3.4.3. *Let X be a $(d, 3, k)$ -graph and $v \in V(X)$. Then, the induced graph $X[N(v)]$ is k -regular and has d vertices. If d is odd, then $X[N(v)]$ is vertex-transitive, and if d is even, $X[N(v)]$ is either vertex transitive or has an automorphism group which partitions $N(v)$ into two orbits of equal size.*

Proof. Note that the triangles containing a vertex v are in bijection with edges in $X[N(v)]$. Moreover, if $u \in N(v)$ then every triangle containing the edge uv has its third vertex in $N(u) \cap N(v)$, so $|N(u) \cap N(v)| = k$. Our claim about the symmetry of $X[N(v)]$ follows from Observation 3.4.2. \square

In the next section, we'll establish some stability theorems. The next observation arises in two of them, so let's do it once in generality and be done.

Observation 3.4.4 (Classification of Double Transitive Line Graphs). *Let $d > 1$. A graph $Y \in [K_d]_2$ if and only if $Y \cong \mathcal{L}(X)$ where X is d -regular, except in the case that $d = 3$ and X has girth 3. Additionally,*

1. *if the girth of X is at least 4, then the induced neighborhood of every vertex $v \in Y$ is precisely two disjoint copies of K_{d-1} , and*
2. *if Y is double transitive, then X is also double transitive.*

Proof. Let X be a d -regular graph. Then, the line graph $Y = \mathcal{L}(X)$ has vertex set $E(X)$ and edges $\{uv, uw\}$. Observe that the set $E_v = \{uv : u \in N(v)\}$ of edges incident to a vertex $v \in V(X)$ form a clique $Y[E_v] \cong K_d$. Any other maximal clique is a set of mutually incident edges: a triangle, since X is a simple graph. Therefore, $Y[N(uv)] \cong 2K_{d-1}$ if and only if X has girth at least four. Likewise, if $d = 3$ then the edges of a triangle in X belong to at least two triangles in $\mathcal{L}(X)$ and so $\mathcal{L}(X) \notin \Delta_2$.

Now, let $Y \in [K_d]_2$. We construct a graph X with vertex set $\{v \subset V(Y) : Y[v] \cong K_d\}$ and edges $u \sim v$ if and only if $|u \cap v| = 1$. We construct an isomorphism $\phi : \mathcal{L}(X) \rightarrow Y$ mapping $uv \mapsto y$, the unique element in $u \cap v$. By definition of Y , every vertex is contained in exactly two d -cliques, so the claimed isomorphism is bijective and X is d -regular. Finally, we note there is a unique induced d -clique in Y containing the vertices y and z if and

only if $yz \in E(Y)$; translating this back to X , we see that $\phi(uv) \sim \phi(wx)$ if and only if $|\{u, v\} \cap \{w, x\}| = 1$, so ϕ is an isomorphism.

Finally, assume that Y is double transitive and $Y = \mathcal{L}(X)$. It's clear that X is edge-transitive since Y is vertex-transitive. Moreover, if $yz \in E(Y)$, there is a unique induced d -clique in Y containing that edge, which corresponds to a vertex in X . Since Y is edge-transitive, $\text{Aut}(Y)$ acts transitively on these d -cliques, so X is vertex-transitive. \square

3.5 Some Stability Theorems

This section presents some theorems which classify graphs based on three parameters: degree, girth and frequency. We will describe these as *stability* theorems. They all have the form “Assume a d -regular double-transitive graph X contains a certain structure. Then, X must be one of a small number of exceptional graphs, or belong to a known family of graphs.” For the most part, we'll be looking at girth cycles. Depending on the frequency and their length, girth cycles gives us some amount of control over the neighborhood of the graph. Together with the vertex- and edge-transitivity, we are able to translate the *local* information we gain about the neighborhood into a *global* characterization of the graph.

When the frequency is too small, the global characterization may be fairly weak, for example, if X is $(4, 3, 1)$ -graph, then X is the line graph of an arc-transitive cubic graph with girth at least 4. This may sound more profound than it truly is; we've just restated the characterization of line graphs in terms of frequency. On the other hand, every arc-transitive cubic graph is either K_4 or has a frequency 1 double transitive line graph, so there isn't anything more to say about this family.

In total, these classification theorems can be summarized as follows.

Theorem 3.5.1. *Let X be a finite d -regular double-transitive graph of girth g such that $dg \leq 2(d + g)$. Then, either*

- $X \cong K_6, \text{GP}(10, 3)$ or Hea^c ,
- X is the 1-skeleton of a regular tiling of the sphere or torus, or
- $X \in \square_2, \triangle_2, \boxtimes_2$ or \triangle_3 .

3.5.1 Degree 3

The first stability theorem is a classification of cubic graphs of girth $g \leq 6$. This classification was done by Miller [35] in 1971, but we prefer to cite a 2006 result of Feng and Nedela [24] because of the form of their classification: where they classify the cubic graphs of $g \leq 7$ which we don't need, they do approach the problem similarly, by looking at the frequency of the cubic graphs in question (they do not define a term to communicate the frequency, and merely say “the number of girth cycles passing through an edge”).

Theorem 3.5.2 (Feng and Nedela, 2006). *The table below lists the $(3, g)$ -graphs with $g \leq 6$ along with their frequency k .*

| g | k | Graphs |
|-----|-----|---|
| 3 | 2 | K_4 |
| 4 | 2 | Q_3 |
| | 4 | $K_{3,3}$ |
| 5 | 2 | Dod |
| | 4 | Pet |
| 6 | 2 | $\mathcal{T}_6 \setminus \{\text{Pap}, \text{Hea}, \text{GP}(8, 3)\}$ |
| | 4 | Pap, GP(10, 3) |
| | 6 | GP(8, 3) |
| | 8 | Hea |

3.5.2 Degree 4

This section is devoted to some stability lemmas concerning 4-regular double transitive graphs. We start by looking at triangles, and spend a significant amount of effort on the classification of those 4-regular graphs of girth 4. That particular result is specialization of joint work with DeVos [10], where we classify edge-transitive 4-regular graphs (which may be infinite) with girth 4.

Theorem 3.5.3. *The table below lists the $(4, 3)$ -graphs along with their frequency k .*

| k | Graphs |
|-----|------------|
| 1 | Δ_2 |
| 2 | $K_{2(3)}$ |
| 3 | K_5 |

Proof. By Lemma 3.4.3, we know that $X[N(v)]$ is a k -regular graph on 4 vertices. For $k = 1$, we have $X[N(v)] = 2K_2$ and so we have $X \in \Delta_2$. For $k = 2$, we have $X[N(v)] \cong C_4 \cong K_{2,2}$ and by Lemma 3.3.3, there is a vertex $u \neq v$ with $N(u) = N(v)$ and we see that $X \cong K_{2(3)}$. Finally, we have $k = 3$ for which $X[N(v)] \cong K_4$ is already 3-regular, so we're already done because $X[N(v) \cup \{v\}] \cong K_5$ is 4-regular. \square

Corollary 3.5.4. *If X is a $(4, 3)$ -graph with a 4-cycle, then X is one of K_5 , $K_{2(3)}$, $\mathcal{L}(K_{3,3})$ or $\mathcal{L}(Q_3)$.*

Proof. The girth of X is 3, so by Theorem 3.5.3 and Observation 3.4.4 X is isomorphic to one of K_5 , $\mathcal{L}(K_4) \cong K_{2(3)}$, or the line graph of an arc-transitive cubic graph with girth $g > 3$. We consider a 4-cycle in the line graph X of a cubic graph W with girth $g > 3$. Since $g > 3$, the 4-cycle must be induced, or the neighborhood criterion of Observation 3.4.4 is violated. Thus, we must have four edges uv, vw, wx and xu where $x \neq v$ and $w \neq u$: an induced 4-cycle in W , so W has girth 4. By Theorem 3.5.2, W is either $K_{3,3}$ or Q_3 . \square

The remainder of this subsection will be spent proving the following classification theorem, along with more precise classifications of the double transitive graphs $X \in \square_2$.

Theorem 3.5.5. *The table below lists the $(4, 4)$ -graphs along with their frequency k .*

| k | <i>Graphs</i> |
|-----|----------------------------|
| 1 | \square_2 |
| 2 | \mathcal{T}_4 |
| 3 | Q_4, Hea^c |
| 5 | $C_m^{(2)}$ for $m \geq 5$ |
| 6 | M_5 |
| 9 | $K_{4,4}$ |

We'll start by examining those graphs with frequency 1 and 2, and then attack the remainder by considering other induced substructures.

3.5.2.1 Frequency 1

This section contains a rough description of the 4-regular double transitive graphs with girth 4 and frequency 1. Simply, they can be obtained from line graphs of double transitive 4-regular graphs by deleting the edges of a 2-regular subgraph. Clearly, not all such deletions will be double transitive, so we will go through some pains to find such. Particularly, we will show that they arise from 4-regular graphs Y equipped with a subgroup $G \leq \text{Aut}(Y)$ which acts vertex- and edge-transitively and has the added property that for every vertex v , the action of $\text{Stab}_G(v)$ on the pairs of subsets of $\partial(v)$ has an orbit of size 4.

This is essentially a negative result for us, as it indicates that the family of $(4, 4, 1)$ -graphs is not likely to have a simple explicit description as do the $(4, 4, k)$ -graphs for $k \geq 2$. In particular, these results demonstrate that classifying all $(4, 4, 1)$ -graphs would require classifying all 4-regular graphs of girth at least 5 which have certain kinds of vertex stabilizers.

Let Y be a 4-regular graph for which G acts transitively on the vertices and edges of Y , and suppose that for every vertex v , the action of $\text{Stab}_G(v)$ on the 2-element subsets of $\partial(v)$ has an orbit \mathcal{O}_v of size four. We define $\square(Y, G)$ to be the graph with vertex set $E(Y)$ and edge set $\cup_{v \in V(Y)} \mathcal{O}_v$. We will show that every graph of the form $\square(Y, G)$ with girth at least 4 is a 4-regular edge-transitive graph of girth 4, and that this class contains all $(4, 4, 1)$ -graphs.

First we will investigate how these vertex stabilizers of interest may act on their incident edges. Let H be a group acting on a four element set $\{a, b, c, d\}$, and suppose that the action of H on pairs of subsets of $\{a, b, c, d\}$ has an orbit O of size four. It follows from the assumption that O is an orbit that the two 2-element subsets of $\{a, b, c, d\}$ not contained in O must be disjoint. So, we may assume without loss that $O = \{\{a, b\}, \{b, c\}, \{c, d\}, \{a, d\}\}$. Let \hat{H} be the subgroup of permutations of $\{a, b, c, d\}$ associated with an element in H . Since

\hat{H} must fix O as a set, we find that \hat{H} is a subgroup of the dihedral group generated by $(abcd)$ and (ac) . Since H acts transitively on O , the group \hat{H} must then be one of:

- The dihedral group generated by $(abcd)$ and (ac)
- The cyclic group generated by $(abcd)$
- The Klein 4-group generated by (ac) and (bd) .

A quick check reveals that all three of these groups have the desired properties. So, for the graphs Y of interest to us, the subgroups $G \leq \text{Aut}(Y)$ will have vertex stabilizers acting in one of these three manners. Next we prove that the operator \square yields 4-regular double transitive graphs of girth 4.

Observation 3.5.6. *Let Y be a 4-regular graph with girth at least 4 and let G act vertex- and edge-transitively on Y . Then, $\square(Y, G)$ is a 4-regular double transitive graph with girth 4.*

Proof. By assumption, for every $v \in V(Y)$ the action of $\text{Stab}_G(v)$ on the 2-element subsets of $\partial_Y(v)$ has an orbit \mathcal{O}_v of size four. By construction, the graph $X = \square(Y, G)$ has vertex set $E(Y)$ and edge set $\cup_{v \in V(Y)} \mathcal{O}_v$. It follows from the above discussion that for every $v \in V(Y)$ the subgraph of X with vertex set $\partial_Y(v)$ and edge set \mathcal{O}_v is a 4-cycle. It follows immediately from this that the graph X will be 4-regular and have girth 4. To prove that X is edge-transitive, we will show that the action of G on X (inherited from its action on Y) is edge-transitive. It follows from the assumption that G acts vertex transitively on Y that G acts transitively on $\{\mathcal{O}_v \mid v \in V(Y)\}$. Combining that property with the assumption that each \mathcal{O}_v is an orbit of the action of $\text{Stab}_G(v)$ demonstrates that X is edge-transitive, as desired. By construction, G acts transitively on the edges of Y and hence the vertices of X . □

Theorem 3.5.7. *If X is a $(4, 4, 1)$ -graph, then there exists a 4-regular double transitive graph Y and a suitable group $G \leq \text{Aut}(Y)$ so that $X \cong \square(Y, G)$.*

Proof. Let S be the set of all 4-cycles in X and define a graph Y with vertex set S by the rule that distinct vertices $s, s' \in S$ are adjacent in Y if these 4-cycles share a vertex. Note that every vertex v of X is contained in exactly two 4-cycles s and s' so there is a natural correspondence between vertices of X and edges of Y (ex. here v corresponds to $\{s, s'\}$) and hence Y is edge-transitive by the vertex-transitivity of X . Furthermore, the group $G = \text{Aut}(X)$ has a natural action on S by which G acts on Y .

It follows immediately from the edge-transitivity of X (and the fact that every edge of X is in a unique 4-cycle) that G acts vertex-transitively on Y . Now consider a vertex s of Y and let v_1, v_2, v_3, v_4 be the cyclically ordered vertices of X corresponding to s as a 4-cycle in X . It follows from the edge-transitivity of X that the action of the stabilizer of s on $\{v_1, v_2, v_3, v_4\}$

must be transitive on the pairs $\{v_i, v_{i+1}\}$ (working modulo 4), but cannot map any such pair to either $\{v_1, v_3\}$ or $\{v_2, v_4\}$. In short, the set $\{\{v_1, v_2\}, \{v_2, v_3\}, \{v_3, v_4\}, \{v_1, v_4\}\}$ is an orbit of the action of the stabilizer of s on the pairs of $\{v_1, v_2, v_3, v_4\}$. Now we find $X \cong \square(Y, G)$ as desired. \square

3.5.2.2 Frequency 2

In this section, we briefly discuss $(4, 4, 2)$ -graphs. In fact, all graphs of this type arise as quadrangulations of the torus, which we will prove momentarily. In [10], we allow infinite graphs, namely quadrangulations of the plane and cylinder. There, we show that all $(4, 4, 2)$ -graphs arise as quotients of the square tiling of the plane, whose vertices correspond to points in the lattice \mathbb{Z}^2 , and classify the subgroups $\Lambda < \mathbb{Z}^2$ for which \mathbb{Z}^2/Λ yields a $(4, 4, 2)$ -graph.

Theorem 3.5.8. *Every $(4, 4, 2)$ -graph is a quadrangulation of the torus.*

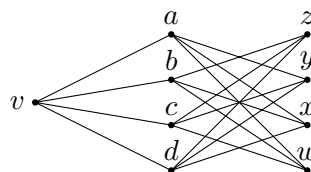
Proof. Let X be a $(4, 4, 2)$ graph. First suppose that there are two adjacent edges which are contained in at least two common 4-cycles. In this case X must have a subgraph isomorphic to $K_{3,2}$. Consider a vertex v of degree 3 in this subgraph and let e be the edge incident with v not in this $K_{3,2}$. Now e must be contained in two 4-cycles, but this gives us at least five 4-cycles through v , which is contradictory. It follows from this that adding a face to each 4-cycle of X results in a graph embedded in a surface. Since X is 4-regular and every face is a 4-cycle, the Euler characteristic is zero. There are two closed surfaces of characteristic zero: the Klein bottle and the torus. Babai [6] classified the vertex transitive maps on the Klein bottle, and a cursory examination of his paper reveals that such a quadrangulation cannot occur. So, the surface must not be a Klein bottle and therefore $X \in \mathcal{T}_4$. \square

3.5.2.3 Larger Frequency

In this section, establish some stability lemmas concerning the existence of $K_{3,2}$ and $K_{4,2}$ subgraphs. These will ease the classification of $(4, 4, k)$ -graphs with $k \geq 3$.

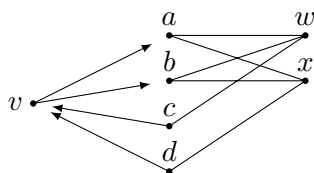
Lemma 3.5.9. *Let X be a $(4, 4)$ -graph with an induced subgraph isomorphic to $K_{3,2}$. If no induced subgraph of X is isomorphic to $K_{4,2}$, then $X \cong M_5$.*

Proof. Choose $v \in V(X)$ and let $\{a, b, c, d\}$ be the neighbors of v . First suppose that every 3 element subset of $\{a, b, c, d\}$ is contained in the neighborhood of a vertex other than v . Since we may assume X has no subgraph isomorphic to $K_{4,2}$ this gives us a subgraph as follows:

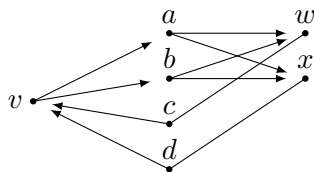


By Lemma 3.3.3, there is one undiscovered vertex remaining, adjacent to $\{w, x, y, z\}$ and so $X \cong M_5$.

We may now assume (without loss) that $\{a, b, c\}$ is contained in the neighborhood of a vertex $w \neq v$ but $\{a, c, d\}$ is not contained in the neighborhood of any vertex but v . In particular, this implies that X is not arc-transitive (since these assumptions forbid the existence of an automorphism mapping the arc (v, b) to (v, d)). By Observation 3.4.2 we can choose an orientation \vec{X} of the graph which is preserved by $\text{Aut}(X)$. We may assume (by possibly reversing orientations) that (v, b) is an edge of \vec{X} , and then (d, v) must also be an edge. Since every orientation of $K_{3,2}$ contains vertices with in-degree at least two, and vertices with outdegree at least two, we find that \vec{X} is 2-regular. We may now assume that (v, b) and (d, v) are edges of \vec{X} , and then choosing an automorphism mapping (c, v) to (d, v) implies the existence of a vertex $x \in V(X)$ which has $\{a, b, d\}$ as neighbors (in the underlying graph). This gives us the following.



Our present assumptions imply that there does not exist a vertex other than v whose neighborhood contains $\{a, c, d\}$ or $\{b, c, d\}$. It follows from this (and vertex-transitivity) that whenever two distinct vertices p, q in X have three common neighbors, these three common neighbors include both out neighbors of p and q in \vec{X} . Applying this property to the vertices a and b (which have v, w, x as common neighbors) implies that we have the following orientations in \vec{X} .



However, now w and v have $\{a, b, c\}$ as common neighbors, but both a, b are in-neighbors of w in \vec{X} . This contradiction completes the proof. \square

Lemma 3.5.10. *Let X be a $(4, 4, k)$ graph with no subgraph isomorphic to $K_{3,2}$. If $k \geq 3$ then X is isomorphic to either Q_4 or Hea^c .*

Proof. We will label vertices with subsets of $\{1, 2, 3, 4\}$ and will write, for example, 12 to represent $\{1, 2\}$. Label a vertex \emptyset and for each $i \geq 0$, let $L_i = \{v : \text{dist}(v, \emptyset) = i\}$ be the set of vertices at distance i from \emptyset . Label the vertices in L_1 with (distinct) singletons 1, 2, 3, and 4.

Observe that every vertex in L_2 is adjacent to at most two vertices in L_1 (since X has no subgraph isomorphic to $K_{3,2}$), and similarly, no two vertices in L_2 have two common neighbors in L_1 . Now for a vertex in L_2 with two neighbors in L_1 , say a and b , we assign this vertex the label ab .

By the above, we know that every 2-edge path with vertex sequence a, \emptyset, b for $1 \leq a, b \leq 4$ completes to at most one 4-cycle. However, the frequency assumption implies that the edge between \emptyset and a must be contained in $k \geq 3$ such 4-cycles. Therefore, $k = 3$ and every 2-edge path of the form a, \emptyset, b completes to a unique 4-cycle using the vertex labelled ab . So, L_2 consists of 6 vertices, each of which is labelled by a distinct 2 element subset.

Next we observe that every 2-edge path with \emptyset as the middle vertex is contained in a unique 4-cycle. So, by vertex-transitivity, we have the *completion property*: every 2-edge path in X is contained in a unique 4-cycle. Using this completion property, it is straightforward to prove that L_2 must be an independent set (an adjacency of the form $ab \sim bc$ would create a 3-cycle, whereas any of type $ab \sim cd$ would impose a 4-cycle through the path a, ab, cd , but $N(a) \cap N(cd) = \emptyset$).

To prepare for working with L_3 , consider a complete graph K_4 with $V(K_4) = \{1, 2, 3, 4\}$. The edges of this K_4 have the same names as the labels of vertices in L_2 . So, we may associate each vertex $x \in L_3$ with the subgraph C_x of K_4 which has edge set $N(x) \cap L_2$ (i.e. all neighbors of x which are in L_2). Let \mathcal{C} denote the set of subgraphs of K_4 associated with vertices in L_3 .

Suppose first that $C_x \in \mathcal{C}$ contains all of the edges 12, 13, and 14 from the K_4 under consideration. Then the corresponding vertex x in L_3 together with the vertices 1, 2, 3, 4 form a subgraph isomorphic to $K_{3,2}$, giving us a contradiction. It follows from this reasoning that every graph in \mathcal{C} has maximum degree at most 2.

By applying the completion property to the two paths in X given by 12, 1, 13 and 12, 1, 14 we deduce that L_3 must contain a vertex x adjacent to 12 and 13 and another vertex x' adjacent to 12 and 14. Since X is 4-regular, these are the only vertices in L_3 adjacent to 12. It follows from this property that every graph in \mathcal{C} is a cycle, and further the cycles in \mathcal{C} cover every edge of the K_4 exactly twice.

The only possibilities are for \mathcal{C} to consist of the three 4-cycles in K_4 , or the four 3-cycles in K_4 . In the former case, every vertex in L_3 has all of its neighbors in L_2 and we find that X is isomorphic to Hea^c . In the latter case, each vertex x in L_3 is associated with a 3-cycle C_x in K_4 and we may label each such x with $V(C_x)$ (a 3-element subset of 1234). Using these labels, we see that the graph induced by $L_0 \cup L_1 \cup L_2 \cup L_3$ is isomorphic to the graph obtained from Q_4 by removing a vertex. Now applying the completion property to the edges between L_3 and L_4 implies that $X \cong Q_4$. \square

Lemma 3.5.11. *Let $X = (V, E)$ be a $(4, 4)$ -graph with a subgraph isomorphic to $K_{4,2}$. Then X is either isomorphic to $K_{4,4}$, or $C_m^{(2)}$ for some $m \geq 5$.*

Proof. Call two vertices $u, v \in V$ clones if $N(u) = N(v)$ and note that this implies $\{u, v\} \notin E$. Clones give an equivalence relation on V and we let V^\bullet denote the corresponding partition of V into equivalence classes (so every $S \in V^\bullet$ is a maximal set of clones). Let X^\bullet be the graph with vertex set V^\bullet and two sets $S, T \in V^\bullet$ adjacent in X^\bullet if there is a vertex in S adjacent to a vertex in T (in the original graph X). Note that X^\bullet will still be connected and double transitive since these properties are inherited from X .

Since X contains a subgraph isomorphic to $K_{4,2}$, we know that it has distinct vertices which are clones. By vertex-transitivity, every vertex has another clone. It then follows that X^\bullet has maximum degree at most 2, so X^\bullet must be isomorphic to either K_2 or C_m . In the first case $X \cong K_{4,4}$. In the second case we find that $X \cong C_m^{(2)}$ for some $m \geq 3$. If $m = 3$ we have a contradiction to the assumption that X has girth 4, and for $m = 4$ note that $C_4^{(2)} \cong K_{4,4}$. So in this case we must have $m \geq 5$ as desired. \square

We are now ready to prove the classification of $(4, 4)$ -graphs.

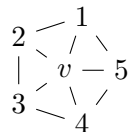
Proof of Theorem 3.5.5. Let X be a $(4, 4, k)$ -graph. If X has a subgraph isomorphic to $K_{4,2}$ then by Lemma 3.5.11, it is isomorphic to $K_{4,4}$, to $C_m^{(2)}$ for some $m \geq 5$. If it has a $K_{3,2}$ subgraph but no $K_{4,2}$ subgraph, then by Lemma 3.5.9 we find that X is isomorphic to $K_{5,5} - M$. If X has no $K_{3,2}$ subgraph and $k \geq 3$ then by Lemma 3.5.10 it is isomorphic to either Q_4 or Hea^c . The only remaining possibilities are $k = 1$ and $k = 2$ which were dealt with in Sections 3.5.2.1 and 3.5.2.2. \square

3.5.3 Degree 5

Theorem 3.5.12. *If X is a $(5, 3)$ -graph then either $X \cong K_6$ or $X \cong \text{Ico}$.*

Proof. First, look at the induced graph $X[N(v)]$, which has at least one edge since X has girth 3. Since X is arc-transitive, $\text{Stab}(v)$ acts transitively on $N(v)$, so $X[N(v)]$ is a vertex-transitive 5-vertex graph, hence $X[N(v)]$ must be either 2- or 4-regular. If $X[N(v)]$ is 4-regular, then it must be K_5 , and X is K_6 .

Now we consider the case where $X[N(v)]$ is 2-regular. Happily, the only 2-regular graph on 5 vertices is C_5 , so we can draw the neighborhood of a vertex below.



Here, we see that every edge is contained precisely two triangles. Looking at $\text{Stab}(v)$ again, we see that edge-transitivity implies that $\text{Stab}(v)$ acts transitively on the triangles containing v . Thus we construct a graph Y whose vertex set is the triangles of X , with edges between triangles which share an edge. Since the frequency of X is 2, Y is a cubic graph. Triangle-transitivity implies that Y is vertex-transitive, edge-transitivity of X implies that

Y is edge-transitive. By Theorem 3.5.2, Y is either Pet or Dod since it contains a 5-cycle. Completing the vertex neighborhood around 5, we find that the frequency for Y is 2, so $Y \cong \text{Dod}$. Therefore, X is the planar dual of Dod, the Icosahedron. \square

3.5.4 Degree 6

Theorem 3.5.13. *A graph $X \in \Delta_3$ if and only if there is a connected bipartite cubic graph Z with girth $g \geq 6$ and bipartition $V(Z) = (A, B)$ such that X is obtained by taking a $Y - \Delta$ transformation of every vertex $v \in A$. Additionally, X is double transitive if and only if Z is edge-transitive.*

Proof. Let $X = (V, E) \in \Delta_3$, and let T be $\{S \subset V : X[S] \cong K_3\}$. Let $Z = \mathcal{I}(T)$, so by construction Z is bipartite. Since every edge in X is contained in exactly one triangle $t \in T$, every vertex is contained in exactly three triangles, and every triangle contains three vertices, so Z is cubic. Now, consider a cycle of length 4 in Z : (x_1, t_1, x_2, t_2) must have $\{x_1, x_2\} \subset t_1 \cap t_2$, and so the edge $\{x_1, x_2\}$ must belong to two different triangles. Since $X \in (V, E)$ and Z is bipartite, its girth must be at least 6.

Now, assume that X is edge-transitive and consider two edges uv and xy in $E(X)$, which belong to the unique triangles uvw and xyz . There is an automorphism $\phi \in \text{Aut}(X)$ with $\phi(uv) = xy$ and by the uniqueness of triangles containing a given edge, we find $\phi(w) = z$. So, consider two (vertex, triangle) incidence pairs (x_1, t_1) and (x_2, t_2) , or equivalently, two edges in $E(Z)$. Then, $t_1 \setminus \{x_1\}$ and $t_2 \setminus \{x_2\}$ are edges in X , so by the above, Z is edge-transitive.

Now we'll work on the converse. Let Z be a cubic graph with girth $g > 4$ and bipartition $V(Z) = (A, B)$. Then define X to be a graph with vertex set B and edges $E(X) = \{N(a) \setminus \{b\} : a \in A, b \in N(a)\}$. Since Z is cubic, $E(X)$ is a set of sets with size two, so X is a graph, and every edge xy belongs to a triangle $xyz = N(a)$. Since Z has girth $g > 4$, there are no two vertices a_1 and a_2 with $|N(a_1) \cap N(a_2)| > 1$, so every edge contains at most one triangle. Finally, we note that because Z is cubic, each $b \in B$ belongs to precisely three triangles, one per original edge $ab \in E(Z)$.

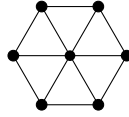
Now, assume that Z is edge-transitive and connected, and consider two edges of X , $\{u, v\} \subset N_Z(a)$ and $\{x, y\} \subset N_Z(a')$ for $a, a' \in A$. If $N_Z(a) \setminus \{u, v\} = \{w\}$ and $N_Z(a') \setminus \{x, y\} = \{z\}$, then there is an automorphism $\phi \in \text{Aut}(Z)$ with $\phi(\{a, w\}) = \{a', z\}$. More specifically, Z is either arc-transitive, or $\text{Aut}(Z)$ respects the bipartition (A, B) by Observation 3.4.2 and the fact that Z is connected. Therefore, we can take $\phi(a) = a'$ without loss of generality. Therefore, $\phi(N_Z(a)) = N_Z(a')$ and $\phi(\{u, v\}) = \{x, y\}$, and so X is edge-transitive, and hence double transitive by Observation 3.4.2 since it contains triangles. \square

Theorem 3.5.14. *The table below lists the $(6, 3)$ -graphs along with their frequency k .*

| k | <i>Graphs</i> |
|-----|------------------------------|
| 1 | Δ_3 |
| 2 | $\mathcal{T}_3, \boxtimes_2$ |
| 3 | $K_{3(3)}, \mathcal{L}(K_5)$ |
| 4 | $K_{2(4)}$ |
| 5 | K_7 |

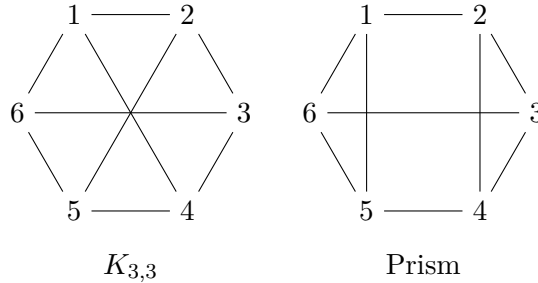
Proof. We'll begin with frequency 1. By Lemma 3.4.3, $X[N(v)]$ is a 1-regular graph, so the induced graph $X[N(v) \cup \{v\}]$ consists of the three triangles which share the vertex v . This is precisely the definition of Δ_3 , the family we characterize in Theorem 3.5.13.

Now, consider the frequency 2 case. Here, construct a graph Y with vertex set $T = \{\{u, v, w\} \subset V : X[\{u, v, w\}] \cong K_3\}$ and edges between triangles that share an edge. Then, Y is a double transitive cubic graph, and the set of triangles $T_v \subset T$ containing a vertex $v \in V$ form a 2-regular induced subgraph of $Y[T(v)]$. In the case that $Y[T_v]$ is two disjoint triangles, those triangles correspond to a pair of K_4 subgraphs which intersect at v ; by Observation 3.4.4, Y is the line graph of a 4-regular double transitive graph. In the case that $Y[T_v]$ is a 6-cycle, the neighborhood is shown below.

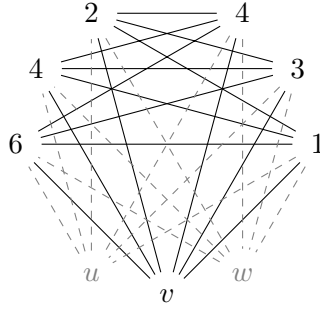


Thus, the triangles give an embedding, and Y is the geometric dual. By Theorem 3.5.2, Y is a hexangulation of the torus and therefore $X \in \mathcal{T}_3$.

In the frequency 3 case, we cite Lemma 3.4.3 to examine the induced neighborhood $X[N(v)]$: a 3-regular graph on 6 vertices. There are two such graphs, which we show below.

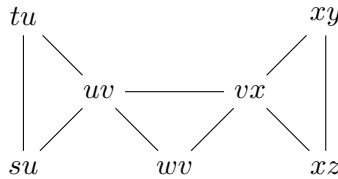


In the case where $K[N(v)] \cong K_{3,3}$, we redraw the neighborhood together with v in a way that will assist further reasoning, with the yet-undiscovered vertices of X shown in gray.



Consider the neighbors of the vertex 1 – we already see the neighbors $v, 2, 4,$ and $6,$ and we need two more (we'll call them u and w) that form a complete bipartite graph between $\{u, v, w\}$ and $\{2, 4, 6\}$. At this point, we have accounted for all of the neighbors of $\{2, 4, 6\}$. When we attempt to fill out the neighborhoods of 3 and $5,$ we need those neighborhoods to be disjoint from $\{1, 3, 5\}$ and form a complete bipartite graph with one half being $\{2, 4, 6\}$. The graph we've drawn above is the unique completion: $K_{3(3)}$.

In the case where $X[N(v)]$ is the prism, we see that the vertex v is the intersection of two copies of K_4 . Using Observation 3.4.4, we see that X is the line graph of a 4-regular double transitive graph Y ; however, the additional edges $\{1, 4\}, \{2, 5\},$ and $\{3, 6\}$ show that Y contains triangles. By Theorem 3.5.3, Y is either K_5 or the line graph of a cubic graph. Suppose for contradiction that Y is the line graph of a cubic graph Z . Then, the local picture around an edge $\{uv, vx\}$ in Y is shown below, where we may end up identifying some of the vertices in $\{t, s, y, z\} \subset V(Z)$ where $Y = \mathcal{L}(Z)$.



The cliques of Z induced by $\partial_Y(uv)$ and $\partial_Y(vx)$ intersect at $\{uv, vx\}$, and we already see one edge between those cliques in Z , $\{uv, vw\} \sim \{vx, vw\}$. A second edge between those cliques will mean identifying, for example, $t = y$. If we identify the other pair, $s = z$ we see three triangles through the edge uv : $\{w, u, x\}, \{t, u, x\},$ and $\{s, u, x\}$, so both u and x have degree 4. Therefore, Y cannot be the line graph of a cubic graph, so we have $Y \cong K_5$ and $X \cong \mathcal{L}(K_5)$.

In the frequency 4 case, we again cite Lemma 3.4.3. Here, the neighborhood of v is a 4-regular graph on 6 vertices, and there is only one such graph that is symmetric enough, $K_{2(3)}$. Observe that $N(v) \cup \{v\}$ induces a 6 edge cut in a vertex-transitive 6-regular graph. By Tindell's theorem, $V \setminus (N(v) \cup \{v\})$ is a single vertex, so $X \cong K_{2(3)}$.

Finally, we have frequency 5. The induced neighborhood is K_6 by Lemma 3.4.3, so X is the complete graph K_7 . \square

3.6 Proof of The Main Theorem

Now we'll start working on the main theorem proper. We first establish three lemmas wherein most of the case analysis is done. The first rules out counterexamples to Theorem 3.3.4 among the exceptional graphs. The next two are summarizing statements about the table in Theorem 3.3.4, whose proofs are collections of mostly one-line proofs of simple statements. A small number of these could be left to the reader but morally we cannot omit such a large number of proofs, however short. Where these cases are considered in the main proof, they would detract from the flow of the main argument.

Lemma 3.6.1 (Nothing Exceptional). *There are no counterexamples to Theorem 3.3.4 among the exceptional graphs K_4 , K_5 , K_6 , K_7 , $K_{3,3}$, $K_{4,4}$, $K_{2(3)}$, $K_{3(3)}$, $K_{2(4)}$, $\mathcal{L}(K_5)$, $\mathcal{L}(K_{3,3})$, $\mathcal{L}(Q_3)$, Q_3 , Q_4 , M_5 , Pet, GP(8, 3), GP(10, 3), Hea, Pap, Hea^c, Dod or Ico.*

This lemma was verified by computer. We computed all nonisomorphic induced subgraphs of size up to $|V|/2$ for each graph and didn't find any new cuts. Code and results for this are in Appendix C.

Lemma 3.6.2 (Stability). *For each halfrow (d, n, C, F) of the table in Theorem 3.3.4, we obtain a true statement, "let $X = (V, E)$ be a d -regular double transitive graph. If $A \subset V$ with $X[A] \cong C$ and $|A| < |V|/2$ then $X \in F$ ".*

Proof. We'll work up the table, first in the right column, and then the left. We skip any entry where G can be any double transitive graph with degree d .

Theorem 3.5.2 gives us a classification of cubic graphs of girth $g < 6$, which is consistent with the table after the consideration that $|A| < |V|/2$. The remaining graphs with $g = 6$ are hexangulations of the torus with $k = 2$. The two exceptional cuts in GP(10, 3) and GP(8, 3) require $k > 2$, and so the table is correct for $d = 3$.

We classify the 4-regular graphs with triangles in Lemma 3.5.3, and the only ones with at least 6 vertices are in Δ_2 . In Corollary 3.5.4, find that all 4-regular graphs which contain both squares and triangles are exceptional. Thus, the table is correct for all listed cuts in 4-regular graphs with triangles.

For the three infinite families of cuts, the smallest nontrivial (that is, those with edges) are C_4 , $K_{3,2}$, and $K_{4,2}$ (respectively, working upwards) – any larger member of those family contains a $K_{4,2}$. We have listed C_4 and $K_{3,2}$ elsewhere in the table (we'll discuss those in the next paragraph), so we omit those smallest cuts except $K_{4,2}$ from the families. By Lemma 3.5.11, the only 4-regular double-transitive graphs containing $K_{4,2}$ are the graphs $C_m^{(2)}$.

By Lemma 3.5.9, if a double transitive X contains $K_{3,2}$ and no $K_{4,2}$, then $X \cong M_5$. Otherwise, if a 4-regular double transitive graph contains a 4-cycle, the girth is 3 or 4. If X is not one of the exceptions, then it's in \mathcal{T}_4 or \square_2 by Theorem 3.5.5.

The final structure to consider in 4-regular graphs is an induced Q_3 . There are two 4-cycles through every edge in the $X[A]$, and any edge in $\partial(A)$ must also be contained in 4-cycles which implies that $k \geq 3$. By Theorem 3.5.5, X is exceptional.

For $d = 5$, there isn't much to say because every $X[A]$ contains at least one triangle, so X is exceptional by Theorem 3.5.12.

For $d = 6$, we first look at those double transitive graphs containing tetrahedra. Looking at Theorem 3.5.14, the only allowable family is \boxtimes_2 .

The double transitive graphs containing triangles, of course, is the entire list from Theorem 3.5.14. \square

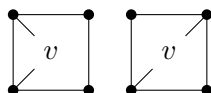
Lemma 3.6.3. *Let $X = (V, E)$ be a d -regular double transitive graph, and suppose $X[A]$ appears in the statement of Theorem 3.3.4. If $v \in V \setminus A$ and $c(A \cup \{v\}) \leq 2d$, then $A \cup \{v\}$ satisfies Theorem 3.3.4.*

Proof. By Lemma 3.6.1 and Lemma 3.6.2, we need only look at adding a vertex to each listed cut in the eight families: $\mathcal{T}_3, \mathcal{T}_4, \mathcal{T}_6, \Delta_2, \Delta_3, \square_2, \boxtimes_2$ and $C_m^{(2)}$.

Let $X \in \mathcal{T}_3, \Delta_3$, or \boxtimes_2 and $X[A] \cong K_3$. Since $c(A) = 12$, the only way to produce a small enough cut $c(A \cup \{v\}) \leq 12$ is if there is a vertex $v \notin A$ for which $|N(V) \cap A| = 3$, hence $N[A \cup \{v\}] \cong K_4$. By Lemma 3.6.2, we find that $X \in \boxtimes_2$, so $A \cup \{v\}$ satisfies the theorem for all $v \in V$.

Let $X \in \boxtimes_2$ and $X[A] \cong K_4$. Since $c(A) = 12$, the only way to produce a small enough cut $c(A \cup \{v\}) \leq 12$ is if there is a vertex $v \notin A$ for which $|N(V) \cap A| \geq 3$, and we find edges which belong to more than one induced K_4 and $X \notin \boxtimes_2$.

Let X be 4-regular and $X[A] \cong C_4$. Since $c(A) = 8$, the only way to produce a small enough cut $c(A \cup \{v\}) \leq 8$ is if there is a vertex $v \notin A$ for which $|N(V) \cap A| \geq 2$, and there are two potential ways to add such a vertex:



In the first we find a square and a triangle. In the second, we find an induced $K_{3,2}$. In either case, we find exceptional graphs by Theorem 3.5.5 and Lemma 3.5.9 respectively.

In the case of $C_m^{(2)}$, we note that there are three large families of cuts. When we add a vertex v with $|N(v) \cap A| \geq 2$, we find that $A \cup \{v\}$ belongs to one of the other three families. If we add a vertex v with $|N(v) \cap A| \leq 1$, we have $c(A \cup \{v\}) \geq 10$. In any case, $A \cup \{v\}$ satisfies the theorem.

Let $X \in \Delta_2$ and $X[A] \cong K_3$. Since every vertex $v \notin A$ has at most two neighbors in A , we either find $c(A \cup \{v\}) = 10$ if $A \cap N(v) = \emptyset$, or $c(A \cup \{v\}) = 8$ otherwise. In the latter case, we find the graph K_3 with one pendant vertex, which we will denote K_3^+ since it appears on the list and we'll consider it next. As it does appear on the list, we've satisfied the theorem in both cases.

Let $X \in \Delta_2$ and $X[A] \cong K_3^+$. There are three kinds of vertices $v \notin A$. The first kind is far away from A , and $N(v) \cap A = \emptyset$ so $c(A \cup \{v\}) = 12$ and we needn't worry. The next is adjacent to one vertex in $X[A]$, and $c(A \cup \{v\}) = 10$ and again, the theorem holds. The third kind is adjacent to two vertices in A , and so $c(A \cup \{v\}) = 8$. Since X has frequency 1, the only possible result of adding a vertex adjacent to two vertices in A is to add the last neighbor of the vertex of degree 3, which is also adjacent to the vertex of degree 1. This yields two copies of K_3 which share a vertex, which is on the list. We'll denote the resulting "bowtie" graph by $K_3 \bullet K_3$, and consider it next.

Let $X \in \Delta_2$ and $X[A] \cong K_3 \bullet K_3$. Here, we consider the possibility of adding a vertex $v \notin A$ which is adjacent to two vertices in A . Any vertex $v \notin A$ must be adjacent to at most two vertices, otherwise we'd create a triangle through an edge we already see, and the frequency of X is 1. We note that X is the line graph of a cubic graph by Observation 3.4.4, and if v is adjacent to two of the nonadjacent vertices in A , we produce a 4-cycle. By Theorem 3.5.3 X must be exceptional. Therefore, a vertex $v \notin A$ is adjacent to at most one vertex in A , so $c(A \cup \{v\}) \geq 10$ and $A \cup \{v\}$ satisfies the theorem.

We're left with cubic graphs. The only case here to check is when $X \in \mathcal{T}_6$, $X[A] \cong C_6$ and the girth g of X is 6. Any vertex $v \notin A$ must be adjacent to at most one vertex in A , otherwise adding it in would produce a cycle of length at most 5, contradicting the assertion that $g = 6$. Therefore, $c(A \cup \{v\}) \geq 7$, and $A \cup \{v\}$ satisfies the theorem for all v . \square

Now, we've gotten nearly all of the hard details out of the way, and we are almost ready to prove the theorem. We'll be proving the theorem by contradiction, picking a minimum counterexample in the lexicographic ordering of tuples $(c(A), |A|)$. An important tool in navigating this space is *uncrossing*. Taking a minimal counterexample A to the theorem, if we can find an automorphism ϕ for which $|\phi(A) \cap A| = z$, we can find a cut B which satisfies the theorem and has $z \leq |B| \leq |V|/2$.

Lemma 3.6.4 (Uncrossing). *Let $X = (V, E)$ be a graph. If $|A| \leq |V|/2$, $\phi \in \text{Aut}(X)$ and $z = |A \cap \phi(A)| < |A|$, we have one of two outcomes*

1. *some $B \in \{\phi(A) \cup A, V \setminus (\phi(A) \cup A)\}$ satisfies $c(A) > c(B)$ and $|V|/2 \geq |B| \geq z$, or*
2. $c(A \cap \phi(A)) \leq c(A)$.

In the proof of this lemma, we use the notation $E_{A,B} = \{(a,b) \in E : a \in A, b \in B\}$ to denote the edges with endpoints in both A and B .

Proof. The principal observation is that the action of ϕ partitions the vertices in V into four nonempty parts by intersecting A , $\phi(A)$ and their complements,

| | | |
|-----------------------|-----|-----------------|
| | A | $V \setminus A$ |
| $\phi(A)$ | P | Q |
| $V \setminus \phi(A)$ | R | S |

$$P = A \cap \phi(A), \quad Q = A \setminus \phi(A), \quad R = \phi(A) \setminus A, \quad S = V \setminus (A \cup \phi(A)),$$

which in turn partitions $\partial(A)$

$$\partial(A) = E_{P,Q} \cup E_{P,S} \cup E_{R,Q} \cup E_{R,S},$$

and likewise $\partial(\phi(A))$

$$\partial(\phi(A)) = E_{A,V \setminus A} = E_{P,R} \cup E_{P,S} \cup E_{Q,R} \cup E_{Q,S},$$

into disjoint sets, some of which may be empty. Furthermore, we partition the cut edges of $A \cap \phi(A) = P$ and $A \cup \phi(A) = P \cup Q \cup R$,

$$\partial(A \cap \phi(A)) = E_{P,Q} \cup E_{P,R} \cup E_{P,S}$$

and

$$\partial(A \cup \phi(A)) = E_{P,S} \cup E_{Q,S} \cup E_{R,S}.$$

Thus,

$$\begin{aligned} c(A) + c(\phi(A)) &= (|E_{P,R}| + |E_{P,S}| + |E_{Q,R}| + |E_{Q,S}|) \\ &\quad + (|E_{P,Q}| + |E_{P,S}| + |E_{R,Q}| + |E_{R,S}|) \\ &\geq |E_{P,Q}| + |E_{P,R}| + |E_{P,S}| + |E_{P,S}| + |E_{Q,S}| + |E_{R,S}| \\ &= c(A \cap \phi(A)) + c(A \cup \phi(A)). \end{aligned}$$

Unless $c(A \cap \phi(A)) = c(A \cup \phi(A)) = c(A)$, we have either $c(A \cap \phi(A)) < c(A)$ or $c(A \cup \phi(A)) < c(A)$. Finally, we note that

$$z = |A \cap \phi(A)| < |A| \leq |A \cup \phi(A)| \leq |A| + |\phi(A)| - |A \cap \phi(A)| \leq |V| - z$$

since $|A| \leq |V|/2$, so each of $A \cap \phi(A)$, $A \cup \phi(A)$ and $V \setminus (A \cup \phi(A))$ have at least z elements. \square

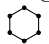
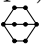

The general plan is proof by contradiction, interleaving two strategies. The first strategy is to organize the proof by degree, small to large. The second strategy is to establish a

sequence of claims which narrow down the possibilities for what the cut $X[A]$ may look like. Frequently, we will use the uncrossing lemma to find a cut for which the theorem holds, which necessitates checking a few specific cuts. As we rule out the smaller degrees, we are able to say successively more about $X[A]$, and we are left with fewer cuts to check after uncrossing.

Proof of Theorem 3.3.4. Choose a counterexample such that (1) $c(A)$ is minimum, and (2) subject to (1), $|A|$ is minimum. Note that there's nothing to say about double transitive graph with $d \leq 2$.

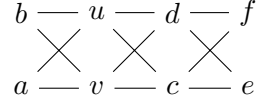
Claim 1. Our first claim is that the minimum degree of $X[A]$ is greater than $d/2$. If $v \in A$ has degree $d_A(v) \leq d/2$, then $c(A \setminus \{v\}) \leq c(A)$ and $|A \setminus \{v\}| < |A|$ so $A \setminus \{v\}$ satisfies the theorem, by the minimality of the counterexample. By Lemma 3.6.3, A is not a counterexample.

Degree 3. First, suppose that $X[A]$ has an edge uv between two vertices of degree 3. By Claim 1, there is an edge xy where $\deg_A(x) = 3$ and $\deg_A(y) = 2$. Take $\phi \in \text{Aut}(X)$ mapping $\phi : uv \mapsto xy$. Then, $A \cap \phi(A)$ contains all but one vertex in $N(x) \cup N(y)$, so we apply the uncrossing lemma. In outcome 1, we have a set B with $|V|/2 \geq |B| \geq 5$ and $c(B) < c(A) \leq 6$ contradicting the choice of A . In outcome 2 we have $B = A \cap \phi(A)$, $c(B) < c(A)$ and $|B| \geq 5$ where $X[B]$ contains a vertex of degree 3. Again, B is a more minimal counterexample.

Now, we know that $X[A]$ is a connected subcubic graph with at most 6 vertices of degree 2 and has no two adjacent vertices of degree 3. So, $X[A]$ is either a cycle or a subdivision of a cubic graph (possibly a multigraph) with ≤ 6 edges. By Lemma 3.6.1, the girth of X is at least 6, so $X[A]$ is one of , , or  so A satisfies the theorem.

Claim 2. Our next claim is that $X \notin \Delta_2$; equivalently, X is not the line graph of a cubic graph with girth $g > 3$. Let $X \cong \mathcal{L}(Y)$ and define $A^* = \{x \in V(X) : |N(x) \cap A| \geq 2\}$, so by Claim 1, $A \subset A^*$ and $c(A^*) \leq c(A)$. By definition of Δ_2 , the degree 3 vertices in $X[A]$ come in adjacent pairs which are missing the same neighbor, so $|A^* \setminus A| \leq 4$ and $X[A^*]$ is a union of triangles, and we denote their underlying vertices $B \subset V(Y)$, whence $8 \geq c(A) \geq c(A^*) = 2c(B)$. Since we've proved the theorem for $d = 3$, we see that $Y[B]$ is one of (a vertex, an edge, a square) or the complement thereof (by growing A to A^* , we may be looking at the larger half of the graph). In the case where Y contains a square, we're looking at an exceptional graph. Additionally, $Y[B]$ can't be a vertex or edge, since $X[A]$ would have at least one vertex of degree 1. We're left looking at B being the complement of a vertex or an edge, at which point $|A| + 4 \geq |A^*| \geq |V| - 5$ and $|A| \leq |V|/2$, which leaves us with the exceptionally small $|V(Y)| \leq 6$.

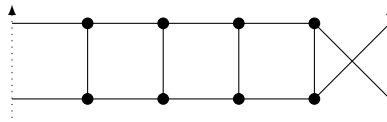
Claim 3. Our third claim is that $X \not\cong C_m^{(2)}$. By Claim 1, we should have a vertex v of degree 3 in $X[A]$, so we look at its neighborhood.



If $u \notin A$, we have $c(A \cup \{u\}) \leq d + 1$ and $A \cup \{u\}$ satisfies the theorem, so $A \cup \{u\}$ is the complement of a single vertex, leaving us in the ridiculous situation that $m = 2$ and X is 2-regular. So, we conclude that both u and v have degree 3 in $X[A]$. Without loss of generality, suppose that $c \notin A$ and therefore $d \in A$. Whether d has degree 3 or 4, we find that $c(A \cup \{c\}) \leq d + 1$. Ridiculous.

Claim 4. Next, we claim that $X[A]$ has maximum degree less than d . Suppose that $v \in A$ is a vertex of degree d in $X[A]$, and that $u \in A$ has degree $\lceil d/2 \rceil \leq \deg_A(u) < d$. Then, find $\phi \in \text{Aut}(X)$ mapping $\phi : v \mapsto u$. Then, $|\phi(A) \cap A| \geq 1 + \lceil d/2 \rceil \geq 4$. Uncrossing, we find a set B with $|V|/2 \geq |B| \geq 4$ which satisfies the theorem (since A was a minimal counterexample) and has $c(B) \leq c(A)$. If any $c(B) < 2d$ then we find an immediate contradiction since $|B| \geq 4$. Otherwise, we take $B = A \cap \phi(A)$ and $c(B) \leq 2d$ and $X[B]$ contains a vertex u with degree $d/2 < d_u < d$: looking at the list, the only such non-exceptional cut is Υ , which only occurs in Δ_2 , which we took care of with Claim 2.

Degree 4. By Claims 1 and 4, we see that $X[A]$ is 3-regular. If X contains a triangle, then by Theorem 3.5.3, X is an exceptional graph or $X \in \Delta_2$. Therefore, $X[A]$ is a 3-regular graph with girth at least 4, and $|A| \leq 8$ since $c(A) \leq 8$. If $|A| = 6$ then we have either $X[A] \cong K_{3,3}$ or Q_3 , whence $k \geq 3$. By Theorem 3.5.5, either $X \cong C_m^{(2)}$ or X is an exceptional graph, and we're done in either case. Otherwise $|A| = 8$ and $X[A]$ must be the Möbius band V_8 shown below, where the left and right sides are identified top edge to top edge, bottom edge to bottom edge.



By Theorem 3.5.5, either $k > 3$ and we're looking at an exceptional graph, or $k = 2$ and there is a toroidal embedding of V_8 where the 4-cycles displayed above are faces. That cannot be, as traversing those four faces necessitates a change in orientation. Therefore, the theorem is true for all 4-regular graphs.

Claim 5. Now, we claim that $X[A]$ has maximum degree less than $d - 1$. Otherwise, let $v \in A$ have degree $d_v = d - 1$ in $X[A]$ (by Claim 4, this is the only exception to the current claim). By Observation 3.4.2, there is an automorphism $\phi \in \text{Stab}(v)$ mapping an edge $vx \in E_A$ to an edge $vy \in \partial(A)$. Therefore, $|N(v) \cap A \cap \phi(A)| = d - 2$ so $|A \cap \phi(A)| \geq d - 1$. Uncrossing, we find a set B with $c(B) \leq c(A)$ and $|V|/2 \geq |B| \geq d - 1$, which satisfies the theorem. Therefore, either $2d < c(B) \leq c(A)$ and we don't have a counterexample after all, or $X = \text{Ico}$, an exceptional case that we've already checked.

Degree 5. By Claims 1 and 5, $X[A]$ is 3-regular with $|A| \leq 5$. The only possibility here is that $X[A] \cong K_4$ and by Theorem 3.5.12, $X \cong K_6$, an exceptional graph.

Degree 6. By Claims 1 and 5, $X[A]$ is 4-regular with $|A| \leq 6$. Here, we have either $X[A] \cong K_5$ or $X[A] \cong \text{Oct}$, so $g = 3$ and $k \geq 3$. By Theorem 3.5.14, X is an exceptional graph, and we're done.

Claim 6. Our final claim is that d is odd and $X[A]$ is $(d+1)/2$ -regular. Otherwise, by Claims 1 and 5, there is a vertex $v \in A$ with $\deg_A(v) > (d+1)/2$. Pick $\phi \in \text{Stab}(v)$ such that $\phi(N_A(v)) \neq N_A(v)$. Thus, $A \cap \phi(A)$ contains v and at least two neighbors of v , so $|A \cap \phi(A)| \geq 3$. Uncrossing, we find a set B with $c(B) \leq c(A)$ and $|V|/2 \geq |B| \geq 3$, which satisfies the theorem: $c(A) \geq c(B) > 2d$, so we didn't have a counterexample after all.

Degree $d = 2e + 1, e > 3$. By Claim 6, we see that $X[A]$ is $e + 1$ -regular and $e|A| = c(A) \leq 4e + 2$. That is, $X[A]$ is at least 4-regular and has at most 4 vertices: absurd. \square

Bibliography

- [1] Tameem Albash et al. “Consistency tests of classical and quantum models for a quantum annealer”. In: *Physical Review A* 91.4 (2015), p. 042314.
- [2] Dan Archdeacon. “Heffter Arrays and Biembedding Graphs on Surfaces”. In: *The Electronic Journal of Combinatorics* 22 (1 2015).
- [3] Dan Archdeacon et al. “On Partial Sums in Cyclic Groups”. In: *Journal of Combinatorial Mathematics and Combinatorial Computing (to appear)* (2015).
- [4] Dan S. Archdeacon, Tomas Boothby, and Jeffrey H. Dinitz. “Tight Heffter Arrays Exist for all Possible Values”. In: *submitted* (Sept. 2015).
- [5] Dan S. Archdeacon, Tomas Boothby, and Jeffrey H. Dinitz. “Tight Heffter Arrays Exist for all Possible Values: The Research Report”. In: *arXiv preprint arXiv:1509.00430* (Sept. 2015). arXiv: 1509.00430 [math.CO].
- [6] László Babai. “Vertex-transitive graphs and vertex-transitive maps”. In: *Journal of Graph Theory* 15.6 (1991), pp. 587–627. ISSN: 1097-0118. DOI: 10.1002/jgt.3190150605.
- [7] Thøger Bang. “On the sequence $[n\alpha], n = 1, 2, \dots$. Supplementary note to the preceding paper by Th. Skolem”. In: *Mathematica Scandinavica* 5.1 (1957), pp. 69–76.
- [8] Jens-P. Bode and Heiko Harborth. “Directed paths of diagonals within polygons”. In: *Discrete Mathematics* 299.1–3 (2005). Graph Theory of Brian Alspach, pp. 3–10. ISSN: 0012-365X. DOI: <http://dx.doi.org/10.1016/j.disc.2005.05.006>.
- [9] Sergio Boixo et al. “Computational Role of Collective Tunneling in a Quantum Annealer”. In: *arXiv preprint arXiv:1411.4036* (2014).
- [10] Tomas Boothby and Matt DeVos. “The 4-Regular Edge-Transitive Graphs of Girth 4”. In: *arXiv preprint arXiv:1511.06794* (Nov. 2015). arXiv: 1511.06794 [math.CO].
- [11] Tomas Boothby, Andrew D. King, and Aidan Roy. “Fast clique minor generation in Chimera qubit connectivity graphs”. In: *Quantum Information Processing* (2015). ISSN: 1570-0755. DOI: 10.1007/s11128-015-1150-6. URL: <http://dx.doi.org/10.1007/s11128-015-1150-6>.
- [12] Jun Cai, William G. Macready, and Aidan Roy. “A practical heuristic for finding graph minors”. In: *arXiv preprint arXiv:1406.2741* (2014).
- [13] Augustin-Louis Cauchy. “Recherches sur les nombres”. In: *J. École Polytech.* 9 (1813), pp. 99–116.
- [14] Vicky Choi. “Minor-embedding in adiabatic quantum computation: I. The parameter setting problem”. In: *Quantum Information Processing* 7.5 (2008), pp. 193–209.

- [15] Vicky Choi. “Minor-embedding in adiabatic quantum computation: II. Minor-universal graph design”. In: *Quantum Information Processing* 10.3 (2011), pp. 343–353.
- [16] Harold Davenport. “A historical note”. In: *J. London Math. Soc.* 22 (1947), pp. 100–101.
- [17] Harold Davenport. “On the addition of residue classes”. In: *J. London Math. Soc.* 10 (1935), pp. 30–32.
- [18] Matt DeVos. “The Structure of Critical Product Sets”. In: *arXiv preprint arXiv:1301.0096* (Jan. 2013). arXiv: 1301.0096 [math.CO].
- [19] N.G. Dickson et al. “Thermally assisted quantum annealing of a 16-qubit problem”. In: *Nature Communications* 4.May (Jan. 2013), p. 1903. ISSN: 2041-1723. DOI: 10.1038/ncomms2920. URL: <http://www.ncbi.nlm.nih.gov/pubmed/23695697>.
- [20] Reinhard Diestel. *Graph Theory, 4th Edition*. Vol. 173. Graduate texts in mathematics. Springer, 2012. ISBN: 978-3-642-14278-9.
- [21] Jeff Dinitz and Amelia Mattern. “Biembedding Steiner Triple Systems and n-cycle Systems on Orientable Surfaces”. In: *arXiv preprint arXiv:1505.04070* (May 2015). arXiv: 1505.04070 [math.CO].
- [22] Jeffrey H Dinitz. “CRC Handbook of Combinatorial Designs”. In: CRC Press Boca Raton, FL, 2007. Chap. Starters, pp. 612–628.
- [23] Jacek Dziarmaga. “Dynamics of a quantum phase transition: Exact solution of the quantum Ising model”. In: *Physical review letters* 95.24 (2005), p. 245701.
- [24] Yan-Quan Feng and Roman Nedela. “Symmetric Cubic Graphs of Girth At Most 7”. In: *Acta Universitatis Matthiae Belii. Mathematics* 13 (2006), pp. 33–35.
- [25] David J. Grynkiewicz. “A Step Beyond Kemperman’s Structure Theorem”. In: *Mathematika* 55 (1-2 Dec. 2009), pp. 67–114. ISSN: 2041-7942. DOI: 10.1112/S0025579300000966.
- [26] Lothar Heffter. “Über Tripelsysteme”. In: *Math. Annalen* 49 (1897), pp. 101–112.
- [27] M.W. Johnson et al. “Quantum annealing with manufactured spins”. In: *Nature* 473.7346 (2011), pp. 194–198.
- [28] Gyula Károlyi. “The Cauchy-Davenport theorem in group extensions”. In: *L’Enseignement Mathématique* 51 (2005), pp. 239–254.
- [29] Johannes Henricus Bernardus Kemperman. “On small sumsets in an abelian group”. In: *Acta Mathematica* 103.1 (1960), pp. 63–88.
- [30] Andrew D. King and Catherine C. McGeoch. “Algorithm engineering for a quantum annealing platform”. In: *arXiv preprint arXiv:1410.2628* (2014).
- [31] Christine Klymko, Blair D. Sullivan, and Travis S. Humble. “Adiabatic quantum programming: minor embedding with hard faults”. In: *Quantum Information Processing* 13.3 (2014), pp. 709–729.
- [32] Martin Kneser. “Ein Satz über abelsche Gruppen mit Anwendungen auf die Geometrie der Zahlen”. In: *Mathematische Zeitschrift* 61.1 (1954), pp. 429–434.
- [33] László Lovász and Michael David Plummer. “Matching Theory”. In: AMS Chelsea Publishing Series. AMS Chelsea Pub., 2009, pp. 208–211. ISBN: 9780821847596. URL: <https://books.google.ca/books?id=0aoJBAAQBAJ>.

- [34] Wolfgang Mader. “Minimale n -fach zusammenhängende Graphen mit maximaler Kantenzahl.” In: *Journal für die reine und angewandte Mathematik* 249 (1971), pp. 201–207.
- [35] Robert C Miller. “The trivalent symmetric graphs of girth at most six”. In: *Journal of Combinatorial Theory, Series B* 10.2 (1971), pp. 163–182.
- [36] Rose Peltesohn. “Eine Lösung der beiden Heffterschen Differenzenprobleme”. In: *Compositio Mathematica* 6 (1939), pp. 251–257.
- [37] Alejandro Perdomo-Ortiz et al. “A Performance Estimator for Quantum Annealers: Gauge selection and Parameter Setting”. In: *arXiv preprint arXiv:1503.01083* (2015).
- [38] Stephen R Schmidt. “Effects of humor on sentence memory.” In: *Journal of Experimental Psychology: Learning, Memory, and Cognition* 20.4 (1994), p. 953.
- [39] Nabil Shalaby. “Skolem sequences: generalizations and applications”. PhD thesis. McMaster University, 1992.
- [40] James E Simpson. “Langford sequences: perfect and hooked”. In: *Discrete Mathematics* 44.1 (1983), pp. 97–104.
- [41] Thoralf Skolem. “On certain distributions of integers in pairs with given differences”. In: *Mathematica Scandinavica* 5.1 (1957), pp. 57–68.
- [42] Vincent Vatter and Steve Waton. “On points drawn from a circle”. In: *Electronic Journal of Combinatorics* 18.1 (2011), P223.
- [43] D. Venturelli et al. “Quantum Optimization of Fully-Connected Spin Glasses”. In: *arXiv preprint arXiv:1406.7553* (2014).
- [44] Alan Gordon Vosper. “The critical pairs of subsets of a group of prime order”. In: *Journal of the London Mathematical Society* 1.2 (1956), pp. 200–205.
- [45] Jozef Širáň and Martin Škoviera. “Characterization of the maximum genus of a signed graph”. In: *Journal of Combinatorial Theory, Series B* 52.1 (1991), pp. 124–146.
- [46] Jeffrey Paul Wheeler. “The Cauchy-Davenport Theorem for Finite Groups”. In: *arXiv preprint arXiv:1202.1816* (Feb. 2012). arXiv: 1202.1816 [math.CO].
- [47] K.C. Young, R. Blume-Kohout, and D.A. Lidar. “Adiabatic quantum optimization with the wrong Hamiltonian”. In: *Physical Review A* 88.6 (2013), p. 062314.

Appendix A

Skolem-like Sequences

In this appendix, we will review the history of Skolem sequences, demonstrate the constructions of K -near Skolem sequences that we use, and briefly describe how we found them.

In his 1957 seminal paper [41] on the topic, Thoralf Skolem proved that $[n]$ -Skolem sequences exist if and only if $n \equiv 0, 1 \pmod{4}$. The necessity result boils down to counting the number of odd terms in a sum. To demonstrate sufficiency, Skolem defined two families of these sequences, one for $n \equiv 0 \pmod{4}$ and one for $n \equiv 1 \pmod{4}$. The below is copied verbatim¹ from [41], his construction for $n \equiv 0 \pmod{4}$:

1. all pairs $(4m + r, 8m - r)$ for $r = 0, 1, 2, \dots, 2m - 1$,
2. the pairs $(2m + 1, 6m)$ and $(2m, 4m - 1)$,
3. the pairs $(r, 4m - 1 - r)$ for $r = 1, 2, \dots, m - 1$,
4. the pair $(m, m + 1)$,
5. the pair $(m + 2 + r, 3m - 1 - r)$ for $r = 0, 1, \dots, m - 3$.

Note that $\{1\}$ -near Skolem sequences are also known as *Langford sequences of defect 2* and $\{1, 2\}$ -near Skolem sequences are Langford sequences of defect 3. Skolem [41] proved that Skolem sequences exist for all positive $n \equiv 0, 1 \pmod{4}$. Shalaby [39] investigated the existence of $\{k\}$ -near Skolem sequences in his PhD thesis, finding that a $\{k\}$ -near Skolem sequences of order $n > k$ exist if and only if $n \equiv 0, 1 \pmod{4}$ when k is odd and $n \equiv 2, 3 \pmod{4}$ when k is even. Simpson [40] proved that $[1, d - 1]$ -near Skolem sequences of order $d + m - 1$ exist if and only if $m \geq 2d - 1$ and $m \equiv 0, 1 \pmod{4}$ if d is odd and $m \equiv 0, 3 \pmod{4}$ if d is even – that is, $\{1, 2\}$ -near Skolem sequences of order n exist if and only if $m \geq 7$ and $m \equiv 2, 3 \pmod{4}$.

Many of the constructions found in the literature [40, 39] are recursive, and involve further generalizations of Skolem sequences. For example, a “hooked” Skolem sequence is similar to a Skolem sequence, with a single zero in the second or penultimate position of the sequence.

¹less one typo

To construct a Skolem sequence of order 12, we can assemble a hooked Skolem sequence of order 4, 303242114, together with a hooked $\{1, 2, 3, 4\}$ -near Skolem sequence of order 15,

$$[5, 12, 13, 14, 15, 5, 6, 7, 8, 9, 10, 11, 6, 12, 7, 13, 8, 14, 9, 15, 10, 0, 11]$$

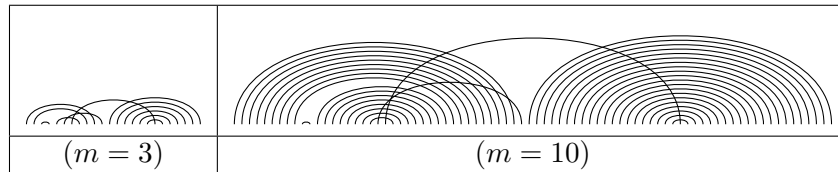
to produce a Skolem sequence of order 15,

$$[5, 12, 13, 14, 15, 5, 6, 7, 8, 9, 10, 11, 6, 12, 7, 13, 8, 14, 9, 15, 10, 3, 11, 3, 2, 4, 2, 1, 1, 4].$$

Simpson's constructions use particularly nice $[1, k - 1]$ -near Skolem sequences of order $3k$, together with similarly nice looped and hooked sequences to recursively construct his Langford sequences of defect d .

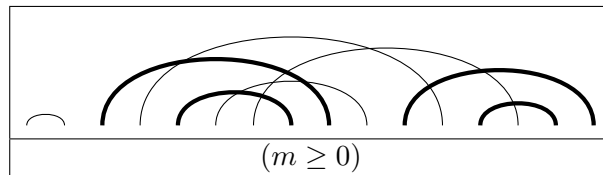
Hoping to use the Heffter system constructions presented in the Section 2.5.1, we want direct, explicit, one-shot constructions like Skolem's. Our desire to find a nice set of tiles with zero row- and column-sum directs us to throw away even Skolem's original constructions. Annoying as that sounds, we'll be finding these constructions by computer search and it generally takes a few seconds to produce the requisite constructions.

We can visualize Skolem partitions by drawing arcs between paired points on a number line, as shown below.



Prominent in these pictures are rainbow-like groups of lines. There are three such groups in Skolem's construction, all of different sizes. For our purposes, it is most convenient if there are four equal-sized groups. The reasoning behind this convenience will be apparent when we use the Skolem partitions to finally construct Heffter arrays, but it all boils down to our favorite sum: $x + \overline{x + a} + \overline{y} + (y + a) = 0$.

Should all the groups have equal size, we are able to represent a family of Skolem partitions with a single diagram:



here, a group of pairs is represented as a thick line. This represents the family of partitions defined by

1. the pairs $(1, 2)$, $(2m + 4, 4m + 6)$, $(2m + 5, 6m + 8)$ and $(m + 3, 5m + 7)$,
2. the pairs $(r + 5m + 8, -r + 7m + 8)$ for $0 \leq r < m$,
3. the pairs $(r + m + 4, -r + 3m + 5)$ for $0 \leq r < m$,

4. the pairs $(r + 4m + 7, -r + 8m + 8)$ for $0 \leq r < m$, and
5. the pairs $(r + 3, -r + 4m + 5)$ for $0 \leq r < m$.

We found this construction, and seven more like it, as follows:

1. Use an EXACTCOVER solver to find an explicit partition of $[1, 2n_0 - 2|K|]$ into differences $[1, n_0] \setminus K$ for some sufficiently large $n_0 = 4m_0 + k$.
2. Select four pairs from the partition to *thicken*.
3. Symbolically compute the set of differences of a thickened partition and check if that set is a Skolem partition for all $m \geq m_0$. If not, pick a new K -near Skolem sequence from the EXACTCOVER solver.

Given a partition P of $I = [I_0, I_f]$ into distances D and a set $T = \{t_1, t_2, t_3, t_4\} \subset D$, we will describe the family obtained by thickening the pairs (a_t, b_t) for all $t \in T$. We define the set E of endpoints $\{a_t : t \in T\} \cup \{b_t : t \in T\}$, and for $t \in \mathbb{Z}$, define $A(t) = \{e \in E : e < t\}$ and $B(t) = \{e \in E : e \leq t\}$. Then, the set of pairs

$$P(m) = \{(a_d + mA(a_d), b_d + mB(b_d)) : d \in D\} \cup \bigcup_{i=1}^4 \{(a_{t_i} + mA(a_{t_i}) + r, b_{t_i} + mB(b_{t_i}) - r) : 0 < r < m\}$$

is a partition of $I(m) = [I_0, I_f + 8(m - 1)]$ into pairs.

While it is conceivable that any set of pairs could be thickened to construct a family of K -near Skolem sequences, we impose some additional conditions that narrow down the search space and facilitate easy proof that we produce a partition into the desired differences (by definition of thickening, we will always produce partitions, the difficulty is in discovering the desired differences). We say that two pairs (a_i, b_i) and (a_j, b_j) are *crossed* if $a_i < a_j < b_i < b_j$ and *nested* if $a_i < a_j < b_j < b_i$. We require the following:

1. The pairs (a_{t_1}, b_{t_1}) and (a_{t_2}, b_{t_2}) are nested, as are (a_{t_3}, b_{t_3}) and (a_{t_4}, b_{t_4}) , and there are no other crossings or nestings among these pairs
2. $b_{t_1} - a_{t_1} = b_{t_3} - a_{t_3} \pm 1$ and $b_{t_2} - a_{t_2} = b_{t_4} - a_{t_4} \pm 1$, and
3. $b_{t_1} - a_{t_1} \not\equiv b_{t_2} - a_{t_2} \pmod{2}$ and $b_{t_3} - a_{t_3} \not\equiv b_{t_4} - a_{t_4} \pmod{2}$.

Note that a group of pairs $\{(a_t + mA(a_t) + r, b_t + mB(b_t) - r) : 0 \leq r < m\}$ has differences $\{t + m(B(b_t) - A(a_t)) - 2r : 0 \leq r < m\}$: a “half interval” where every other element is skipped. The requirements above ensure that these half intervals are interleaved to make a whole interval of size $2m$.

Once we have interleaved the half intervals, we are left with a collection of “sporadic differences” coming from non-thickened pairs and two intervals of differences. To check that $P(m)$ is a partition of $I(m)$ into distances $D(m) = [1, 4m + n_0] \setminus K$, we construct a graph whose vertices have three types: sporadic differences, difference interval endpoints, and “holes”

from K . For our purposes, the sets of holes we consider are $\emptyset, \{1\}, \{2\}$ and $\{1, 2\}$. We place edges in our graph between vertices which differ by 1, and between the two endpoints of each distance interval. If the resulting graph is a path and contains the vertex $\max D(m)$, then every difference in $D(m)$ occurs precisely once as a difference from $P(m)$. We will duplicate this line of reasoning later, in Section 2.7, to prove that our final constructions indeed produce Heffter arrays.

For example, let us consider the construction above. We have the sporadic differences $1, 2m+2, 4m+3$, and $4m+4$ coming from the pairs $(1, 2), (2m+4, 4m+6), (2m+5, 6m+8)$, and $(m+3, 5m+7)$ respectively. We have two difference intervals, $[2, 2m+1]$ obtained by interleaving the pairs $(r+5m+8, -r+7m+8)$ and $(r+m+4, -r+3m+5)$ for $0 \leq r < m$, and likewise $[2m+3, 4m+2]$ from the remaining groups of pairs. Thus, we have the complete interval

$$[1, 4m+4] = \{1\} \cup [2, 2m+1] \cup \{2m+2\} \cup [2m+3, 4m+2] \cup \{4m+3\} \cup \{4m+4\},$$

so this is a Skolem sequence for all $m \geq 0$.









| Type | Pair Families ($0 \leq r < m$) | Sporadic Pairs | |
|-------------------|---|---|---|
| \emptyset -near | $(r+2, 4m-r+3)$ $(4m+r+4, 8m-r+8)$ $(m+r+3, 3m-r+3)$ $(5m+r+7, 7m-r+6)$ | $(1, 2m+3)$ $(m+2, 5m+5)$ $(5m+4, 7m+8)$ $(5m+6, 7m+7)$ |  |
| \emptyset -near | $(r+2, 4m-r+3)$ $(m+r+3, 3m-r+3)$ $(4m+r+6, 8m-r+10)$ $(5m+r+9, 7m-r+8)$ | $(1, 4m+4)$ $(m+2, 5m+7)$ $(2m+3, 4m+5)$ $(5m+6, 7m+10)$ $(5m+8, 7m+9)$ |  |
| $\{2\}$ -near | $(r+2, 4m-r+5)$ $(m+r+4, 3m-r+5)$ $(5m+r+8, 7m-r+10)$ $(4m+r+8, 8m-r+10)$ | $(1, 4m+7)$ $(m+2, m+3)$ $(2m+4, 6m+8)$ $(4m+6, 6m+9)$ $(2m+5, 6m+10)$ |  |
| $\{2\}$ -near | $(r+3, 4m-r+7)$ $(4m+r+9, 8m-r+12)$ $(5m+r+9, 7m-r+11)$ $(m+r+4, 3m-r+5)$ | $(1, 4m+8)$ $(2, 2m+5)$ $(m+3, 3m+7)$ $(6m+10, 6m+11)$ $(2m+4, 6m+9)$ $(3m+6, 7m+12)$ |  |
| $\{1\}$ -near | $(r+3, 4m-r+5)$ $(m+r+3, 3m-r+4)$ $(4m+r+7, 8m-r+8)$ $(5m+r+7, 7m-r+7)$ | $(1, 4m+6)$ $(2, 2m+4)$ $(2m+3, 6m+7)$ $(3m+5, 7m+8)$ |  |
| $\{1, 2\}$ -near | $(4m+r+9, 8m-r+15)$ $(5m+r+12, 7m-r+13)$ $(m+r+3, 3m-r+5)$ $(r+2, 4m-r+5)$ | $(2m+3, 6m+13)$ $(m+2, 5m+11)$ $(5m+9, 7m+15)$ $(4m+8, 8m+16)$ $(5m+10, 7m+14)$ $(2m+5, 6m+12)$ $(1, 4m+6)$ $(2m+4, 4m+7)$ |  |
| $\{1, 2\}$ -near | $(r+1, 4m-r+4)$ $(4m+r+6, 8m-r+10)$ $(m+r+1, 3m-r+2)$ $(5m+r+7, 7m-r+9)$ | $(2m+1, 6m+8)$ $(3m+4, 7m+10)$ $(2m+2, 6m+7)$ $(4m+5, 6m+9)$ $(3m+3, 5m+6)$ |  |
| $\{1\}$ -near | $(5m+r+6, 7m-r+6)$ $(4m+r+5, 8m-r+6)$ $(m+r+2, 3m-r+3)$ $(r+1, 4m-r+3)$ | $(m+1, 5m+5)$ $(2m+2, 4m+4)$ $(2m+3, 6m+6)$ |  |

Table A.1: Our constructions of Skolem-like sequences

Appendix B

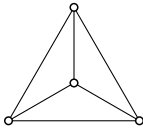
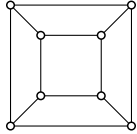
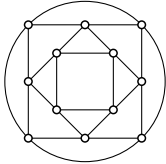
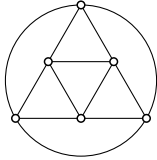
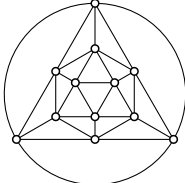
Two Row Tiles

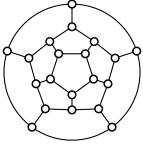
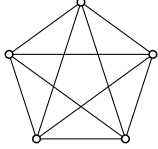
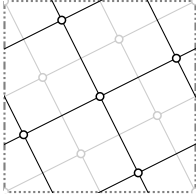
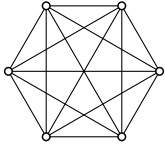
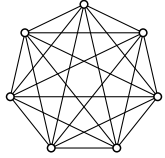
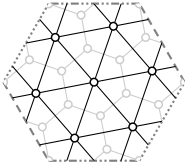
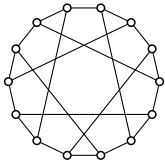
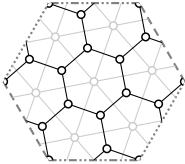
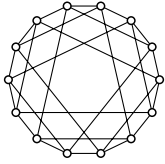
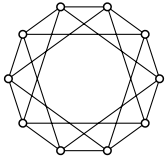
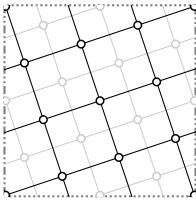
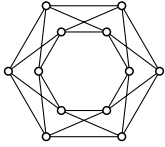
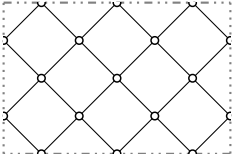
| | | | |
|--|--|--|--|
| $\begin{bmatrix} 1 & \bar{2} & \bar{3} & 4 \\ \bar{5} & 6 & 7 & \bar{8} \\ \hline 4 & 4 & 4 & 4 \end{bmatrix}$ | $\begin{bmatrix} 1 & \bar{2} & \bar{3} & 4 \\ \bar{8} & 7 & 6 & \bar{5} \\ \hline \bar{7} & 5 & 3 & \bar{1} \end{bmatrix}$ | $\begin{bmatrix} 1 & \bar{2} & \bar{7} & 8 \\ \bar{3} & 5 & 4 & \bar{6} \\ \hline 2 & 3 & \bar{3} & 2 \end{bmatrix}$ | $\begin{bmatrix} 1 & \bar{3} & \bar{5} & 7 \\ \bar{4} & 8 & 2 & \bar{6} \\ \hline \bar{3} & 5 & \bar{3} & 1 \end{bmatrix}$ |
| $\begin{bmatrix} 1 & \bar{2} & \bar{3} & 4 \\ \bar{5} & 7 & 6 & \bar{8} \\ \hline 4 & 5 & 3 & 4 \end{bmatrix}$ | $\begin{bmatrix} 1 & \bar{2} & \bar{5} & 6 \\ \bar{3} & 4 & 7 & \bar{8} \\ \hline \bar{2} & 2 & 2 & \bar{2} \end{bmatrix}$ | $\begin{bmatrix} 1 & \bar{2} & \bar{7} & 8 \\ \bar{4} & 6 & 3 & \bar{5} \\ \hline \bar{3} & 4 & \bar{4} & 3 \end{bmatrix}$ | $\begin{bmatrix} 1 & \bar{3} & \bar{5} & 7 \\ \bar{8} & 4 & 6 & \bar{2} \\ \hline \bar{7} & 1 & 1 & 5 \end{bmatrix}$ |
| $\begin{bmatrix} 1 & \bar{2} & \bar{3} & 4 \\ \bar{6} & 5 & 8 & \bar{7} \\ \hline \bar{5} & 3 & 5 & \bar{3} \end{bmatrix}$ | $\begin{bmatrix} 1 & \bar{2} & \bar{5} & 6 \\ \bar{3} & 7 & 4 & \bar{8} \\ \hline \bar{2} & 5 & \bar{1} & \bar{2} \end{bmatrix}$ | $\begin{bmatrix} 1 & \bar{2} & \bar{7} & 8 \\ \bar{5} & 3 & 6 & \bar{4} \\ \hline 4 & 1 & \bar{1} & 4 \end{bmatrix}$ | $\begin{bmatrix} 1 & \bar{3} & \bar{6} & 8 \\ \bar{2} & 5 & 4 & \bar{7} \\ \hline \bar{1} & 2 & \bar{2} & 1 \end{bmatrix}$ |
| $\begin{bmatrix} 1 & \bar{2} & \bar{3} & 4 \\ \bar{6} & 8 & 5 & \bar{7} \\ \hline \bar{5} & 6 & 2 & \bar{3} \end{bmatrix}$ | $\begin{bmatrix} 1 & \bar{2} & \bar{5} & 6 \\ \bar{4} & 3 & 8 & \bar{7} \\ \hline \bar{3} & 1 & 3 & \bar{1} \end{bmatrix}$ | $\begin{bmatrix} 1 & \bar{2} & \bar{7} & 8 \\ \bar{6} & 4 & 5 & \bar{3} \\ \hline \bar{5} & 2 & \bar{2} & 5 \end{bmatrix}$ | $\begin{bmatrix} 1 & \bar{3} & \bar{6} & 8 \\ \bar{7} & 4 & 5 & \bar{2} \\ \hline \bar{6} & 1 & \bar{1} & 6 \end{bmatrix}$ |
| $\begin{bmatrix} 1 & \bar{2} & \bar{3} & 4 \\ \bar{7} & 8 & 5 & \bar{6} \\ \hline \bar{6} & 6 & 2 & \bar{2} \end{bmatrix}$ | $\begin{bmatrix} 1 & \bar{2} & \bar{5} & 6 \\ \bar{4} & 8 & 3 & \bar{7} \\ \hline \bar{3} & 6 & \bar{2} & \bar{1} \end{bmatrix}$ | $\begin{bmatrix} 1 & \bar{3} & \bar{5} & 7 \\ \bar{2} & 4 & 6 & \bar{8} \\ \hline \bar{1} & 1 & 1 & \bar{1} \end{bmatrix}$ | |
| $\begin{bmatrix} 1 & \bar{2} & \bar{3} & 4 \\ \bar{8} & 6 & 7 & \bar{5} \\ \hline \bar{7} & 4 & 4 & \bar{1} \end{bmatrix}$ | $\begin{bmatrix} 1 & \bar{2} & \bar{5} & 6 \\ \bar{8} & 4 & 7 & \bar{3} \\ \hline \bar{7} & 2 & 2 & 3 \end{bmatrix}$ | $\begin{bmatrix} 1 & \bar{3} & \bar{5} & 7 \\ \bar{2} & 6 & 4 & \bar{8} \\ \hline \bar{1} & 3 & \bar{1} & \bar{1} \end{bmatrix}$ | |

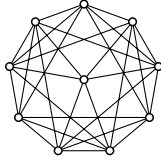
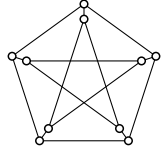
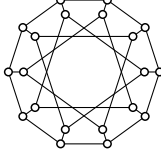
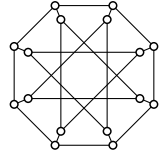
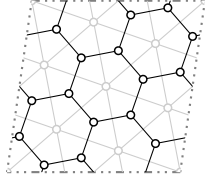
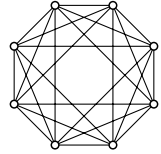
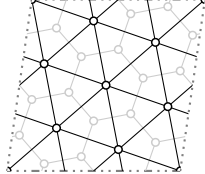
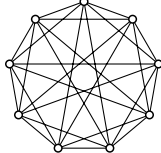
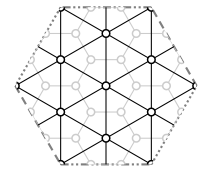
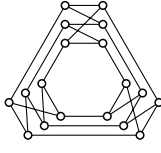
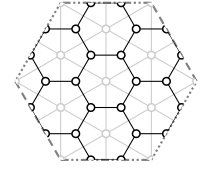
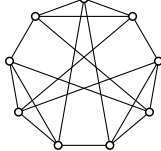
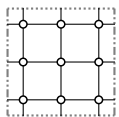
Table B.1: Representative shifttable 2×4 tiles whose row sums are zero. All possible column sums (up to reordering and negation) are represented. Third row is the column sums.

Appendix C

Additional Info for Chapter 3 and Main Theorem Tearout

| Graph Name(s) | Family | Plane Drawing | Torus Embedding |
|--|-----------------------|--|-----------------|
| $K_4 \cong$ Tetrahedron | |  | |
| $Q_3 \cong M_4$ | |  | |
| $\mathcal{L}(Q_3) \cong$ Medial(Q_3) \cong Medial(Oct) \cong Cubeoctahedron | Δ_2, \square_2 |  | |
| Oct $\cong K_{2(3)} \cong$ $\mathcal{L}(K_4) \cong C_3^{(2)}$ | |  | |
| Ico | |  | |

| Graph Name(s) | Family | Plane Drawing | Torus Embedding |
|---------------------------------|-----------------|--|---|
| $\text{Dod} \cong \text{Ico}^*$ | |  | |
| K_5 | \mathcal{T}_4 |  |  |
| K_6 | |  | No regular torus embeddings by Euler characteristic. |
| K_7 | \mathcal{T}_3 |  |  |
| $\text{Hea} \cong K_7^*$ | \mathcal{T}_6 |  |  |
| Hea^c | |  | No 4-cycle double cover. |
| M_5 | \mathcal{T}_4 |  |  |
| $C_m^{(2)}, m \geq 4$ | \mathcal{T}_4 |  |  |

| Graph Name(s) | Family | Plane Drawing | Torus Embedding |
|--|---------------------------|--|---|
| $\mathcal{L}(K_5) \cong \overline{\text{Pet}}$ | \boxtimes_2 |  | Every triangle double cover makes pinch points. |
| $\text{Pet} = \text{GP}(5, 3) \cong \overline{\mathcal{L}(K_5)}$ | |  | Every 6-cycle double cover makes pinch points. |
| $\text{GP}(10, 3)$ | |  | No 6-cycle double cover. |
| $\text{GP}(8, 3)$ | \mathcal{T}_6 |  |  |
| $K_{2(4)} \cong \text{GP}(8, 3)^*$ | \mathcal{T}_3 |  |  |
| $K_{3(3)}$ | \mathcal{T}_3 |  |  |
| $\text{Pap} \cong K_{3(3)}^*$ | \mathcal{T}_6 |  |  |
| $\mathcal{L}(K_{3,3}) \cong K_3 \times K_3$ | Δ_2, \mathcal{T}_4 |  |  |

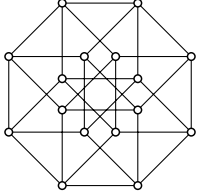
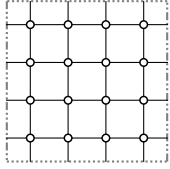
| Graph Name(s) | Family | Plane Drawing | Torus Embedding |
|---------------|-----------------|--|---|
| Q_4 | \mathcal{T}_4 |  |  |

Table C.1: Table of exceptional graphs and their familial inclusions. Note that the graph G^* is the 1-skeleton of the geometric dual of G as drawn in this table.

Below is the code that we used to prove Lemma 3.6.1

```

def UniqueLabel(X):
    return X.canonical_label().graph6_string()
def SmallCuts(X):
    V = set(X.vertices())
    d = X.degree_sequence()[0]
    cuts = {}

    for k in range(3,1+len(V)/2):
        for A in Subsets(V,k):
            XA = X.subgraph(A)
            cA = d*k - sum(XA.degree_sequence())
            if cA <= 2*d:
                cuts[UniqueLabel(XA)] = XA

    return cuts

Fano = [(1,2,3),(3,4,5),(1,5,6),(1,4,7),(2,5,7),(3,6,7),(2,4,6)]
ExceptionalGraphs = {
    'K_4': graphs.CompleteGraph(4),
    'K_5': graphs.CompleteGraph(5),
    'K_6': graphs.CompleteGraph(6),
    'K_7': graphs.CompleteGraph(7),
    'K_{2^3}': graphs.CompleteMultipartiteGraph([2,2,2]),
    'K_{2^4}': graphs.CompleteMultipartiteGraph([2,2,2,2]),
    'K_{3,3}': graphs.CompleteMultipartiteGraph([3,3]),
    'K_{3^3}': graphs.CompleteMultipartiteGraph([3,3,3]),
    'K_{4,4}': graphs.CompleteMultipartiteGraph([4,4]),
    'L(K_4)': graphs.CompleteGraph(4).line_graph(),
    'L(K_5)': graphs.CompleteGraph(5).line_graph(),
    'L(K_{3,3})': graphs.CompleteMultipartiteGraph([3,3]).line_graph(),
    'Q_3': graphs.CubeGraph(3),
    'Q_4': graphs.CubeGraph(4),
    'L(Q_3)': graphs.CubeGraph(3).line_graph(),

```

```

'M_5': Graph({i:[j+5 for j in range(5) if i!=j] for i in range(5)}),
'Pet': graphs.PetersenGraph(),
'GP(8,3)': graphs.GeneralizedPetersenGraph(8,3),
'GP(10,3)': graphs.GeneralizedPetersenGraph(10,3),
'Hea': Graph({i:[s for s in Fano if i in s] for i in range(1,8)}),
'coHea': Graph({i:[s for s in Fano if i not in s] for i in range(1,8)}),
'Pap': graphs.PappusGraph(),
'Dod': graphs.DodecahedralGraph(),
'Ico': graphs.IcosahedralGraph()
}
SpecialCuts = {
'triangle': graphs.CycleGraph(3),
'three path': graphs.PathGraph(3),
'four path': graphs.PathGraph(4),
'tetrahedron': graphs.CompleteGraph(4),
'theta': Graph({0:[1,2,3],1:[2,3]}),
'wheel5': graphs.WheelGraph(6),
'cube': graphs.CubeGraph(3),
'K_{2,3}': graphs.CompleteMultipartiteGraph([2,3]),
'bowtie': Graph({0:[1,2,3,4],1:[2],3:[4]}),
'yield': Graph({0:[1,2,3],1:[2]}),
'house': Graph({0:[1,2,3],1:[4],3:[2,4]}),
'cat': Graph({0:[1,2,3,4],1:[2,5],3:[4,5]}),
'pill': Graph({0:[1,2,3],1:[2,5],3:[4,5],4:[5]}),
'three star': graphs.StarGraph(3),
'hexagon': graphs.CycleGraph(6),
'pentagon': graphs.CycleGraph(5),
'square': graphs.CycleGraph(4),
'pentagon plus': Graph({0:[1,2,3],3:[5],4:[1,5]}),
'bipentagon': Graph({0:[1,2,3],1:[4,5],6:[2,4],7:[3,5]}),
'tripentagon': Graph({0:[1,2,3],1:[4,5],3:[8,9],6:[2,5],7:[2,8],9:[4]}),
'split tetrahedron': Graph({0:[4,5,7],1:[4,6,9],2:[7,8,9],3:[5,6,8]}),
'split triple edge': Graph({0:[1,2,3],4:[1,7],5:[2,7],6:[3,7]}),
}
TrivialNames = {'vertex', 'two vertices', 'two path',
                'three path', 'four path', 'three star'}
SpecialCutID = {UniqueLabel(X):Name for Name,X in SpecialCuts.items()}

for d in range(3,7):
    GraphsWithCuts = {Name:[] for Name in SpecialCuts}
    print "Degree", d
    for Name,X in ExceptionalGraphs.items():
        if X.degree_sequence()[0] == d:
            for cut in SmallCuts(X):
                #There's some implicit completeness checking happening here
                #since SpecialCutID contains info about known cuts -- if we
                #found something new, we'd get screamed at.

```

```

CutName = SpecialCutID[cut]
GraphsWithCuts[CutName].append(Name)

for Name,Graphs in GraphsWithCuts.items():
    if Name not in TrivialNames and Graphs:
        print " with %s as a small cut: "%Name, ", ".join(Graphs)

```

Output from the above is below.

Degree 3

```

with square as a small cut: Q_3
with pentagon as a small cut: Pet, Dod
with split tetrahedron as a small cut: GP(10,3)
with bipentagon as a small cut: Dod
with pentagon plus as a small cut: Dod
with split triple edge as a small cut: GP(8,3)
with tripentagon as a small cut: Dod
with hexagon as a small cut: Pap, GP(10,3), Hea, GP(8,3)

```

Degree 4

```

with square as a small cut: L(K_{3,3}), M_5, coHea, Q_4, L(Q_3), K_{4,4}
with house as a small cut: L(Q_3)
with K_{2,3} as a small cut: M_5
with pill as a small cut: L(Q_3)
with cube as a small cut: Q_4
with triangle as a small cut: L(K_{3,3}), K_{2^3}, L(Q_3)
with bowtie as a small cut: L(Q_3)
with yield as a small cut: L(K_{3,3}), L(Q_3)
with cat as a small cut: L(Q_3)

```

Degree 5

```

with theta as a small cut: Ico
with wheel5 as a small cut: Ico
with triangle as a small cut: Ico, K_6

```

Degree 6

```

with tetrahedron as a small cut: K_{2^4}, L(K_5)
with triangle as a small cut: K_{2^4}, K_7, L(K_5), K_{3^3}

```

With so many cases to consider in the proof of our main theorem, it may be useful to tear the next page out for a quick reference guide.

We define two parametrized families of graphs:

- We denote the tilings of the torus where every face is a m -cycle by \mathcal{T}_m .
- For a graph \mathcal{V} and natural number m , we define the family $[\mathcal{V}]_m$ to be graphs (V, E) for which the edges E may be partitioned into induced subgraphs isomorphic to \mathcal{V} such that every vertex $v \in V$ belongs to exactly m parts. In particular, we use the symbols \triangle, \square and \boxtimes as shorthand for $[K_3], [C_4]$ and $[K_4]$ respectively.

For a subset $A \subset V$ of vertices of a graph, we define the *edge cut* induced by A to be the edges between A and $V \setminus A$, $\partial(A) = \{uv \in E : u \in A, v \in V \setminus A\}$. We denote the size of the edge cut $c(A) = |\partial(A)|$.

Theorem 3.3.4. *Let $X = (V, E)$ be a connected d -regular double transitive graph and $A \subset V$. If $c(A) \leq 2d$ and $|A| \leq |V|/2$ then $X[A]$ is isomorphic to one of the following:*

| d | $c(A)$ | $X[A]$ | X | d | $c(A)$ | $X[A]$ | X |
|-----|----------|---------------------------------------|---|-----|----------|---|-------------------------|
| any | $2d$ | $\cdot \cdot$ | any | 4 | $2d$ | \boxtimes | $\mathcal{L}(Q_3)$ |
| any | $2d - 2$ | \dashrightarrow | any | 4 | $2d$ | \diamond | $\mathcal{L}(Q_3)$ |
| any | d | \cdot | any | 4 | $2d$ | \boxtimes | $\mathcal{L}(Q_3)$ |
| 6 | $2d$ | \triangle | $\mathcal{T}_3, \triangle_3, \boxtimes_2$ | 4 | $2d - 2$ | \triangle | $\triangle_2, K_{2(3)}$ |
| 6 | $2d$ | \triangle | $\boxtimes_2, K_{2(4)}$ | 3 | $2d$ | \dashrightarrow | any |
| 5 | $2d$ | \diamond | Ico | 3 | $2d$ | \frown | any |
| 5 | $2d$ | \star | Ico | 3 | $2d$ | \hexagon | \mathcal{T}_6 |
| 5 | $2d - 1$ | \triangle | Ico, K_6 | 3 | $2d$ | \heptagon | Dod |
| 4 | $2d$ | \dashrightarrow | any | 3 | $2d$ | \heptagon | Dod |
| 4 | $2d$ | \square | Q_4 | 3 | $2d$ | \heptagon | Dod |
| 4 | $2d$ | \square | $\mathcal{T}_4, \square_2, \text{Hea}^c$ | 3 | $2d$ | \heptagon | GP(10, 3) |
| 4 | $2d - 2$ | \diamond | M_5 | 3 | $2d$ | \heptagon | GP(8, 3) |
| 4 | $2d$ | $\boxtimes \dashrightarrow \boxtimes$ | $C_m^{(2)}$ | 3 | $2d - 1$ | \dashrightarrow | any |
| 4 | $2d$ | $\boxtimes \dashrightarrow \boxtimes$ | $C_m^{(2)}$ | 3 | $2d - 1$ | \heptagon | Pet, Dod |
| 4 | $2d$ | $\boxtimes \dashrightarrow \boxtimes$ | $C_m^{(2)}$ | 3 | $2d - 2$ | \square | Q_3 |
| 4 | $2d$ | \boxtimes | \triangle_2 | 2 | $2d$ | $\dashrightarrow \dashrightarrow \dashrightarrow$ | any |
| 4 | $2d$ | ∇ | \triangle_2 | 2 | d | $\dashrightarrow \dashrightarrow \dashrightarrow$ | any |

Note that there are three large families of cuts in $C_m^{(2)}$. Some of the smaller members of those families, notably \diamond and \square , appear elsewhere on the table and we do not list $C_m^{(2)}$ there. Also, when an exceptional graph is known to belong to a particular family, it is not shown alongside that family. For example, $K_{2(4)}$ contains \triangle but is not listed since $K_{2(4)} \in \mathcal{T}_3$.